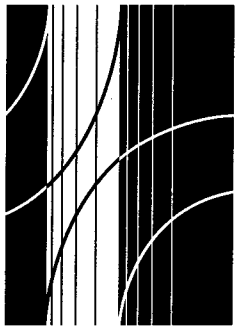

Joint
Transportation
Research
Program

JTRP

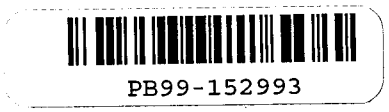

FHWA/IN/JTRP-96/22

Final Report

Contributions of Performance-Graded Asphalt to Low Temperature Cracking Resistance of Pavements

Ssu-Wei Loh
Jan Olek

May 1999

Indiana
Department
of Transportation

Purdue
University

FHWA/IN/JTRP-96/22

Final Report

Contributions of Performance-Graded Asphalt to Low Temperature Cracking Resistance of Pavements

Ssu-Wei Loh
Jan Olek

May 1999

Final Report

FHWA/IN/JHRP-96/22

CONTRIBUTION OF PERFORMANCE-GRADED ASPHALT TO LOW TEMPERATURE CRACKING RESISTANCE OF PAVEMENTS

By

Ssu-Wei Loh
Research Assistant
and
Jan Olek
Research Engineer

Purdue University
Department of Civil Engineering

Joint Transportation Research Program
Project No: C-36-24C
File No: 2-10-3

Prepared in Cooperation with the
Indiana Department of Transportation and
U.S. Department of Transportation
Federal Highway Administration

Purdue University
West Lafayette, Indiana 47907

May 1999

TECHNICAL REPORT STANDARD TITLE PAGE

1. Report No.	2. Government Accession No.	3. F
FHWA/IN/JTRP-96/22		PB99-152993

4. Title and Subtitle	5. Report Date
Contribution of Performance-Graded Asphalt to Low Temperature Cracking Resistance of Pavements	May 1999
	6. Performing Organization Code

7. Author(s)	8. Performing Organization Report No.
Ssu-Wei Loh and Jan Olek	FHWA/IN/JHRP-96/22

9. Performing Organization Name and Address	10. Work Unit No.
Joint Transportation Research Program 1284 Civil Engineering Building Purdue University West Lafayette, Indiana 47907-1284	
	11. Contract or Grant No. SPR-2130

12. Sponsoring Agency Name and Address	13. Type of Report and Period Covered
Indiana Department of Transportation State Office Building 100 North Senate Avenue Indianapolis, IN 46204	Final Report
	14. Sponsoring Agency Code

15. Supplementary Notes

Prepared in cooperation with the Indiana Department of Transportation and Federal Highway Administration.

16. Abstract

The purpose of this research was to study and evaluate the role that asphalt binders play in the resistance of asphalt pavements to low temperature cracking.

As part of the Strategic Highway Research Program (SHRP) new specifications for asphalt binders were developed that are based on the performance of the material. The asphalt binder graded and specified according to these new performance-based specifications is called PG binder. These new specifications are commonly referred to as Superpave (Superior Performing Asphalt Pavement) binder specifications.

A section of Interstate 64 in southern Indiana was experiencing severe low temperature cracking before it was reconstructed over the summers of 1995 and 1996. The binder used in the new pavement mixes was PG material. Dynamic Shear Rheometer (DSR) tests, Bending Beam Rheometer (BBR) tests, and viscosity tests were performed on this binder. Comparisons were made between test results obtained from the binders in the old pavement and the new pavement. All tests and comparisons were based on the Superpave binder specifications.

A portion of this study involved a review of the extraction and recovery procedures used in the laboratories. Much of the asphalt used in this project had to be extracted from cores or pavement mixes, and it was important to ensure that the extraction and recovery process did not significantly change the properties of the material.

Also, as a part of this research project, plans were developed for field monitoring of the temperature distribution within the pavement and its variation with time, in order to correlate these changes with pavement performance. Data generated during this monitoring program will be used in the future for validation of low temperature algorithms developed as a part of Superpave system.

17. Key Words	18. Distribution Statement
performance graded asphalt, low temperature cracking, extraction and recovery procedures, temperature algorithms and models, IDT testing, weather station, temperature sensors.	No restrictions. This document is available to the public through the National Technical Information Service, Springfield, VA 22161

19. Security Classif. (of this report)	20. Security Classif. (of this page)	21. No. of Pages	22. Price
Unclassified	Unclassified	159	

IMPLEMENTATION REPORT

The research was directed towards comparing the binder used in the new pavement and the old pavement of Interstate 64 in southern Indiana. The binder used in the new pavement was PG 64-34, while the binder used in the old pavement was PG 64-22. The procedures for extracting and recovering asphalt binder from mixes and cores were also investigated.

The following recommendations are made for the implementation of the findings of this research.

1. Modified ASTM D 2172 procedures and solvents can be used for extraction and recovery of asphalt from mixes and cores without changing the properties of the asphalt. Toluene should be used as the solvent for the extraction. During the recovery process, the temperature of the bath should be carefully monitored and maintained at 130°C, and the rotovapor should continue to run for 60 minutes past the time when solvent stops dripping into the recovery flask.

2. The procedures and solvents used for the extraction and recovery of asphalt binders from mixes and cores should be studied and compared further for effects they may have on modified asphalts.

3. Weather and pavement temperature data from the instrumentation at the study site should be collected and analyzed over a period of several years. These data include climatic factors such as air temperature, air humidity, and solar radiation. Such data will be invaluable in assessing the validity of the existing pavement temperature algorithms and pavement performance prediction models.

TABLE OF CONTENTS

LIST OF TABLES

LIST OF FIGURES

1. INTRODUCTION

Low temperature cracking, also sometimes referred to as thermal cracking, in asphalt pavements is a result of extreme temperature gradients or changes present in the pavement, and frequently is attributed to the tensile stress developed due to shrinkage of the pavement material. When the tensile stress resulting from such thermal contraction is greater than the inherent tensile strength of the pavement, cracks form and will generally propagate in a direction perpendicular to that of traffic flow.

The Strategic Highway Research Program (SHRP) developed a method of specifying asphalt binders to meet the climatic conditions in which the pavement will have to perform. This method is based on a series of binder tests at specific temperatures. The objective of SHRP was to develop test methods that better correlate with pavement performance. The product of the program is the system of tests and specifications known as the Superpave (Superior Performing Asphalt Pavements) system.

The purpose of this research was to evaluate the role that asphalt binders play in the resistance of the pavement to low temperature cracking. An asphalt pavement that experienced extensive thermal cracking was studied and binder properties from this pavement were compared to properties of materials used in rehabilitation. These new materials are expected to have the capability of withstanding the same conditions under which the old pavement had failed. In an effort to ensure that accurate data is obtained, a comparison research on the various methods of extracting asphalt from pavement cores and mixes, including a method recommended by SHRP, was conducted. The goal of this portion of the study was to select an extraction and recovery procedure that minimizes the potential for additional aging of the binders.

Tests conducted during this research included the Dynamic Shear Rheometer (DSR) and the Bending Beam Rheometer (BBR). Three kinds of materials were tested.

The virgin asphalt from the new pavement was tested as original tank asphalt binder, after aging in the Rolling Thin Film Oven (RTFO) to simulate aging during construction, and after aging in the Pressure Aging Vessel (PAV) to simulate aging during pavement life. The binder extracted from the pavement mixes was considered as having already undergone RTFO aging. They were tested as RTFO material, then pressure-aged in the PAV and tested as PAV material. Finally, binder was extracted from cores obtained from the old pavement. This was considered and tested as PAV material, then aged again in the PAV and tested once more in the same equipment to see if any additional aging could occur.

1.1 Asphalt Binder Characteristics

Asphalt pavements are constructed from asphalt binder and aggregates. The asphalt binder acts as a water-proofing agent and holds the aggregate framework together, while the aggregate framework is the primary contributor to the strength of the asphalt pavement.

An important characteristic of an asphalt binder related to pavement performance is its susceptibility to temperature changes. At high temperatures, asphalt binder is a viscous fluid and flows easily. At low temperatures, it behaves like a elastic solid, which means it is generally capable of returning to its original shape, to a certain extent, upon the removal of an applied load. Asphalt binders are also sensitive to load duration. Therefore, when testing asphalt materials, it is often necessary to specify temperature and loading conditions under which the tests have been performed (1). Asphalt binders can also react with oxygen, resulting in what is known as age or oxidative hardening. Age hardening occurs more rapidly when an asphalt is exposed to high temperatures. This is an inevitable process during the life of binder material, though it occurs to different degrees for different binders and increases binder stiffness (2), which could in turn lead to a greater susceptibility to thermal cracking. Aging, then, can have a significant effect on pavement performance.

1.2 Current Methods of Binder Classification

The current methods of classifying asphalt binders use viscosity or penetration tests. When using these methods, viscosity values are obtained at two temperatures (typically, 60°C and 135°C) using two different procedures, and penetration is done at one temperature (typically, 25°C). The results from these tests are plotted on a graph. There is a possibility that two asphalts may share the same grade, and because of that, they are also expected to provide the same performance when in use. However, these could be two very different asphalt binders (3).

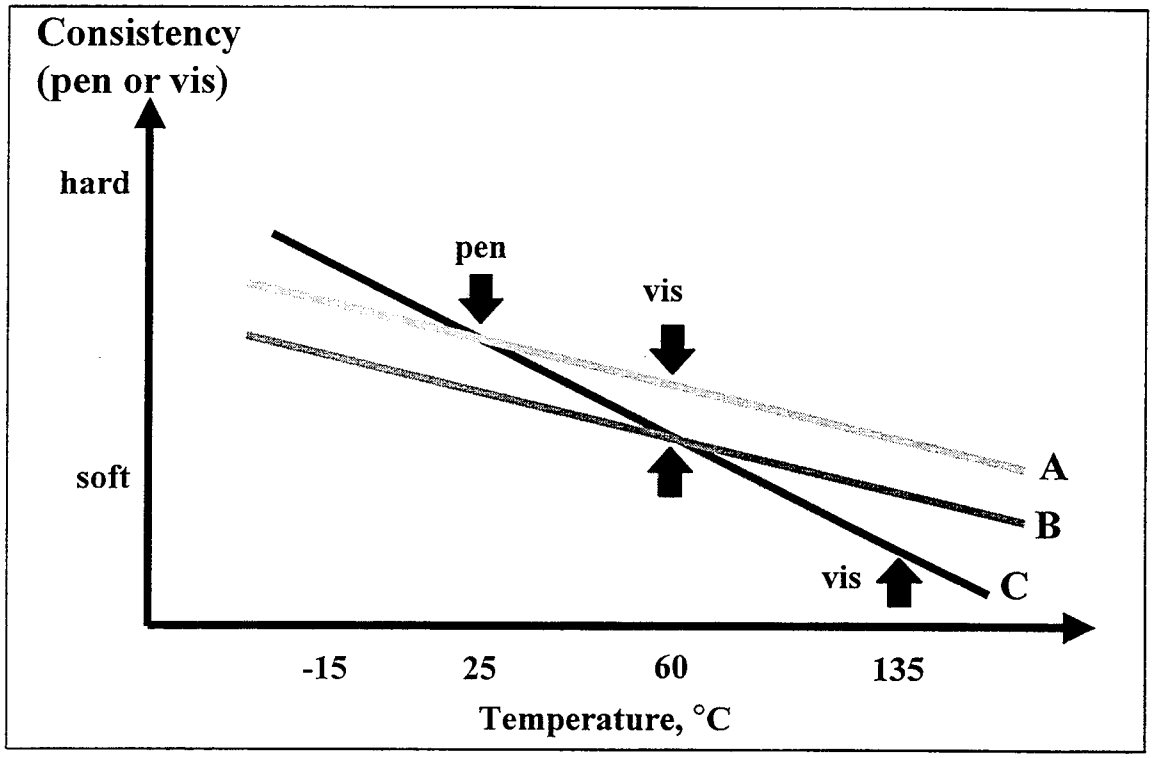

Figure 1.2.1 Comparison of asphalt consistency (8)

For example, consider three asphalt binders A, B, and C as shown in Figure 1.2.1 (8). Asphalts A and C have the same consistencies at low temperatures, but are completely different at high temperatures. Asphalt B has the same consistency as Asphalt C at the specification temperature, 60°C, but otherwise it is very different from asphalt C.

All three are classified as the same grade, only because they fall within the specified viscosity range at 60°C. In reality, they behave in different ways.

1.3 Superpave Classification of Asphalt Binders

The Superpave specifications classify asphalt binders based on their performance at temperatures that are expected to occur in pavements during their service life. Asphalt binders are placed in the same grade only if they have the same physical properties (within a range), and pass the same criteria. An example of a performance-graded asphalt is a PG 64-34 asphalt binder. PG stands for Performance Grade, the first number, 64, indicates that the asphalt performs adequately at a high temperature up to 64°C. The second part of the classification, -34, indicates that the asphalt binder is able to perform acceptably at temperatures as low as -34°C.

1.4 Low Temperature Cracking

Low temperature cracking is a serious problem in the United States and Canada (4). It is related to binder composition. If the binder is too stiff, its ability to deform elastically diminishes. At low temperatures, asphalt materials shrink due to a reorganization of the low polarity and non-polar components of the material. The top of a pavement contracts during cooling, but this contraction is resisted by friction with underlying layers that are warmer, or have lower coefficients of thermal expansion. Micro cracks develop at the edge and surface of the pavement (5). At critically low temperatures, or after repeated temperature cycles, these micro-cracks extend and penetrate through the depth and across the width of the pavement. Asphalt binders play a key role in low temperature cracking.

Age hardening produces harder asphalt, and harder asphalts are more prone to cracking. As a result, if an asphalt binder has been subjected to aging, the chances of this

binder cracking at low temperatures is increased significantly. Therefore, in order to avoid cracking in pavements, softer asphalt binders need to be used.

1.5 Problem Statement

Low-temperature cracking of hot mix asphalt (HMA) pavements has been a sporadic but persistent problem on some highway projects in Indiana. One of the projects showing the signs of distress attributed to low-temperature cracking is the 21 km-long stretch of highway I-64 in southwestern Indiana. The affected segment of the highway has been scheduled for rehabilitation and part of the work (segment about 6.5 km long) has been completed during the 1995 construction season. The work on the remaining portion continued in 1996. The rehabilitation process involved removal of the top (cracked) layer to the depth of about 5 cm and replacement with a layer of Superpave mixture containing PG 64-34 binder. In preparation for the rehabilitation work INDOT personnel removed several cores from various sections of the cracked pavement to study the binder content and aggregate gradation of the asphalt concrete mixtures. Twenty of these cores were made available to the research team. All twenty cores were collected from sites showing severe signs of low-temperature cracking.

From the discussions with the INDOT personnel it appeared that the pavement most likely failed because the binder used in the top layer was too stiff for the local environmental conditions. It is expected that new mixtures containing PG-graded asphalt will perform better in the same environment as the Superpave binder selection process addresses the issue of temperature-stiffness incompatibility. Selection of binders in Superpave is driven at the high temperature by "mean 7-day high temperature" of the pavement and at low temperatures by "lowest anticipated temperature" of the pavement with appropriate adjustments based on selected risk (or reliability) levels (1).

Superpave recommends that agencies determine pavement temperatures for each climatic area within their jurisdiction. However, in the event actual pavement temperature data are not available, Superpave provides an algorithm which converts air

temperature (available from the local weather station) to pavement temperature. Testing of this algorithm was limited by time constraints during the original SHRP program, and it has been found inadequate in some regions of the country.

Inaccurate determination of pavement temperature can cause changes of at least two binder grades resulting in over-specifying or, worse, using binders that will crack at the average low temperature expected in a given area. This will lead to premature deterioration and ultimately failure of the pavement. It is therefore necessary to work on establishing a database of actual pavement temperatures in a region and adjusting the Superpave algorithm for specific local environmental conditions. There is also an urgent need for cores to be analyzed from pavements that have cracked. Accompanying temperature records would also be needed. Such data could provide a clearer understanding of the mechanical properties of the binder when thermal cracking occurs.

Another issue related to low temperature performance of binders is the unproved relationship between low temperature cracking resistance and the "m" parameter of the binder. The issue is being heavily debated by the members of the Expert Task Group (ETG). Since the ability of binder to efficiently relax stresses associated with contraction at low temperature is of paramount importance in controlling the amount of strain at failure, it appears that having such information available for local materials will be very useful.

1.6 Objectives

The major objectives of the research can be summarized as follows:

1. To make comparisons between the properties of asphalt binder used in the old pavement and the properties of asphalt binder used in the new pavement of Interstate 64 to determine how binder used in the old pavement will classify under Superpave specifications.
2. To determine how extraction and recovery procedures, as well as a solvent used influence PG classification of asphalt binder recovered from the pavement.

3. To install instrumentation for the monitoring of environmental conditions at the test site. The results of these observations will be used for future evaluation of the pavement temperature algorithm used by Superpave.
4. To assess the reliability of Superpave binder selection with respect to low temperature cracking prevention by estimating critical pavement temperature based on IDT testing and comparing it with low temperatures predicted by existing pavement temperature models.

2 STRATEGIC HIGHWAY RESEARCH PROGRAM

It is a general understanding that all pavements, unless rehabilitated or rebuilt regularly, will eventually fail. The service lives of pavements are approximately ten to twenty years. Transverse cracks are considered one form of failure, and these occur when pavements experience extreme temperatures, particularly low temperatures (5). As temperature drops, the pavement contracts, and stresses develop in the material. When the tensile stress in the material exceeds the critical stress, cracks begin to form, and as time progresses, these cracks expand and propagate across the pavement, and deeper into the pavement layers.

Low temperature cracking can be controlled by the proper selection of asphalt binders. The important point in the selection of a binder is to ensure that the stiffness of the asphalt material is lower than the critical stiffness this material will experience when exposed to the lowest temperature expected to occur in the pavement (6). Asphalt stiffness varies based on its grade, consistency, and temperature susceptibility. Age also plays a role in the stiffness of the material. An aged binder that has undergone a great amount of oxidation has a higher stiffness value than one that is un-aged.

The goal of SHRP was to develop asphalt binder specifications to improve the performance of asphalt binders in pavements (7). Table 2.0.1 shows the binder specifications developed by SHRP. The specification considers low, intermediate, and high temperatures in classifying an asphalt binder. Due to the fact that exposure to field conditions affects the properties of asphalt binders as well, SHRP factors in the results of asphalt properties.

Table 2.0.1 Superpave Specifications (7)

Performance Grade	PG 46			PG 52							PG 58					PG 64					
	-34	-40	-46	-10	-16	-22	-28	-34	-40	-46	-16	-22	-28	-34	-40	-10	-16	-22	-28	-34	-40
Average 7-day Maximum Pavement Design Temperature, °C [a]	<46			<52							<58					<64					
Minimum Pavement Design Temperature, °C [a]	>-34	>-40	>-46	>-10	>-16	>-22	>-28	>-34	>-40	>-46	>-16	>-22	>-28	>-34	>-40	>-10	>-16	>-22	>-28	>-34	>-40
Original Binder																					
Flash Point Temp, T48: Minimum °C	230																				
Viscosity, ASTM D 4402: [b] Maximum, 3 Pa·s (3000 cP), Test Temp, °C	135																				
Dynamic Shear, TP5: [c] G*/sin δ, Minimum, 1.00 kPa Test Temperature @ 10 rad/s, °C	46			52							58					64					
Rolling Thin Film Oven (T 240) or Thin Film Oven (T 179) Residue																					
Mass Loss, Maximum, %	1.00																				
Dynamic Shear, TP5: G*/sin δ, Minimum, 2.20 kPa Test Temp @ 10 rad/sec, °C	46			52							58					64					
Pressure Aging Vessel Residue (PP1)																					
PAV Aging Temperature, °C [d]	90			90							100					100					
Dynamic Shear, TP5: G*sin δ, Maximum, 5000 kPa Test Temp @ 10 rad/sec, °C	10	7	4	25	22	19	16	13	10	7	25	22	19	16	13	31	28	25	22	19	16
Physical Hardening [e]	Report																				
Creep Stiffness, TP1: [f] S, Maximum, 300 MPa m-value, Minimum, 0.300 Test Temp, @ 60 sec, °C	-24	-30	-36	0	-6	-12	-18	-24	-30	-36	-6	-12	-18	-24	-30	0	-6	-12	-18	-24	-30
Direct Tension, TP3: [f] Failure Strain, Minimum, 1.0% Test Temp @ 1.0 mm/min, °C	-24	-30	-36	0	-6	-12	-18	-24	-30	-36	-6	-12	-18	-24	-30	0	-6	-12	-18	-24	-30

Performance Grade	PG 70						PG 76					PG 82				
	-10	-16	-22	-28	-34	-40	-10	-16	-22	-28	-34	-10	-16	-22	-28	-34
Average 7-day Maximum Pavement Design Temperature, °C [a]	<70						<76					<82				
Minimum Pavement Design Temperature, °C [a]	>-10	>-16	>-22	>-28	>-34	>-40	>-10	>-16	>-22	>-28	>-34	>-10	>-16	>-22	>-28	>-34
Original Binder																
Flash Point Temp, T48: Minimum °C	230															
Viscosity, ASTM D 4402: [b] Maximum, 3 Pa·s (3000 cP), Test Temp, °C	135															
Dynamic Shear, TP5: [c] G*/sin δ, Minimum, 1.00 kPa Test Temperature @ 10 rad/s, °C	70						76					82				
Rolling Thin Film Oven (T 240) or Thin Film Oven (T 179) Residue																
Mass Loss, Maximum, %	1.00															
Dynamic Shear, TP5: G*/sin δ, Minimum, 2.20 kPa Test Temp @ 10 rad/sec, °C	70						76					82				
Pressure Aging Vessel Residue (PP1)																
PAV Aging Temperature, °C [d]	100(110)						100(110)					100(110)				
Dynamic Shear, TP5: G*sin δ, Maximum, 5000 kPa Test Temp @ 10 rad/sec, °C	34	31	28	25	22	19	37	34	31	28	22	40	37	34	31	28
Physical Hardening [e]	Report															
Creep Stiffness, TP1: [f] S, Maximum, 300 MPa m-value, Minimum, 0.300 Test Temp, @ 60 sec, °C	0	-6	-12	-18	-24	-30	0	-6	-12	-18	-24	0	-6	-12	-18	-24
Direct Tension, TP3: [f] Failure Strain, Minimum, 1.0% Test Temp @ 1.0 mm/min, °C	0	-6	-12	-18	-24	-30	0	-6	-12	-18	-24	0	-6	-12	-18	-24

2.1 Pavement Temperature and Binder Selection

In order to select an asphalt binder grade for the construction of a pavement, one uses the Superpave software. The first step includes determining the air temperature range in the service area; these temperatures are then converted to pavement temperatures, and an asphalt binder is selected based on the pavement temperatures. The software contains temperature data from weather stations across the country. Only those weather stations were included in the database for which at least 20 years worth of observations were available.

To obtain the pavement temperature, the high and low air temperatures are first obtained. To do so, the software uses the mean and standard deviation of annual 7-day maximum temperatures, and the mean and standard deviation of annual minimum temperatures. These temperatures are assumed to be normally distributed. Conversions to pavement design temperatures are made using separate methods for high and low temperatures. For high temperatures, Superpave defines the design temperature at 20 mm below the surface of the pavement, and for low temperatures it is defined at the surface (19). With considerations for solar absorption, radiation transmission, atmospheric radiation, and wind speed, the conversion equation for high design pavement temperature developed is:

$$T_{20mm} = (T_{air} - 0.00618\ Lat^2 + 0.2289\ Lat + 42.2)(0.9545)-17.78$$

where, T_{20mm} = high pavement design temperature at depth 20 mm,

T_{air} = seven-day average high air temperature, °C,

Lat = geographical latitude of the project, degrees.

SHRP researchers recommended that the low pavement design temperature be assumed to be the same as the air temperature, which results in a conservative selection. However, this is being questioned as some researchers believe that another formula for the conversion, used by the Canadian SHRP researchers, may be preferred:

$$T_{min} = 0.859\ T_{air} + 1.7°C$$

where, T_{min} = minimum pavement design temperature in °C,

T_{air} = minimum air temperature in average year in °C.

There have also been suggestions that more environmental parameters may play a role in the conversion. These possibilities are being studied by LTPP (Long-Term Pavement Performance) under the Seasonal Monitoring Program (SMP). They developed the following equations using data gathered from 30 SMP test sites (20).

$$T_{max} = 54.32 + 0.78\ T_{air} - 0.0025\ Lat^2 - 15.14\ \log(H+25) + z(9 + 0.61\sigma_{air}^2)^{0.5}$$

where, T_{max} = High AC pavement temperature, °C

T_{air} = High 7-day mean air temperature, °C

Lat = Latitude of the section, degrees

H = Depth to surface, mm

σ_{air} = Standard deviation of the high 7-day mean air temperature, °C

z = From the std. normal distribution table, z = 2.055 for 98% reliability

The equation for low pavement temperature prediction is:

$$T_{min} = -1.56 + 0.72\ T_{air} - 0.004\ Lat^2 + 6.26\ \log(H+25) + z(4.4 + 0.52\sigma_{air}^2)^{0.5}$$

where, T_{min} = Low AC pavement temperature below surface, °C

T_{air} = Mean low air temperature, °C

All other terms are as defined before.

The installation of a weather monitoring station at the site on I-64 will be discussed in Chapter 7.

Figure 2.1.1 illustrates an example of establishing pavement temperature from air temperature. Figure 2.1.1a shows the distribution of the low and high air temperatures. Figure 2.1.1 b shows the low and high pavement temperatures used for binder selection, obtained through conversion from the air temperatures. The Superpave binder grades are reported in increments of 6°C, and using specifications given in Table 2.0.1 for this particular example, a PG 58-28 binder could be selected by "rounding" up and down at

the maximum and minimum temperatures respectively. Through calculations, this results in reliability values of more than 95 %, which is desirable.

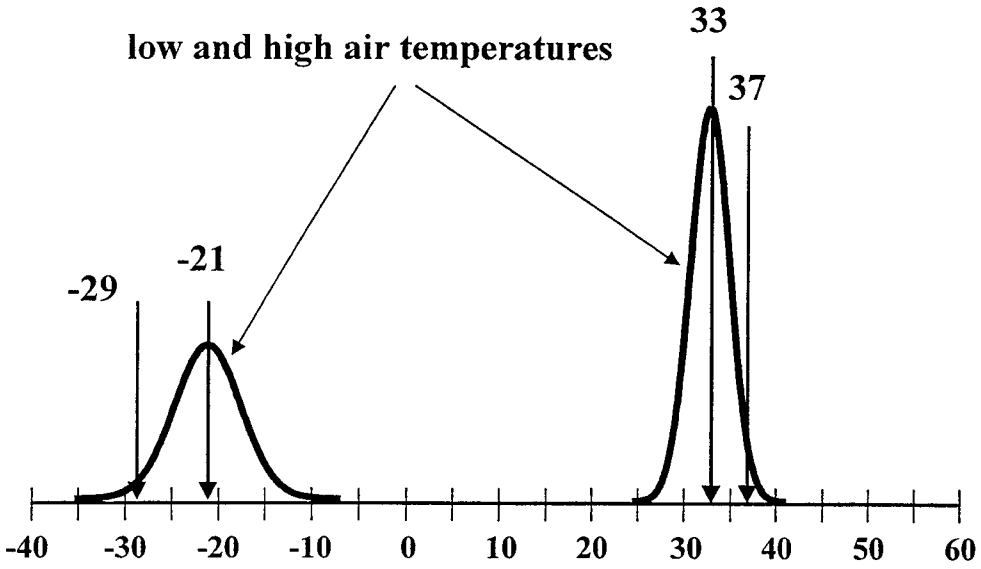

(a)

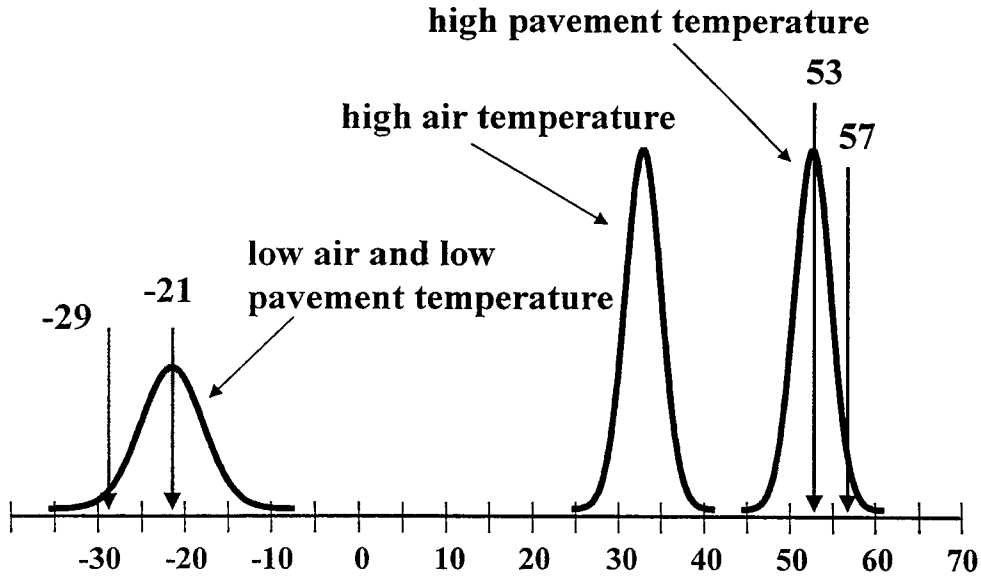

(b)

Figure 2.1.1 Establishment of Pavement Temperature for Binder Selection

2.2 SHRP Model for Thermal Cracking

During the SHRP study, a new mechanistic-based model for low temperature cracking was developed. This model is composed of five major parts with interrelationships as shown in the flow chart in Figure 2.2.1. They are the input module, transformation model for the master relaxation modulus curve, the environmental effects model, the pavement response model, and the pavement distress model. This system of modeling provides the basis for the development of performance based mixture specification for thermal cracking (14).

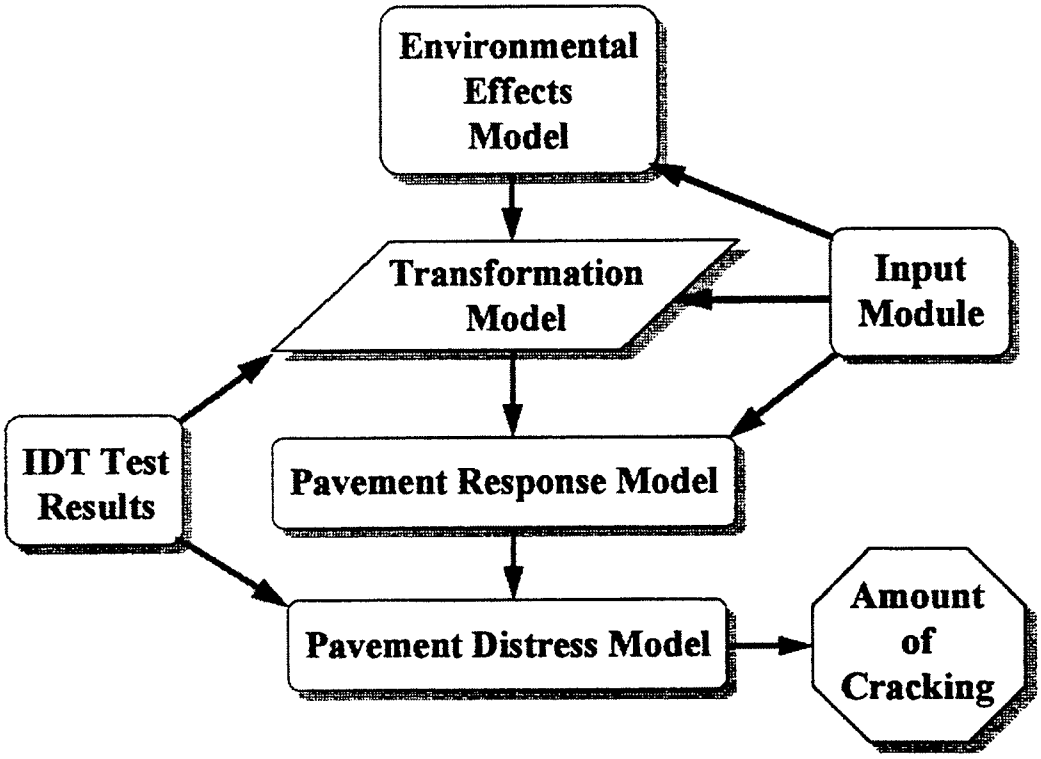

Figure 2.2.1 Flowchart of low temperature cracking modeling components (14)

2.2.1 Input Module

The input module includes pavement structure information, pavement material properties, and site specific environmental data. The pavement structure information includes layer types and the thickness. The pavement material properties include coefficient of thermal contraction, thermal conductivity, and freezing temperature of soil. Examples of environmental data are the maximum and minimum daily air temperatures, and the latitude of the site of study.

The only major output in this model is that of the linear coefficient of thermal contraction of the mix:

$$B_{MIX} = [(VMA \times B_{AC}) + (V_{AGG} \times B_{AGG})] / (3 \times V_{TOTAL}) \quad (2.2.1)$$

where:

B_{MIX} = linear coefficient of thermal contraction of mix, 1/°C

VMA = percent volume of air void in mineral aggregate

B_{AC} = solid state volumetric coefficient of thermal contraction, 1/°C

V_{AGG} = percent volume of aggregate in mix

B_{AGG} = volumetric coefficient of thermal contraction of aggregate, 1/°C

V_{TOTAL} = total volume = 100 percent

This relationship accounts for the differences in the physical mix properties.

2.2.2 Transformation Model for Master Relaxation Modulus Curve

This model determines the master relaxation modulus curve from the creep compliance measurements and determines the relationship between failure strength and temperature. More details are provided in the Asphalt Institute publication of the Superpave Mixture Analysis Manual (8).

The results from this transformation are used in the pavement response model and the pavement distress model described in the next sections.

2.2.3 Environmental Effects Model

The environmental effects model uses information obtained from the inputs module to predict pavement temperatures. The maximum and minimum hourly air temperatures are recorded and the expected temperatures within pavements are calculated.

2.2.4 Pavement Response Model

The pavement response model predicts stresses within the pavement using material properties and pavement structure information, and pavement temperature predictions obtained from the input module and the environmental effects model. It uses a one-dimensional constitutive model, which models the pavement as a uniaxial rod subjected to tensile stresses at each end.

The equation is the Boltzman's Superposition Principle:

$$\sigma(\xi) = IE(\xi - \xi')[d(\alpha(T(\xi') - T_0)]/d\,\xi')d\,\xi' \qquad (2.2.4)$$

where:

$\sigma(\xi)$ = stress at reduced time, psi

$E(\xi - \xi')$ = relaxation modulus at reduced time, psi

α = linear coefficient of thermal contraction, 1/°C

$T(\xi')$ = pavement temperature at reduced time, °C

T_0 = pavement temperature when $\sigma = 0$, °C

ξ' = variable of integration.

The resulting stress distribution predicted is used in the pavement distress model.

2.2.5 Pavement Distress Model

The final component of SHRP low temperature cracking model is the pavement distress model, which consists of three parts -- the stress intensity factor model, the crack depth model, and the crack amount model.

The stress intensity factor is estimated by

$$K = \sigma(0.45 + 1.99C_o^{0.56}) \qquad (2.2.5a)$$

where:

K = stress intensity factor, psi$\sqrt{in}$.

σ = far-field stress from pavement response model at depth of crack tip, psi

C_o = current crack depth, in.

The crack propagation is computed daily and accumulated to obtain the total crack depth over time and is calculated by the Paris Law

$$\Delta C = A(\Delta K)^n \qquad (2.2.5b)$$

where:

ΔC = change in the crack depth due to a cooling cycle, in.

ΔK = change in the stress intensity factor due to a cooling cycle, psi$\sqrt{in}$.

A,n = fracture parameters

The value of A is obtained by the relationship

$$\log A = 4.389 - 2/52\log(kS_t n) \qquad (2.2.5c)$$

where:

S_t = asphalt concrete tensile strength, psi

k = 10,000

and n is determined using

$$n = 0.8(1 + (1/m))$$

where:

m = coefficient or slope of creep compliance curve, predicted from the transformation model for the master relaxation modulus curve, psi/s

The crack amount model predicts the amount of cracking per unit length using the average crack depth and the distribution of crack depths within the section. The equation is

$$C_{AC} = \beta_1 N[(1/\sigma) \log(C/D)] \qquad (2.2.5d)$$

where:

C = crack depth equal to C_0, in.

D = surface thickness, in.

β_1 = regression coefficient determined from field calibration,

$N[(1/\sigma) \log(C/D)]$ = standard normal distribution evaluated at $[(1/\sigma) \log(C/D)]$,

σ = standard deviation of log of pavement crack depths, in.

3. SITE OF STUDY

The site of this study is a section of Interstate 64 approximately 32 km north of Evansville, Indiana. This section is 21 km long and is located from just east of US Highway 41 to just east of State Road 61. This pavement lies in a region where there are extended periods of cold weather and, over the years, the pavement has undergone a great amount of aging leading to extensive temperature cracking.

3.1 Pavement History

The original pavement on this section of Interstate 64 was constructed in 1973 under a contract, R-9247, from the Indiana Department of Transportation. When the pavement began to deteriorate, it was overlaid under contract R-12776. This was done between 1981 and 1982 by Gohmann Asphalt. The most recent work done on the pavement was in 1995, and part of it is still being completed. The first part of the most current paving job was done in the summer of 1995 under contract R-21470 to Koester Contracting Corporation that completed 6.5 km of the highway. The other 14.5 km stretch is expected to be paved by the end of October 1996 under contract R-22347 to Gohmann Asphalt.

An attempt was made to obtain information on the earlier constructions. Unfortunately, the records obtained were incomplete. The materials used in the original construction of the pavement were a No. 5 base, a No. 9 binder, and a Type B surface. The bitumen used was an AP-3 graded asphalt binder, and there was 4.5 percent of asphalt in the base layer, 5.0 percent of asphalt in the binder layer, and 6.1 percent of

asphalt in the surface layer. The base was 222.6 mm thick, but the thicknesses of the other layers are unknown.

In 1981-82, a pavement overlay contract R-12776, was constructed with a No. 5 base, a No. 9 binder, and a Type IV surface. The bituminous materials used were AP-5 for the base and binder layers, and an AE-60 for the surface layer. The base was 62.6 mm thick, the binder layer was 37.6 mm thick, and the surface was 12.5 mm thick. There were no more detailed records found for this contract at the Indiana Department of Transportation, and therefore very little is known of this job.

A second overlay was placed between 1995 and 1996, which consisted of a 25 mm base, a 19 mm binder, and a 19 mm surface. The contractors used the new Performance Graded asphalt binder. The grade selected for the job was a PG 64-34, and the same grade was used in all layers of the pavement. The base was 75 mm thick, the binder layer was 50 mm thick, and the surface was 25 mm thick. Based on the Superpave specifications, the PG-graded asphalt binder should allow the pavement to withstand the weather conditions that it will be exposed to.

3.2 Pavement Condition

In order to get a better understanding of the extent of deterioration in the existing pavement, the site where the paving was being done was surveyed, and photographs were taken to document these failures. These failures were compared and classified according to the standards as specified in ASTM D5340 (Standard Test Method for Airport Pavement Condition Index Surveys). The engineer noted that in most areas, the cracking had propagated to the lower layers, and beyond the depth to which the reconstruction was being made. This is shown in Figure 3.2.1.

Figure 3.2.1 Appearance of the pavement after upper layers of existing pavement have been removed

For the second repaving job, the contractors had milled away 75 mm of the existing pavement and replaced it with 150 mm of new PG-graded asphalt mixture, 75 mm of base, 50 mm of binder, and 25 mm of surface. Along the 21 km of highway, medium severity to high severity transverse cracks could be observed at approximately every 3 to 4.5 m. The cracks ran across the entire width of two lanes and had widths between 32.5 and 75 mm. See photograph in Figure 3.2.2. These kinds of cracks, more often than not, can be attributed to low temperatures. As can be seen in Figure 3.2.2, attempts had been made to seal the cracks, but that had not been very successful, and cracks continued to propagate.

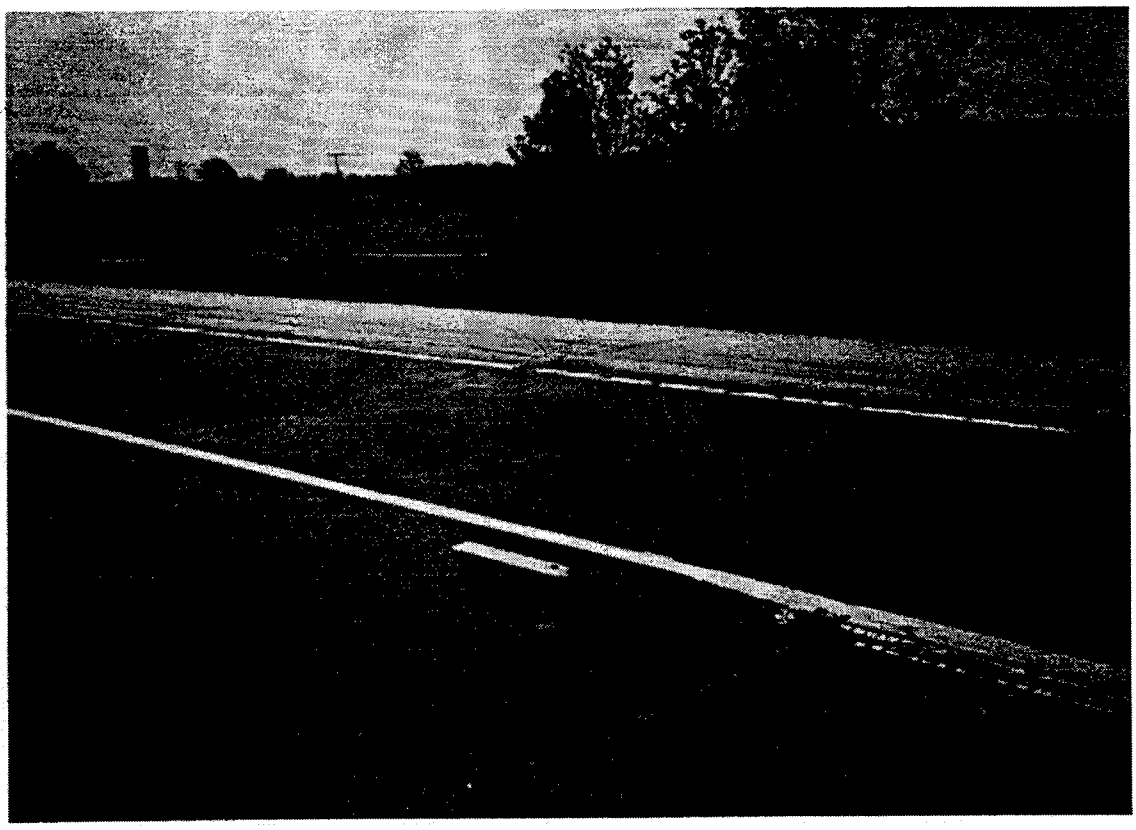

Figure 3.2.2 Transverse cracks due to temperature cracking

Apart from these transverse cracks, there were also some concave cracks at several locations on the highway, Figure 3.2.3. These are cracks that result from fatigue failure due to repeated traffic loading (6).

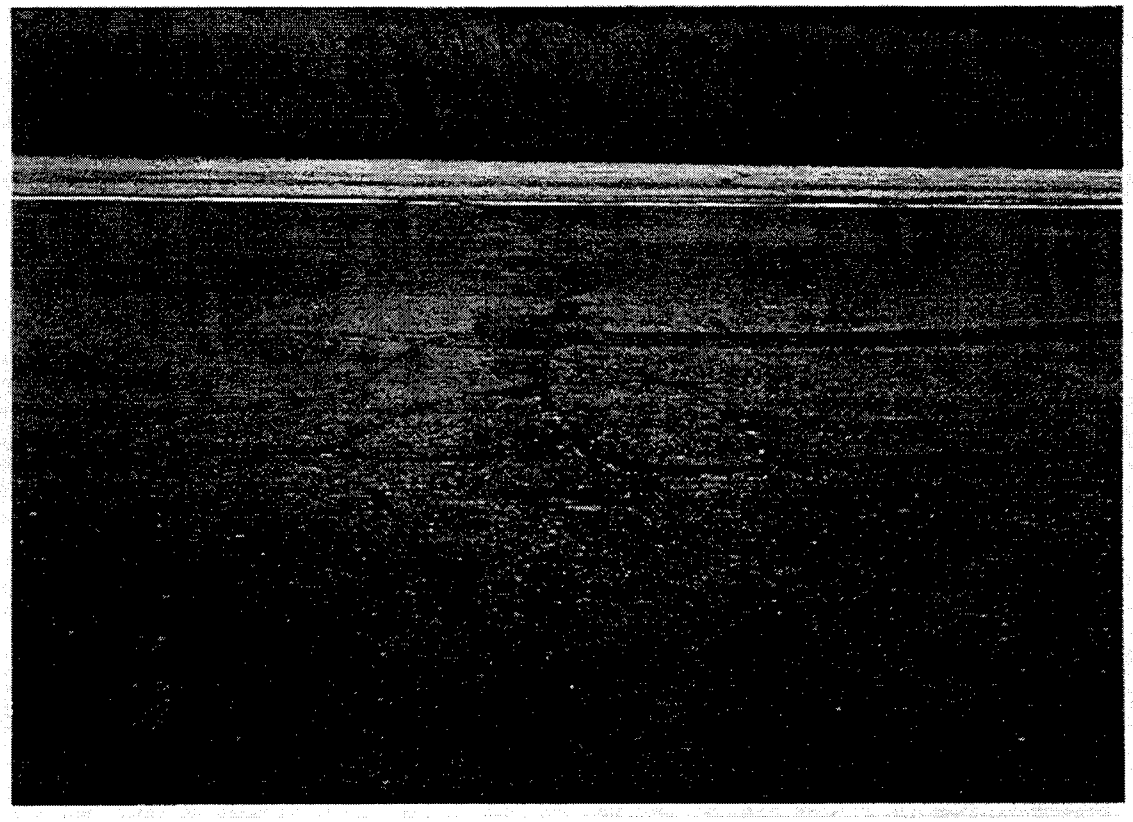

Figure 3.2.3 Transverse and Block cracks due to infiltration of water

4 SAMPLE COLLECTION

This research involved tests conducted using the dynamic shear rheometer, the rotational viscometer, and the bending beam rheometer. Binders from both the old and new pavements were obtained to perform these tests. Some binders were extracted from new pavement mixes, some were extracted from old pavement cores and some samples were obtained as liquid asphalt.

Since the previous paving of the highway occurred in 1983, there were only cores available for testing. Twenty of these cores were obtained from the storage at INDOT and used in this research. Unfortunately, that was all the material that was available from the old existing pavement. The only information that was known about the cores obtained were the mile markers and highway lane they were taken from. It was unknown if they were taken from the wheel-path or the center of the lane. Therefore, the samples were assumed to be random. These cores were 150 mm in diameter, and clearly showed the three layers of the pavement. Cores were taken where cracks had developed in the pavement. Out of the twenty cores examined, there was only one core that did not show any signs of failure. The procedure used to extract and recover the asphalt binder from these cores is discussed in the next section.

Due to the limited sampling from the existing pavement, the extracted binder was used very conservatively and cautiously to avoid waste of the material, and to be able to conduct as many tests as possible. In running tests on the binder that was obtained from these cores, they were treated as the equivalent of having been PAV-aged, since they were more than ten years old.

During the construction of the new pavement, arrangements were made with the engineer and contractor to collect samples of the material that was being placed on the highway. The contractor provided several pint-sized tins of tank asphalt, collected on a

variety of production dates. These samples were tested as original binder, aged and tested as RTFO materials simulating aging during processing at the hot mix asphalt plant and during paving operations, and aged again and tested as PAV materials, simulating aging of the binder during the service life of the pavement. The contractors also provided the research team with paving mixtures collected from the pavement during the paving process. According to the materials engineer from INDOT, a plate was placed on the pavement being paved and after the material was placed by the paver and the plate was lifted with the sample. For these mixtures, the asphalt was extracted from the mix using the same procedure that was used to extract asphalt from the cores of the existing pavement. Since binders in these mixtures have already undergone aging during paving procedures, they were treated as RTFO materials during testing. They were also aged using the PAV and tested again to simulate the expected in-service conditioning.

4.1 Review of Extraction and Recovery Procedures

For several years, research has been conducted on the various extraction and recovery procedures of asphalt binders. The purpose of this research was to develop an efficient method for extraction and recovery of binder that would not significantly alter properties of the material. The main concern in these studies was the potential for hardening of binder due to the solvent and temperature effects. Four publications (9,10,11,12) in the Transportation Research Record recently reported the results of these studies. A method had been developed during the SHRP program that produces more accurate results compared to other methods that have been traditionally used for these purposes. At the same time, a modified version of AASHTO T164 (Standard Method of Test for Quantitative Extraction of Bitumen from Bituminous Paving Mixtures) has also been tested and found to give results that are similar to those obtained from the SHRP procedure.

As already mentioned in this research, asphalt had to be extracted and recovered. The extracted and recovered materials were scheduled to be tested for viscosity, stiffness,

and creep rate (m-value). Therefore, it was important that the extraction procedure did not change the binder properties so that consistent and representative data on binder performance-related properties could be obtained. Some of the reasons that extraction techniques could possibly cause changes in binder properties are:

1. Asphalt is not completely extracted from the sample; it is believed that the strongly absorbed asphalt has significantly different characteristics;
2. Presence of residual solvent in the asphalt after recovery;
3. Solvent aging--hardening of the asphalt due to the reaction of asphalt with the solvent during the extraction and recovery procedures.

Many researchers had advised that the Abson recovery method (18), AASHTO T170-90, should not be used in the research as it may cause hardening of the asphalt and change the results of tests on the asphalt recovered due to the high temperature applied during the procedure. It was recommended that the SHRP procedure, adopted by the Asphalt Institute, should be used. As part of this research, the previously mentioned reports on the SHRP method and the modified version of AASHTO T164 (Method A) were reviewed and compared. Other comparisons were noted between using toluene and trichloroethylene (TCE) as a solvent, and using the Abson Flask and the rotary evaporator in the recovery process.

4.1.1 SHRP Extraction Procedure

The SHRP extraction and recovery apparatus is shown in Figure 4.1.1. It uses an extractor drum made of an aluminum pipe and discs, and consists of mesh screens to filter the aggregates. The drum is also fitted with four baffles to improve mixing. The sample and a solvent are first put through the extractor where the asphalt is dissolved and separated from the aggregates. The resultant solution is then filtrated on the coarse filter. The solution that passes the coarse filter is then run through the fine filter. The filtrate from the second filter is transferred to a recovery flask for the distillation of the solvent using a rotary evaporator, also known as the rotovapor in short, in an oil bath at 100°C.

The bath temperature is kept low to reduce the rate of solvent aging. The distilled solvent is recycled for use in subsequent washes of the sample. While the solvent is being distilled, more solvent is added to the extractor for a repeated wash of the aggregates. The wash time is increased from five to thirty minutes between the first and third washes, and then maintained for subsequent washes. After the third wash, the first flask is replaced by a new one. When the solution coming from the extractor is of a light brown color, the process of extraction is considered complete. The use of the second flask reduces the elevated temperature exposure time for the asphalt. The asphalt in the two flasks are mixed and poured into centrifuge flasks where the aggregate fines are centrifuged. This is known as the "two-flask method". A "single-flask method", with only one recovery flask can also be used.

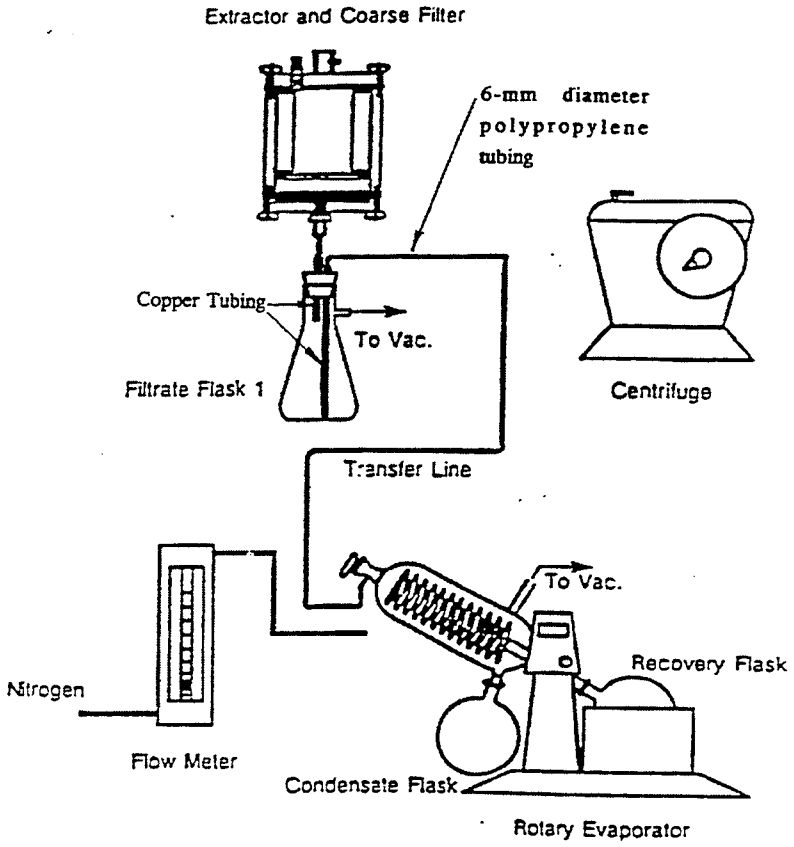

Figure 4.1.1 SHRP extraction and recovery apparatus (9)

4.1.2 AASHTO T164 (Method A) Extraction Procedure

The AASHTO T164-Method A (Quantitative Extraction of Bitumen from Bituminous Paving Mixtures) apparatus is a centrifuge bowl used to separate the coarser aggregates from the binder. Figure 4.1.2 shows the bowl that is used in the AASHTO T164 (Method A). The modified method A essentially follows the AASHTO T164 procedure, except that toluene is used as a substitute for TCE, ethanol is added in later washes, and more solvent is used compared to the standard procedure. Heated asphalt mixture is measured into the bowl and solvent is added to dissolve the binder. The contents of the bowl are centrifuged and the solution is collected in a container. More solvent is added to dissolve the binder, and this is repeated until the liquid that flows out of the centrifuge is a light straw color. In order to compare the method to the SHRP procedure on an equal level, eleven washes of the aggregates were needed as compared to about four to six washes in the standard procedure. The solution collected from this extraction is run through a high-speed fine centrifuge, which further removes finer aggregates from the solution. After the extraction is completed, the extract is recovered using the rotary evaporator in a procedure similar to that used in the SHRP method, except only one flask is used. All of the filtrate is collected in the flask until the extraction process is completed.

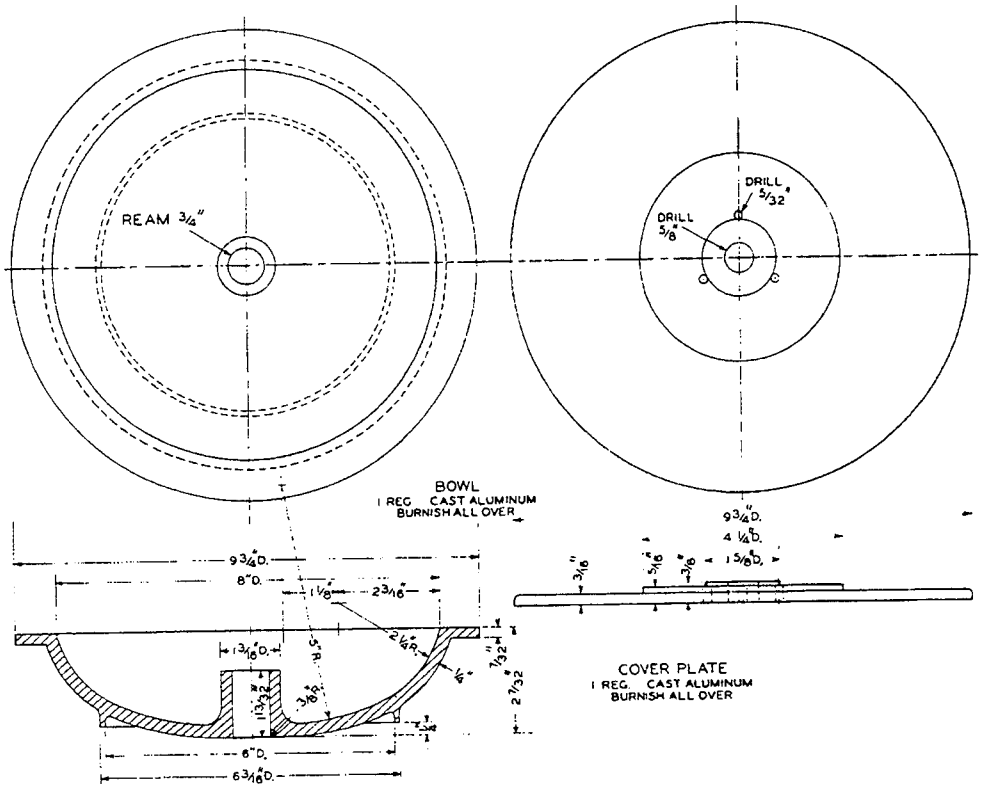

Figure 4.1.2 Bowl used in AASHTO T164-Method A (15)

4.1.3 Abson Recovery Method

As specified in AASHTO T170 (Recovery of Asphalt from Solution by Abson Method), the Abson method for solvent removal calls for distillation using CO_2 as a purging gas. A flask containing a solution of solvent and asphalt is electrically heated to boiling as shown in Figure 4.1.3. At this point, the solvent would evaporate, condense, and collect in a receiving flask. An initial flow of 100 ml/min. of CO_2 is started when the temperature reaches 135°C, and increased to 900 ml/min. when the temperature reaches 157-160°C. The flow rate and a temperature of 166°C are maintained for 10 minutes before the process is considered complete. A problem that comes up in the use of this

procedure is the difficulty in maintaining the constant high temperature. The reported drawback of this method when it comes to asphalt properties is that extended exposure to high temperatures could lead to a potential hardening of the asphalt binder. On the other hand, if the temperature is not set high enough, the solvent removal may be incomplete.

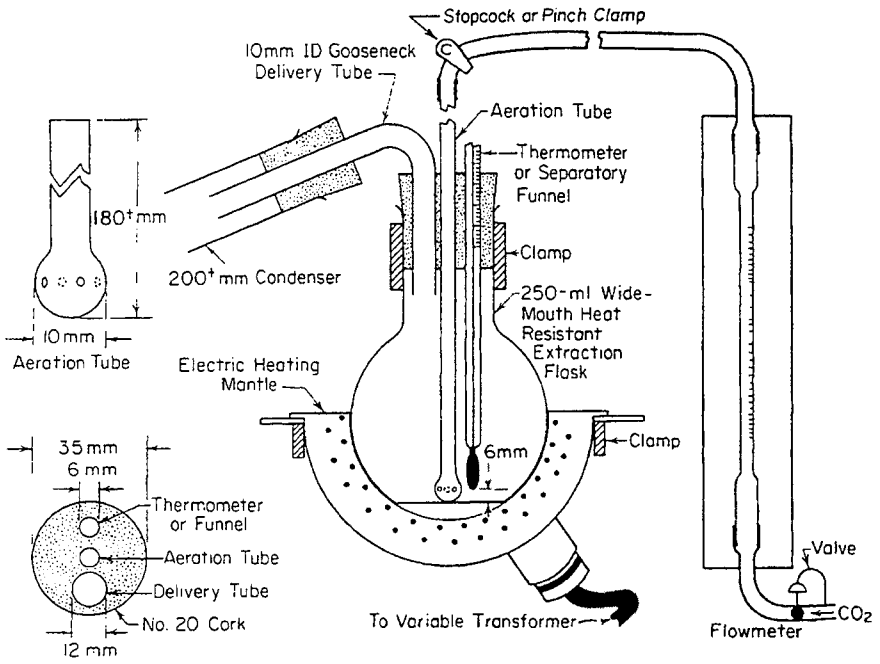

Figure 4.1.3 Apparatus set-up for Abson recovery method (18)

4.1.4 Rotary Evaporator Binder Recovery Method

The rotary evaporator (rotovapor) method uses a rotating evaporator device that mixes the solution and uses a vacuum and vent gas to vaporize and sweep the solvent away. This apparatus, compared to the Abson, can handle a larger volume of solution. The flask rotates in a heated oil-bath, and the flask containing a solution is attached to the rotovapor. Nitrogen gas is fed through a tube that touches the surface of the solution.

The flask rotates in the bath at a fixed speed, and a vacuum is applied with an increased gas flow when most of the solvent has been distilled. These conditions are maintained for a period of time before the process is ended.

After reviewing the methods of extraction and recovery, Burr, et al (9), concludes that the SHRP method is superior to all the other methods, but the tests conducted have also shown that the modified method A used in combination with the rotovapor recovery method appears to produce results that are very comparable to those of SHRP. The SHRP method results in little hardening of the asphalt binder, and the modified method A combination differed from those results by only about 4 percent. The precision of data obtained and the average viscosities of asphalt binders that resulted were also similar for both methods.

The reports (9,10,11,12) indicated that the Abson method of recovery produced greater residual solvent presence than the rotovapor method. The temperature at which the procedure was carried out, as well as the viscosity of the asphalt removed, affected the ability to remove the solvent completely. At lower viscosities and higher temperatures, asphalt removal occurred sooner. However, when the Abson method was used at its standard time and temperature, it left enough solvent to make a significant difference in the properties of asphalt binders tested. In addition to the hardening that took place during the recovery process due to the loss of volatiles, an increase in the temperature of the procedure would also lead to increased aging of the asphalt, regardless of the solvent used.

When addressing the issue of solvents to be used in separating the binder from the aggregates, the quoted reports point out that there is currently no solvent available that would be able to completely remove asphalt from the sample. For the solvents tested, TCE, TCE with the addition of 15 percent ethanol, toluene, and toluene with the addition of 15 percent ethanol, the differences in the efficiency in asphalt binder removal was not significant, especially after several washes. It was observed that using TCE with 15 percent ethanol was more effective than using toluene with 15 percent ethanol. When using TCE in method A, about two to four percent of the asphalt in the mix remained on the aggregates, but if 15 percent ethanol is added to the TCE in later washes, as in

modified method A, more of the asphalt was removed. Toluene with 15 percent of ethanol was somewhat less effective per wash in terms of the amount of asphalt removed, but given enough washes, it would extract an amount of asphalt comparable to that removed by TCE with 15 percent ethanol. TCE is a stronger solvent than toluene, and does have a greater hardening effect on asphalts recovered, but these effects can be minimized if certain precautions are taken and the solvents are thoroughly removed. If the rotovapor method is used in recovery, it also helps to reduce these negative effects to a minimum. In an experiment comparing the degree of hardening caused by the toluene and the TCE solvents used at two different concentrations, it was found that there were no significant differences. It seemed that the solvent hardening was more asphalt dependent than solvent dependent.

4.2 Extraction and Recovery Procedure

Based on the review presented in this research, the modified AASHTO Method A of extraction and the rotovapor method of recovery were selected for this project. The solvent used in the research was TCE, with the addition of 15 percent of ethanol after the third wash. The actual procedure used in this research consisted of the following steps:

1. Mixes and cores were heated to a point where they could be transferred into the extracting bowl.
2. Solvent was added and the aggregates stirred and then immersed for twenty minutes.
3. The aggregates and solvent were then centrifuged to drain the extract.
4. The procedure was repeated for at least six washes, but the time of immersion was much shorter after the first wash. Fifteen percent ethanol was added to the solvent after the third wash. This was done until the extract that flowed through was a light straw colour.

5. The extract was transferred to a high-speed fines centrifuge to separate the fine aggregates from the extract.
6. The final extract was heated and rotovapored in an oil bath with 600 mm Hg of vacuum fed through a tube into the flask.
7. When most of the solvent was distilled, 600 ml/min. of N_2 was fed into the flask until the process was completed. To reduce the hardening process of the asphalt binder, the temperature was kept relatively low, about 100°C, until most of the solvent was distilled.

At this point, the binder was transferred into individual tins where it was stored until test time.

4.3 Revision of Extraction and Recovery Procedures

Results of tests conducted on the binder from the new pavement mix obtained using the previously described method (Section 4.2) of extraction and recovery are reported in Section 6.1.1. The binder, which was considered an RTFO material, could not be classified according to Superpave standards, as it was too soft. These results indicate that some residual solvent may have been left in the binder after the extraction and recovery processes, and that these procedures needed to be revised to eliminate this problem. The next section describes the efforts to overcome the possible softening influences introduced by the extraction and recovery procedures.

4.3.1 Evaluation of Extraction and Recovery Process Variables

A series of experiments were performed to study the effects that the solvents, which were used in the extraction process and recovery procedure, have on a modified asphalt binder. The variables in the experiment were the solvent used, the temperature at which rotovapor recovery was executed, and the length of time that the rotovapor

continues to run after the solvent ceased continuous flow into the distillation flask. The experiment was conducted using combinations of the three variables, and the effect of the resulting changes was monitored by measuring viscosities of the resultant binder compared.

The binder used in this experiment was an original binder sampled directly from the manufacturer's tank. First 100 g of asphalt binder was poured into a tin and dissolved in 1000 ml of solvent. This solution is allowed to sit for one hour, at room temperature, to simulate the amount of time during which the solvent is in contact with the binder during the extraction process. Then, the solution was rotovaped until there was no observable constant dripping of the distilled solvent into the flask. At this point, the timer was started and rotovaping was continued for a set length of time. The binder which had not undergone any processing was used as a standard for comparison of the results. In total, 9 samples were tested, and the results are shown in Table 4.3.1 and illustrated in Figure 4.3.1.

Table 4.3.1 Results of Experiment to Study the Extraction and Recovery Procedures

Sample Description	Viscosity (Pa.s)
Original, unprocessed	0.7096
No solvent, 100°C, 120 min.	0.7342
No solvent, 130°C, 120 min.	0.7542
Toluene, 100°C, 60 min.	0.4900
Toluene, 100°C, 120 min.	0.5750
Toluene, 130°C, 60 min.	0.7333
Toluene, 130°C, 120 min.	0.8308
TCE, 100°C, 120 min.	0.6346
TCE, 130°C, 120 min.	0.8383

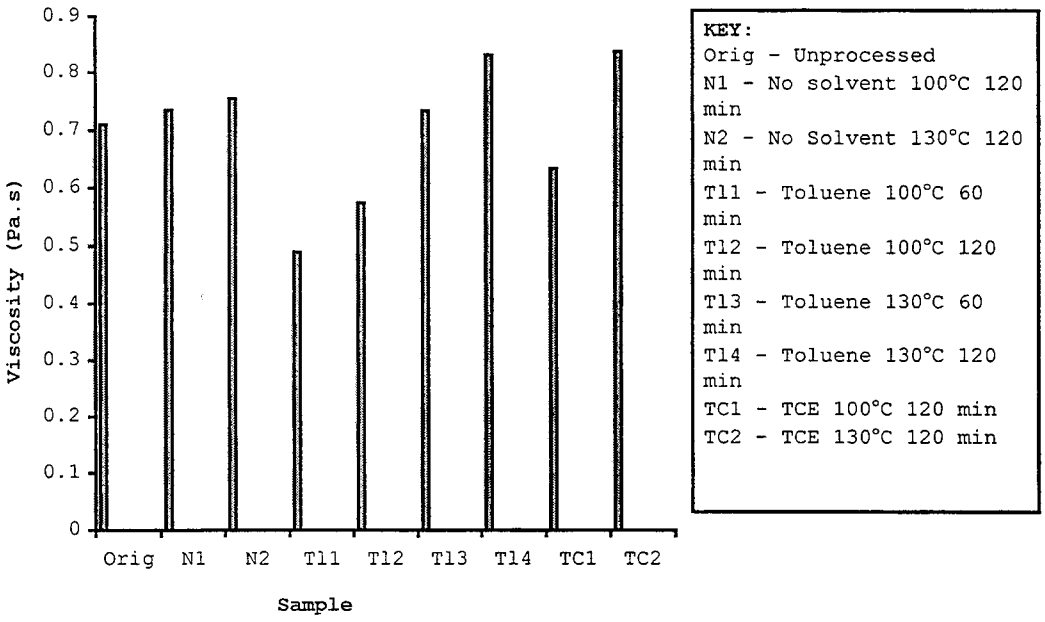

Figure 4.3.1 Viscosity Test Results of Experiment on Extraction and Recovery Procedures

From the results of the viscosity tests, it is observed that using toluene as a solvent and running the rotovapor at 130°C for an additional 60 minutes produced a result closest to the unprocessed binder, and therefore this procedure was adopted in the second series of extraction and recovery operations.

4.3.2 Revised Extraction and Recovery Procedures

Based on the results presented in the previous section, new procedures for extracting and recovering binder from the new construction mixes were selected. An outline of the readjusted procedure is as follows:

1. New pavement mix was heated to a point where it could be weighed into the extracting bowl.
2. Solvent (Toluene) was added and the mix was stirred and then left immersed in solvent for twenty minutes.
3. The aggregates and solution were then centrifuged to drain the extract, and more solvent was added to the mix.
4. The procedure was repeated for at least six washes, but the subsequent times of immersion were reduced two minutes. This was continued until the extract that flowed through was a light straw colour.
5. The extract was transferred to a high-speed fines centrifuge to separate the fine aggregates from the extract.
6. The final extract was transferred to a recovery flask and rotovapored in an oil bath of 130°C, under 600 mm Hg of vacuum until the distilled solvent stopped flowing into the collection flask.
7. The rotovapor was run for an additional hour from this point on, and Nitrogen was introduced for the last thirty minutes of the procedure.
8. When the process was completed, the binder was transferred into a storage tin. Individual tins of binder samples were then combined and homogenized by mixing, and divided into smaller samples for testing.

Results of tests on binder obtained from the modified procedure are reported in Chapter 6.

5 TEST PROCEDURES

For this research, binder tests conducted included the Dynamic Shear Rheometer test, the Bending Beam Rheometer test, and the Rotational Viscometer test. In order to run these tests, some samples also had to be aged to simulate the various stages of conditioning experienced by the pavement material when in service. This was done by placing the samples in the Rolling Thin Film Oven (RTFO) to simulate aging of the binder during construction operations, and the Pressure Aging Vessel (PAV) to simulate binder aging while in service.

This chapter gives summaries of these test and aging procedures.

5.1 Rolling Thin Film Oven

The Rolling Thin Film Oven (RTFO) aging is a method used to simulate the aging of asphalt that occurs during mixing and construction operations. This is an ASTM specified procedure, ASTM D-2872. The set-up used in this test is shown in Figure 5.1.1.

About thirty-five grams of binder is weighed into each of up to eight RTFO bottles. Sometimes two bottles are set aside to measure the mass quantity of volatiles lost from the asphalt during the aging process. The RTFO bottles are set in the oven, one bottle in each hole of the carriage. The carriage rotates at a rate of 15 rpm at 163°C while a jet of air is blown into each bottle when it is at its lowest position in the oven. The samples are aged in the oven for 85 minutes.

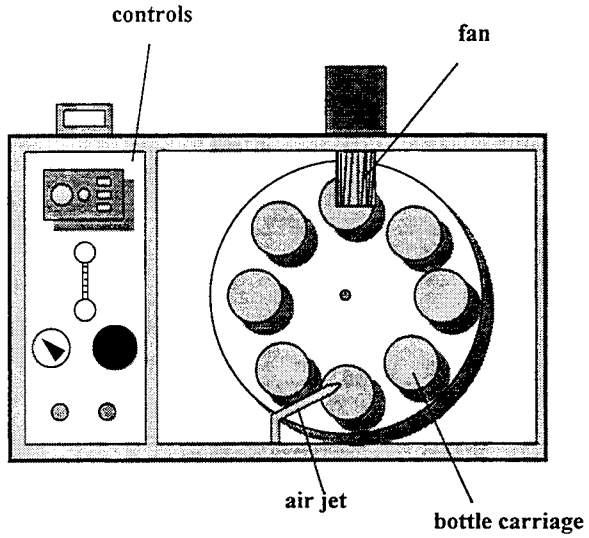

Figure 5.1.1 Rolling Thin Film Oven (3)

5.2 Pressure Aging Vessel

The Pressure Aging Vessel is used to simulate the effect of aging of the asphalt binder when it is in service in the pavement. The schematic of the PAV is shown in Figure 5.2.1.

PAV pans with 50 grams of RTFO materials are weighed and placed on a holder that carries up to ten pans. The PAV oven is preheated to a temperature of either 90°C, 100°C, or 110°C, depending on the design climate. The holder carrying the pans is then placed in the oven, and the oven is allowed to recover the heat lost during the pan placement. Once the heat has been recovered, the binder materials are pressure-aged in air for 24 hours at the selected temperature at 2.07 MPa.

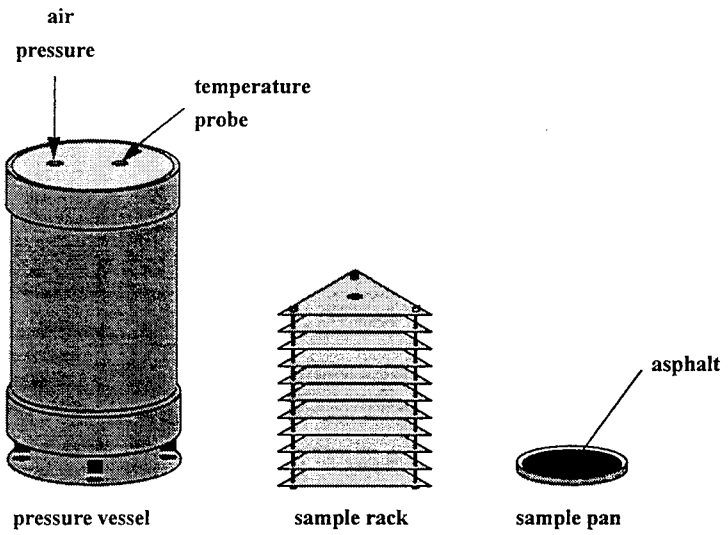

Figure 5.2.1 Components of the Pressure Aging Vessel (3)

The PAV procedure has strict requirements. After the vessel has been placed in the oven, it has to return to the test temperature within 2 hours, and if, during aging, the pressure changes more than 0.5 MPa or the temperature deviates more than 2°C, then the aged binder should not be used for further testing.

5.3 Dynamic Shear Rheometer Test

The Dynamic Shear Rheometer(DSR) is used to determine the complex shear modulus (G*) and phase angle (δ) of the asphalt binder. The complex shear modulus is a measure of total resistance of binder to deformation with repeated pulses of shear stress. The phase angle (δ)is the measure of recoverable and non recoverable deformation.

To run this test, a sample of the asphalt binder in the form of a thin disk is placed between the plates of the DSR. There must be an adequate amount of material between those plates, one of which oscillates.

First the samples of binder to be tested are heated till they are fluid enough to pour. Then they are poured into a mold and cooled. While the material is being cooled, the gap between the plates is set. To test an original unaged binder or an RTFO aged material, the gap should be set at one millimeter and the plates used are twenty-five millimeters in diameter. For a PAV aged material, an eight-millimeter set of plates is used and the gap is set at two millimeters. An extra fifty microns is added to the gap at first.

When the material has been cooled, it is carefully transferred to one of the plates, and the two plates are brought together. Excess asphalt is removed using a trimmer. When that has been done, the extra fifty microns is removed, and the plates readjusted.

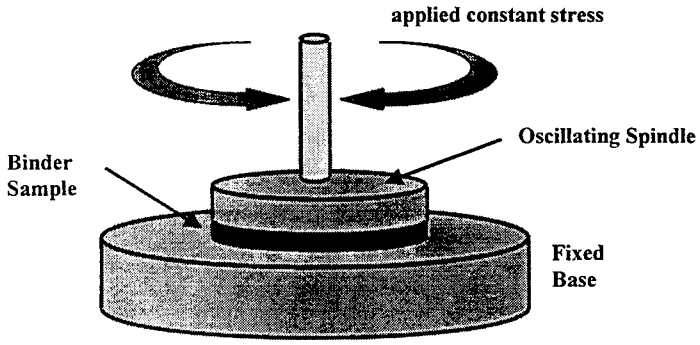

Figure 5.3.1 Plates of the Dynamic Shear Rheometer (3)

During the test, the plates and the sample are submerged in water that has been set at the required test temperature. One plate oscillates, see Figure 5.3.1 and the relationship between the applied torque and the resultant rotation allows the calculation of G* and delta, δ.

According to Superpave specifications, a given binder passes the requirements for a certain grade when it has a minimum $G^*/\sin\delta$ value of 1 kPa for an original binder, a

minimum G*/sinδ value of 2.20 kPa for an RTFO residue material, and a maximum G*sinδ value of 5,000 kPa for a PAV aged binder.

5.4 Bending Beam Rheometer Test

The Bending Beam Rheometer(BBR) test is used to determine the stiffness(s) and the creep rate(m-value) of the asphalt binder. The stiffness is a measure of how much the asphalt resists a constant loading and the creep rate is a measure of the change in this resistance over time (3). This test is performed at low temperatures.

First the sample is heated until it is ready to pour. It is then poured into a rectangular mold, 6.25 mm wide, 125 mm long, and 12.5 mm thick. It is then cooled for about 45 to 60 minutes, and the excess asphalt binder is trimmed from the surface. After the trimming, the specimen remains in the mold at room temperature for no longer than 2 hours before it is cooled in a freezer for demolding. The beam of asphalt binder is then placed in the bath, which has been set at test temperature, for sixty minutes. At the end of the sixty minutes, the beam is ready to be tested.

After a series of initial load conditioning steps, the actual test involves applying a 980 mN load to the beam for a total of 240 seconds. The deflection of the beam is measured as a function of time and computer software calculates creep stiffness and creep rate after 60 seconds of loading, Figure 5.4.1. The Superpave specification requires that the stiffness does not exceed 300 MPa, and a minimum of 0.300 is required for the m-value. Both values have to be met simultaneously.

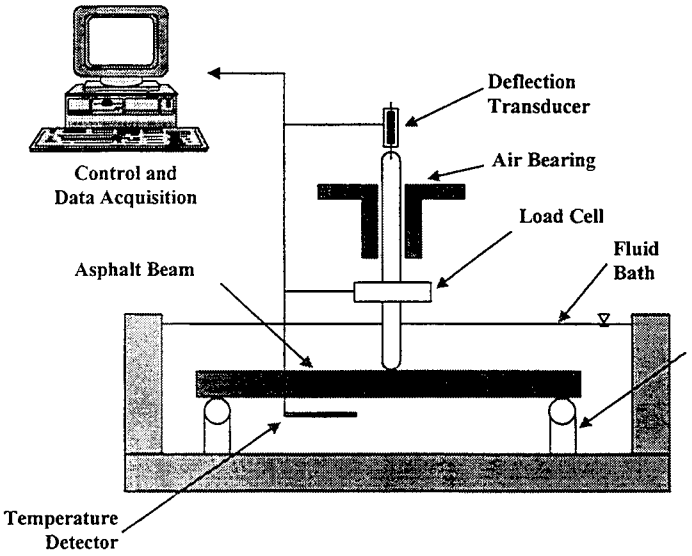

Figure 5.4.1 Set-up of Bending Beam Rheometer (3)

5.5 Rotational Viscometer

The rotational viscometer measures pumpability of an asphalt binder. This method is described in ASTM D-4402, "Standard Test Methods for Viscosity Determination of Unfilled Asphalts Using the Brookfield Thermosel Apparatus".

For testing, asphalt binder is heated until it is fluid enough to be poured. About 8 grams of asphalt is weighed into the sample chamber and the sample chamber is placed in a heated container. A spindle is lowered into the asphalt binder. Once the temperature stabilizes at 135°C, a torque is applied to the spindle, Figure 5.5.1, and the viscometer measures the total torque required to maintain a specified speed of rotation.

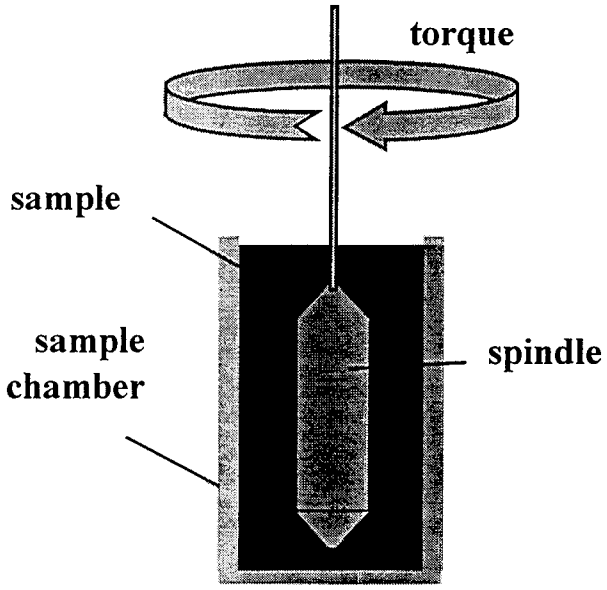

Figure 5.5.1 Rotational viscometer (3)

6 TEST RESULTS AND DATA ANALYSIS

This chapter reports the results of the tests conducted on the binder obtained from the pavement mix from the new construction, and on binder obtained from cores collected from the existing pavement.

The materials were tested at various temperatures based on the extent of aging that has occurred and the extent of aging that was simulated.

6.1 Results for New Pavement Materials

The "new pavement" asphalt binder was obtained in two forms:

1. Binder extracted from mixes collected from the pavement during construction,
2. Binder obtained directly from the manufacturing plant (tank asphalt).

Both forms of binder were tested to verify their PG-grading and to obtain their properties for comparison with the binder extracted from the cores of the existing pavement. Also, to verify that the tests were performed in the correct manner, results for the tank asphalt were obtained from INDOT lab tests and compared to those obtained by the research team.

6.1.1 Binder Extracted from New Pavement Mix

The binder material from the mix was separated from the mix aggregates through an extraction and recovery procedures described in Chapter 4. The material from this collection of samples was initially tested at high temperature using DSR. This material was considered to be and was tested as an RTFO material because it had undergone the

initial aging during the construction process. The samples obtained from individual extractions were assumed to be of equal quality and were not combined prior to DSR testing. However, due to the fact that not all of the solvent was removed from these samples during the recovery process the quality of samples was not uniform and that led to significant scatter of the test results. To correct this problem, extraction and recovery procedures were modified (as described in Section 4.3) and the DSR testing was repeated. For this new series of tests, the samples recovered from individual extractions were combined prior to testing to assure more homogeneous samples.

The first series of DSR tests were performed at 52°C, 58°C, and 64°C, and the complete set of results is presented in Table A1 of Appendix A. Table 6.1.1 shows the average results of these tests. The results show that this material could not be classified using the Superpave specifications. Under the Superpave system of classification, a binder is classified at a certain grade when its G*/sinδ value is less than 2.20 kPa when tested at that temperature but fails that criteria at a lower temperature. As can be seen from the results, this material meets the criteria down to 52°C although it was originally specified as a PG 64-34, meaning that it should have passed the requirement at 64°C but should have failed at 58°C.

Table 6.1.1 Average Results of DSR Test on RTFO-Aged Binder Extracted from Construction Mix (First Run)

% Asphalt = 6.9			
Temperature	G* (kPa)	Delta, δ (°)	G*/sinδ (kPa)
52°C	1.88	68.38	2.03
58°C	1.15	72.76	1.10
64°C	0.60	78.53	0.61

After adjusting the extraction and recovery procedures, the binder obtained from the mix through these processes was tested at 58°C, 64°C, and 70°C. The complete

results of these tests are shown in Table A2 of Appendix A. Table 6.1.2 shows the average values of these results. As can be seen, this binder passes the Superpave specifications at 64°C because it meets the required G*/sinδ value of 2.20 kPa at 64°C, but fails this requirement at 58°C.

Table 6.1.2 Average Results of DSR Test on Binder Extracted from Construction Mix (Second Run)

Temperature	G* (kPa)	Delta, δ (°)	G*/sinδ (kPa)
58°C	3.98	65.03	4.39
64°C	2.10	66.93	2.29
70°C	1.24	69.47	1.32

The material extracted from construction mix was also pressure-aged in the Pressure Aging Vessel (PAV) and tested again on the DSR at intermediate temperatures 16°C, 19°C, and 22°C. This pressure-aged material was also tested at a low temperature, -24°C, in the BBR equipment. The average test results for the first and second series of DSR tests on the PAV material are shown in Tables 6.1.3 and 6.1.4 respectively. Complete results are shown in Tables A3 to A6 in Appendix A.

Table 6.1.3 Average Results of PAV-Aged Mix Material (First Run)

m-value at -24°C = 0.322 Stiffness at -24°C = 223 MPa	
Temperature(°C)	19
G* (kPa)	1,082
Delta, δ (°)	36.08
G*sinδ (kPa)	625

Table 6.1.4 Average Results of PAV-Aged Mix Material (Second Run)

m-value at -24°C = 0.318 Stiffness at -24°C = 257 MPa	
Temperature(°C)	19
G* (kPa)	3,499
Delta, δ (°)	46.55
G*sinδ (kPa)	2,539

6.1.2 "New" Binder Collected from Manufacturer's Tank

The original asphalt binder obtained from the manufacturer was first tested in the DSR at high temperatures, 54°C, 64°C, and 70°C. A rotational viscometer test was also conducted on this material. The binder was then aged in the RTFO to simulate aging during construction operations. The RTFO material was then tested in the DSR at the same high temperatures. Finally, the material was pressured aged in the PAV, and tested in the DSR at intermediate temperatures, 16°C, 19°C, and 22°C, and in the BBR at

-24°C. Average results from these tests are tabulated in Table 6.1.5 and the complete data can be found in Tables A11-A14 in Appendix A.

Table 6.1.5 Average Test Results for Tank Asphalt Binder

Flash Point = 230°C Rotational Viscosity = 0.647 Pa.s Average Percent Change in RTFO Residue = 0.398 % m-value at -24°C = 0.305 Stiffness at -24°C = 305 MPa				
	Temp Passed	G* (kPa)	Delta, δ (°)	Dynamic Shear (kPa)
Original	64°C	1.06	71.20	G*/sinδ = 1.12
RTFO Residue	64°C	2.06	66.86	G*/sinδ = 2.27
PAV	19°C	2,452	48.47	G*sinδ = 2,133

6.1.3 INDOT Test Data

The Indiana Department of Transportation had conducted the same test routines on asphalt binders obtained from the manufacturer. To compare and verify the accuracy of the tests run for this research, results from INDOT tests were obtained, and tabulated in Table 6.1.6. INDOT lab only conducted tests on original (unaged) asphalt, so only these results were used in the comparison.

Table 6.1.6 Average INDOT Test Data

Flash Point = >230°C Rotational Viscosity = 0.734 Pa.s Percent Change in RTFO Residue = 0.311 % m-value at -24°C = 0.302 Stiffness at -24°C = 247 MPa			
	G* (kPa)	Delta, δ (°)	Dynamic Shear (kPa)
Original	1.11	71.45	G*/sinδ = 1.17
RTFO	2.33	66.51	G*/sinδ = 2.54
PAV	3,010	48.10	G*sinδ = 2,235

6.2 Existing Pavement Materials

The asphalt binder from the existing old pavement was obtained by extracting from the cores collected from the pavement using the extraction and recovery procedure described in Chapter 4. Since the pavement had already been in service for more than ten years, the material was considered as having undergone natural aging equivalent to PAV aging. DSR and BBR tests were first conducted on this material to obtain its properties as a PAV-aged material, then the binder was pressured aged in the PAV, and additional low temperature tests (BBR) were conducted. The first series of tests were run to obtain properties needed for Superpave (PG) classification. The second series of tests were run to determine if there were any indication that the stiffness of a material would reach a limit after which no further aging would occur.

The extracted asphalt binder was tested in the DSR at intermediate temperatures, between 7°C and 28°C at increments of 3°C, with the 8-mm discs and a 2-mm gap. All test results for binder extracted from the cores are presented in Tables A15 to A22 in Appendix A. Examination of these tables reveals that the results are highly variable. Table 6.2.1 shows the average results of DSR tests for which the standard deviation of the

data is less than 20 percent. It should be noted that the binder used in the surface layer was an asphalt emulsion. The results of these tests will be further discussed in Section 6.3, Data Analysis.

Table 6.2.1 DSR Data for Binder from Cores from In-Service Existing Pavement

	Base Layer	Binder Layer	Surface Layer
% Asphalt	4.5 %	5.0 %	6.1 %
Temperature Passed	25°C	25°C	1°C
G* (kPa)	10,356	9,341	6,267
Delta, δ (°)	29.98	36.70	40.00
G*sinδ (kPa)	4,854	4,851	4,005

This section also presents the results of the BBR tests that were conducted on the naturally aged (assumed PAV-aged) material to obtain the properties at low temperatures. Table 6.2.2 shows these BBR results and the temperatures they were obtained at. Table 6.2.3 shows the data obtained from the testing of the binder after additional PAV-aging. From these results, the base and intermediate binders would have been classified as PG 64-22 binders under the Superpave system.

Table 6.2.2 BBR Data of Core Materials from Old Pavement (Naturally Aged, Assumed PAV-Equivalent)

	Base Layer	Binder Layer	Surface Layer
Temperature Passed	-12°C	-12°C	-6°C Did Not Pass
m-value	0.372	0.319	0.272
Stiffness (MPa)	59	96	70

As seen in Table 6.2.2, the binder from the surface layer could not pass the required criteria (minimum m-value of 0.300) at -6°C. The temperature of -6°C was the highest temperature at which this material could be tested, as the material became too flexible at 0°C. The material from the surface layer was an asphalt emulsion, and there is currently no knowledge of whether asphalt emulsions can be tested and classified based on the same criteria as the regular binder.

Table 6.2.3 Results for Asphalt Binder from Old Pavement which Underwent Additional PAV-Aging

	Base Layer	Binder Layer	Surface Layer
Properties at -6°C :			
m-value	0.255	0.243	Unable to Test
Stiffness (MPa)	157	73	
Properties at -12°C :			
m-value	0.210	0.243	Unable to Test
Stiffness (MPa)	262	73	

As mentioned before, the surface layer was an asphalt emulsion. After having undergone PAV-aging, it became very sticky and soft. The samples could not be separated from the plastic strips that were part of the BBR mold assembly, and therefore no BBR tests could be conducted on the material.

6.3 Data Analysis

As mentioned before in Section 6.1.1, some errors occurred in the preparation of test samples, leading to tests producing results which were inconsistent. Consequently, the extraction and recovery procedures were evaluated and adjustments were made to ratify the errors.

The results obtained on binder from the second series of tests (after adjustments to extraction and recovery procedures) were much more uniform than the corresponding results from the first series of test. This is very evident from Figure 6.3.1 that shows the deviation of the results from the average, for the first and second series of tests respectively. The line shown on the graph indicates the average value of the dynamic shear, $G^*/\sin\delta$.

It appears that the observed high variability of data from the first series of tests as well as the lack of conformance to Superpave specification could be attributed to the presence of residual solvent in the recovered binder and the fact that samples were not combined before DSR testing.

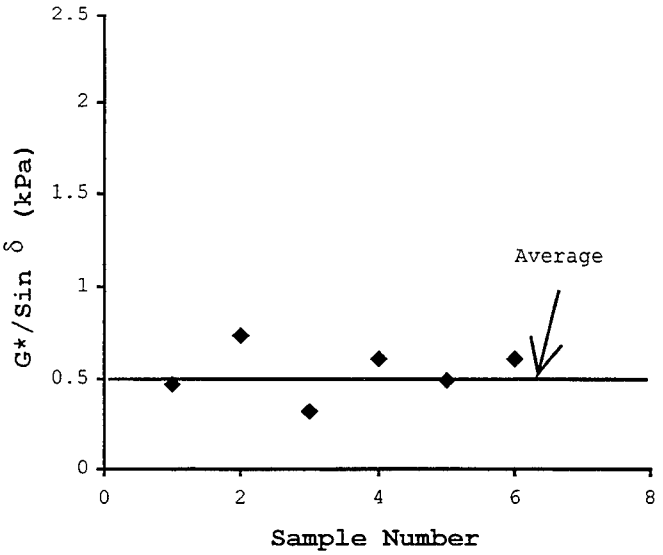

(a) DSR Test Results (First Run)

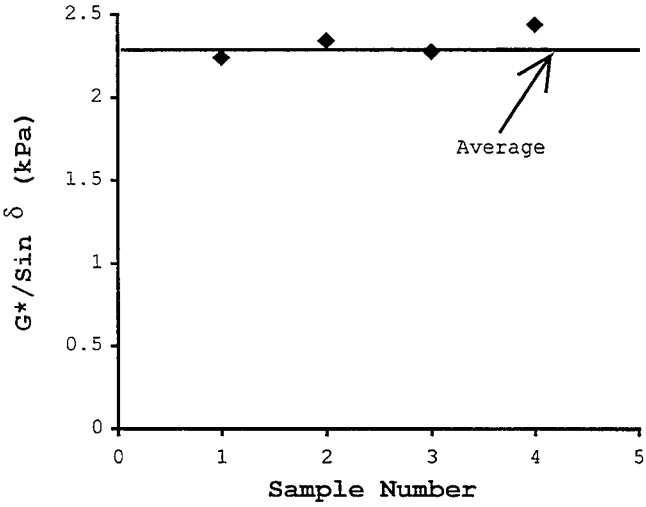

(b) DSR Test Results (Second Run)

Figure 6.3.1 Data Distribution of DSR Tests at 64°C, Before and After Adjustments to Extraction and Recovery Procedures

In order to verify the accuracy of the tests performed by different operators, a comparison was made between the results of tests on tank asphalt conducted by the research team and those by the INDOT lab technicians. Figures 6.3.2a and b show the comparison of the DSR results and Figures 6.3.3a and b show the BBR results. As seen from these figures, the results for the tank asphalt obtained by the research team were very close to those that were obtained at the INDOT lab, with differences ranging between 3 and 11 percent. This good agreement between data obtained by different operators indicated that the observed variability of the results represents real differences in the material properties rather than an operator-related inconsistencies in the test protocols.

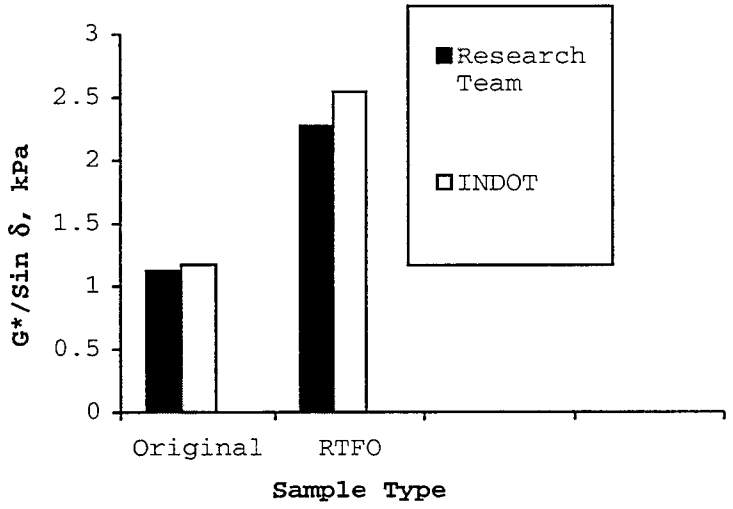

(a) High Temperature DSR Test

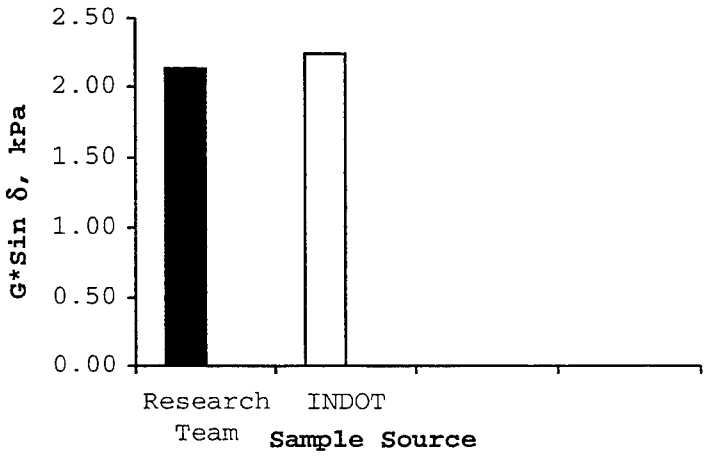

(b) Intermediate Temperature DSR Test

Figure 6.3.2 Comparison of Dynamic Shear Values for Different Sample Types and Operators.

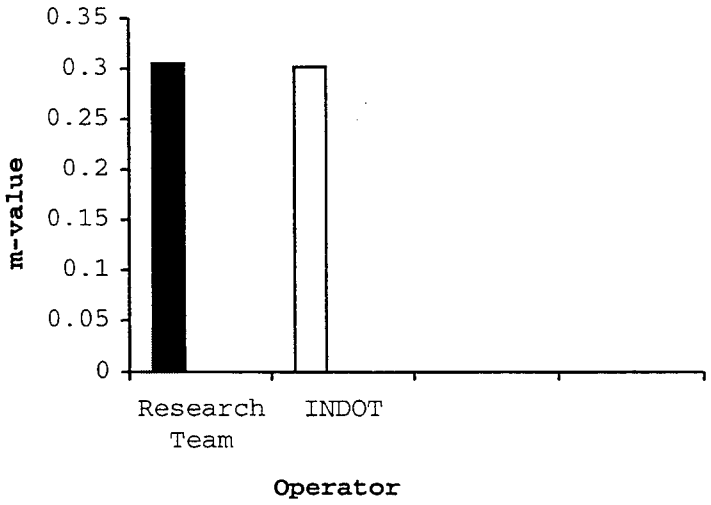

(a) m-value

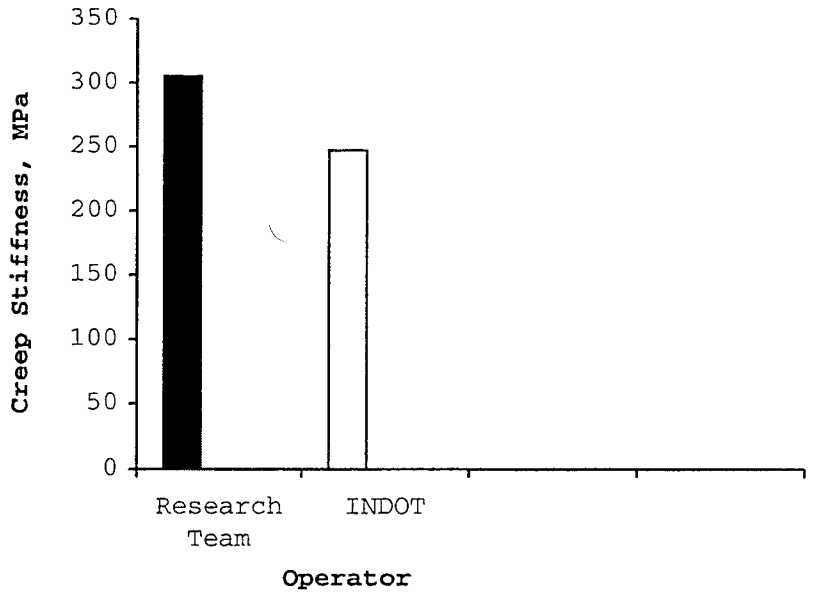

(b) Creep Stiffness

Figure 6.3.3 Comparison of Low Temperature Test Results for Different Operators.

Results from tests performed on binder extracted and recovered after adjustments were made to the procedures were compared to those obtained from tests on the tank asphalt binder (binder obtained from the manufacturer's tank). This series of tests was performed in order to verify the actual grade of asphalt used in the construction of a new pavement. The binder from the new pavement mix was first compared to tank asphalt which was RTFO-aged, then this mix binder was aged in the PAV and compared with similarly aged tank asphalt. The comparisons can be seen in Figures 6.3.4 a, b, c, and d.

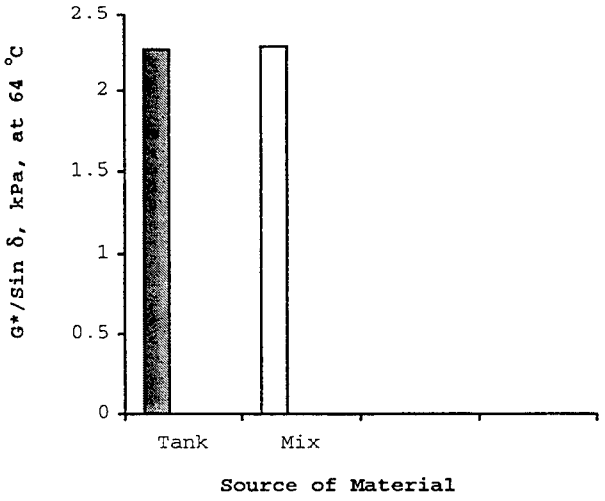

(a) High Temperature DSR Test on RTFO-Aged Binder

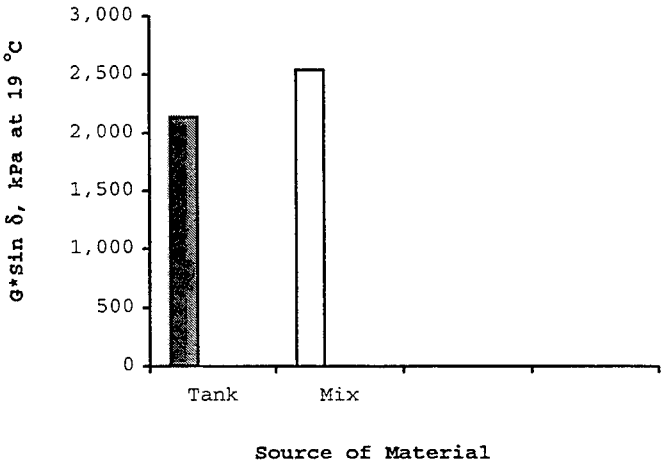

(b) Intermediate Temperature DSR Test on PAV-Aged Binder

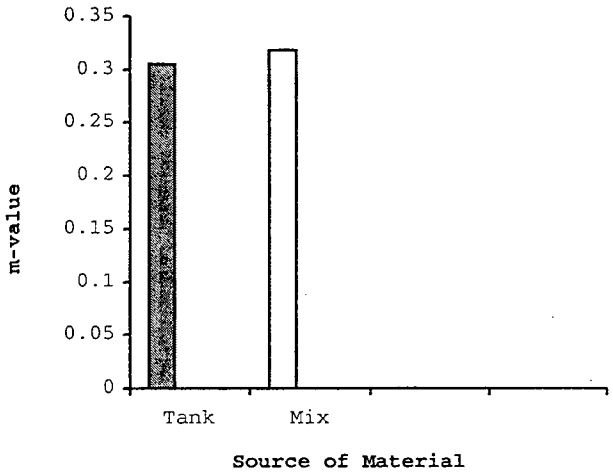

(c) m-value, PAV-Aged Binder

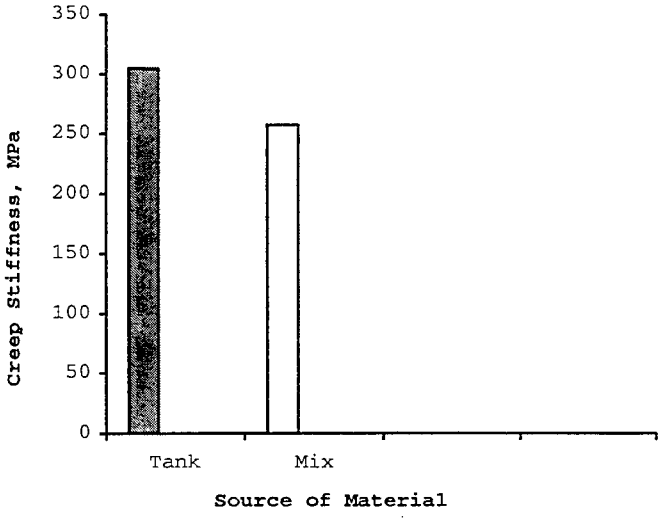

(d) Creep Stiffness, PAV-Aged Binder

Figure 6.3.4 Comparison of Test Results Based on Source of Material.

From these charts, it can be seen that the binder from the manufacturer's tank compares very well to the binder that was extracted from the mix used during construction. The differences in the results of tests on the RTFO-aged binder were insignificant. The results from the two sources of material differed by 0.7 percent. This conforms to expectations, since the RTFO is supposed to simulate the aging that occurs in the binder up to the point when the mix is laid on the pavement. The differences in the in the intermediate and low temperature test results on the PAV-aged materials ranged between 4 and 16 percent. Although these differences are higher, they are still insignificant and can be attributed to a small extent to the different operators and equipment used.

As mentioned in Section 6.2, the tests initially performed on binder extracted and recovered from old pavement cores produced results of very high variability. Figures 6.3.5 a, b, and c illustrate the extent of that variability of test results in each layer at the temperature where the average DSR results satisfied Superpave criteria. Figures A15-A22 in Appendix A show the inconsistencies observed at all test temperatures.

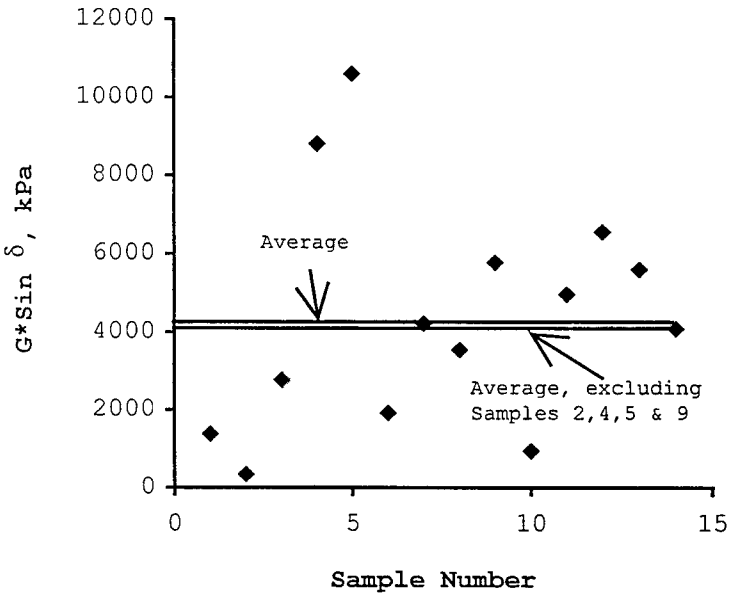

(a) Surface Layer

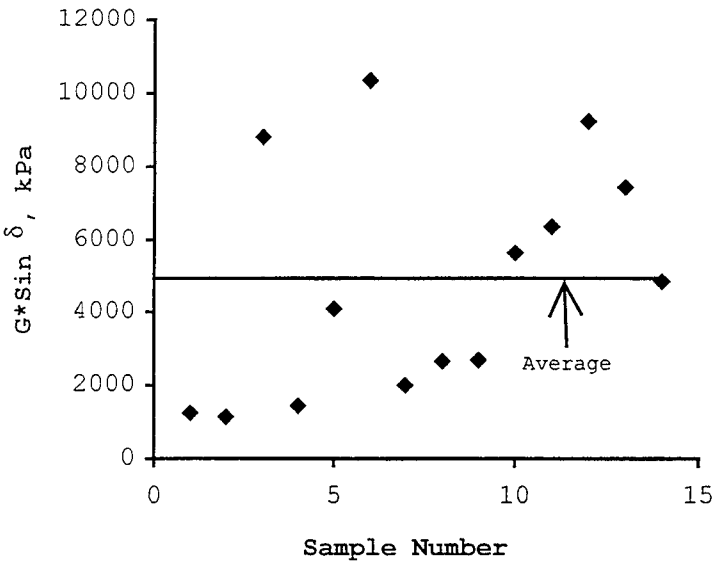

(b) Intermediate Layer

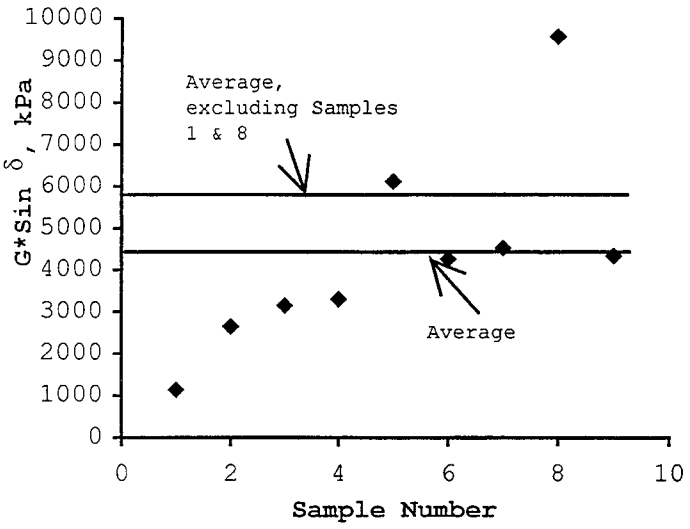

(c) Base Layer

Figure 6.3.5 DSR Test Results for Old Pavement Binder.

Although the binder was extracted from cores obtained from the same pavement, the G*sinδ values differed by as much as 20,000 MPa. A few possible sources of these inconsistencies are described below.

One of the possible sources of the observed variability may be the inconsistencies related to the extraction and recovery procedures themselves. Since the extracted material was not combined before testing but rather was assumed to be of the same quality, any variation in binder properties resulting from the extraction and recovery process will be directly reflected in the test results. Unfortunately, due to limited amount of the material recovered from the old pavement, it was not possible to confirm this theory by additional testing.

Due to the high numbers of parameters that can be adjusted during the extraction and recovery procedures, the process of retrieving asphalt from the mix may be a source of variability of the test results. The experiment conducted to make comparisons among extraction procedures using different solvents, temperatures of rotovapor oil bath, and times of extraction (see Chapter 4) showed that these factors do indeed affect the properties of the material obtained. The results of the experiments were reported in Section 4.3 and illustrated in Figure 4.3.1. All these experiments were performed on tank asphalt, and therefore do not give any indication of whether materials from different sources and at different extents of aging would experience comparable levels of sensitivity to solvent effects. In particular, the binder from the new construction mix has different characteristics than the binder from the base and intermediate layers of the old pavement, the effects of the extraction and recovery procedures on properties of the binder cannot be readily separated and evaluated. Therefore, even though the results show that there is approximately a 380 percent change in the dynamic shear value of the new mix binder before and after adjustments were made to the procedures, it would be unrealistic to apply the same proportional change to the old pavement materials. This would lead to unreasonable results and PG classification of the material would not be possible.

Yet another source of variability may be the origin of the cores itself. No records were available as to the exact location of the cores (that is, driving lane versus passing

lane or wheel path versus centre of the lane). It is also possible that some of the cores were taken from the sections of the pavement that were more extensively cracked than the others and therefore the binder from these cores may have been more aged. The lack of records prevented the development of any potential correlations.

Using the averages of data with standard deviations of less than 20 percent, a comparison was made between the base and intermediate layer binders of the old pavement, and the tank asphalt from the new construction which was aged in the PAV. Figure 6.3.6 shows the results of this comparison. The chart indicates that there is a great difference between the material which was previously used in the pavement and that which is currently in place. That difference is of the order of several thousand kilopascals.

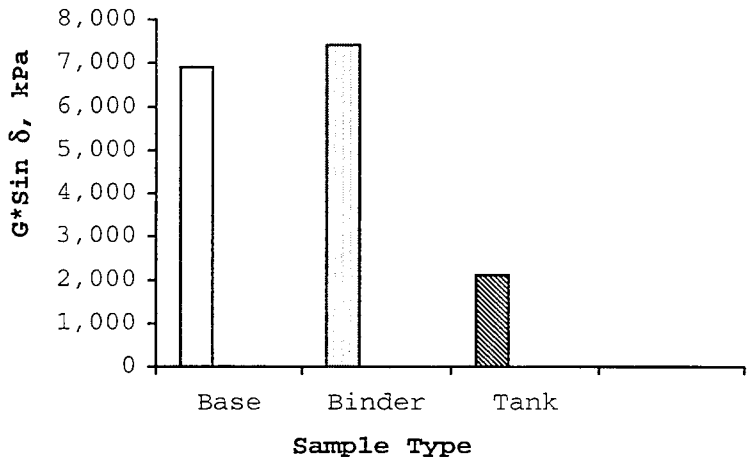

Figure 6.3.6 Shear Properties of Old (Base and Intermediate) and New Tank Binder

Finally, the evaluation was made as to the effects of additional PAV aging on the material that was previously assumed to be PAV-aged equivalent due to in-service exposure. For this purpose the material extracted from old pavement mixes was further PAV-aged. The results of tests for both naturally-aged and naturally-aged plus PAV-aged material are presented in Figures 6.3.7a and b.

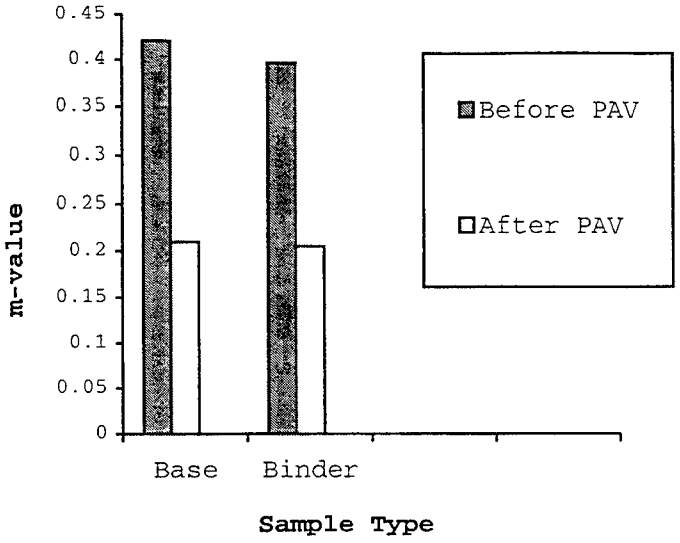

(a) m-value

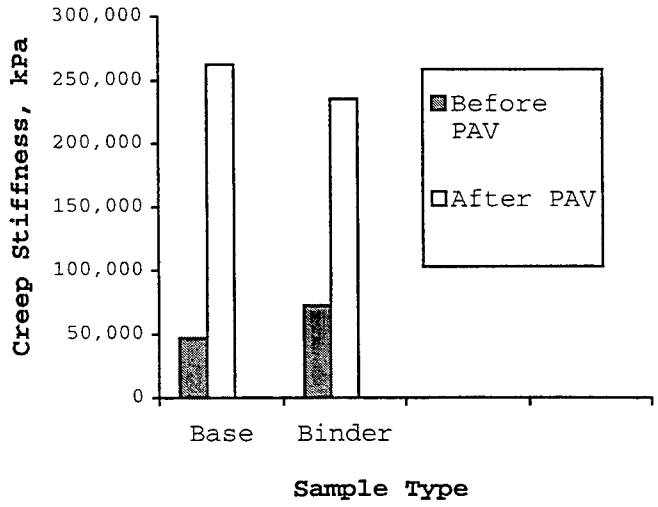

(b) Creep Stiffness

Figure 6.3.7 Comparison of Low Temperature Parameters for Old Pavement Materials Before and After PAV Aging.

Comparisons were only made for the results from the binder and base layers, as stickiness of the material from the surface layers made it impossible to conduct the BBR test. It is clear that for both layers, stiffness of the material has increased quite significantly after it was put through further aging, while the creep rate (m-value) decreased. This shows that for this particular binder, the stiffness limit had not been reached during the field exposure. The PAV simulates binder aging after ten years of service. The old pavement used in this project had been in service for fourteen years at the point of sampling. Another observation from this comparison is there was a significant increase in the stiffness of the material measured before and after the binder underwent additional aging in the PAV. This may suggest that the PAV does not accurately simulate the aging that occurs in the binder during the service life of the pavement.

7. PAVEMENT INSTRUMENTATION

A field monitoring station was installed in the newly constructed section of I-64 near the Indiana State Road 57 interchange. The station will be used to monitor the influence of environment on the performance of the pavement. Data collected by the station will allow for evaluation of the pavement's low temperature cracking resistance and will be used to verify the temperature algorithm of the Superpave model.

The environmental parameters measured by the station include pavement temperature at several depths, air temperature, relative humidity, wind direction and speed, and solar radiation. A combination of thermistors and thermocouples were used for temperature measurements. For redundancy, two sets of thermocouples and one set of thermistors were installed in the pavement. Some sensors were installed on the instrument tower located on the side of the road. The output from all the sensors is collected by the CR10X data acquisition unit also installed on the tower.

7.1 Installation Plans

Figure 7.1.1 shows the original installation plans proposed to and agreed upon by INDOT. The installation involved excavating, after the intermediate asphalt layer has been laid, a 60 cm by 60 cm instrumentation hole in the middle of the lane up to 1 m in depth. A steel conduit 5 cm in diameter was pushed from the side of the road into the hole. The installation of the sensors was performed in two stages. The details of installation are presented in subsequent sections. After installation of probes was completed, the instrumentation hole was filled with Portland cement concrete.

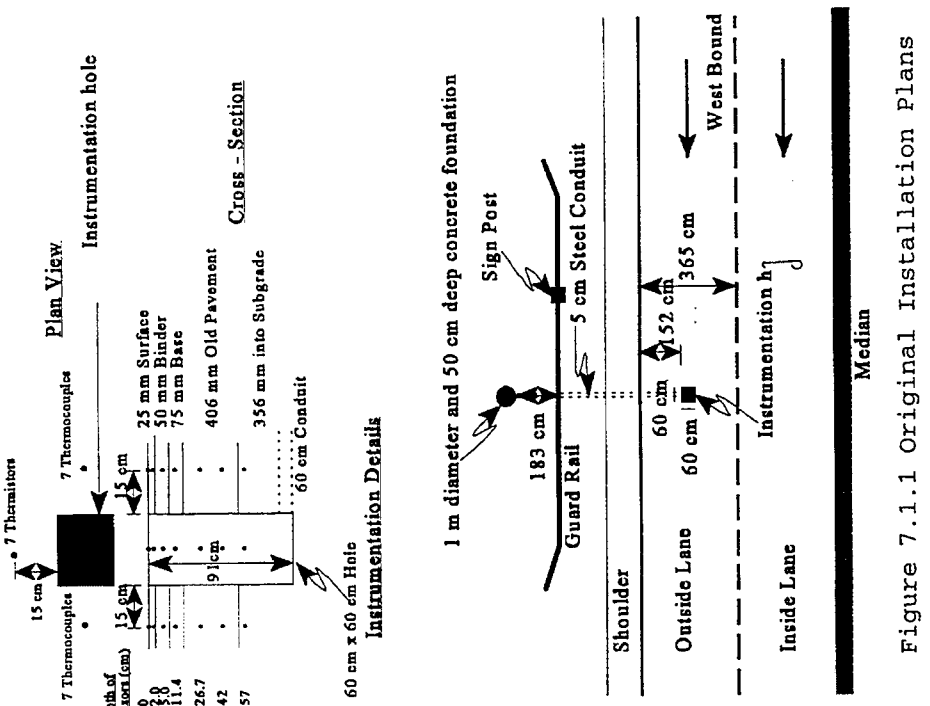

Figure 7.1.1 Original Installation Plans

First, all the sensors up to level of the intermediate asphalt layer were installed. The sensors to be located at the surface and at the depth of 20 mm were buried in a steel box that was installed flush with the intermediate asphalt layer. This box was then paved

over with the surface mix. After the surface paving operation was completed, a block of the surface layer was removed exposing the steel box. The sensors were removed from the box and installed in the pavement. Hot mix asphalt was then used to fill the previously removed block of surface layer.

All sensors and equipment to be installed on the tower were checked in the laboratory before installation. The wind sentry was found to be damaged, and was sent back to the company for repair. It was successfully fixed and installed on the tower.

7.2 Details of Pavement Temperature Sensors Installation Procedure

7.2.1 Installation of Lower Layers (up to the Intermediate Asphalt Layer) Sensors

In preparation for temperature sensors installation, 60 cm by 60 cm by 1 m deep hole was excavated in the driving lane of the pavement as shown in Figure 7.2.1.1. Two sets of thermocouples referred to as East and West were installed on the east and west sides of the hole. In addition, one set of thermistors was installed on the north side of the hole. Each set of these sensors was composed of seven sensors covering the hole depth, at the targeted depths, as shown in Figure 7.1.1. At the targeted sensor location, a mark was made at the appropriate side of the hole. A portable gasoline powered generator was used to power a drill to drill a horizontal hole 15 cm into the side of the excavation. The process was repeated for each sensor with the exception of all sensors to be located at the depths of 20 and 0 mm. Figure 7.2.1.2 shows the thermistors at their drilled locations. Figure 7.2.1.3 shows the thermocouples inserted in their drilled holes. The probe holes were sealed using silicone to prevent moisture infiltration from the concrete that was used to fill in the hole. Figure 7.2.1.4 shows all three sets of probes at their locations.

Figure 7.2.1.1 Instrumentation Hole

Figure 7.2.1.2 Installed Thermisters

Figure 7.2.1.3 Installed Thermocouples

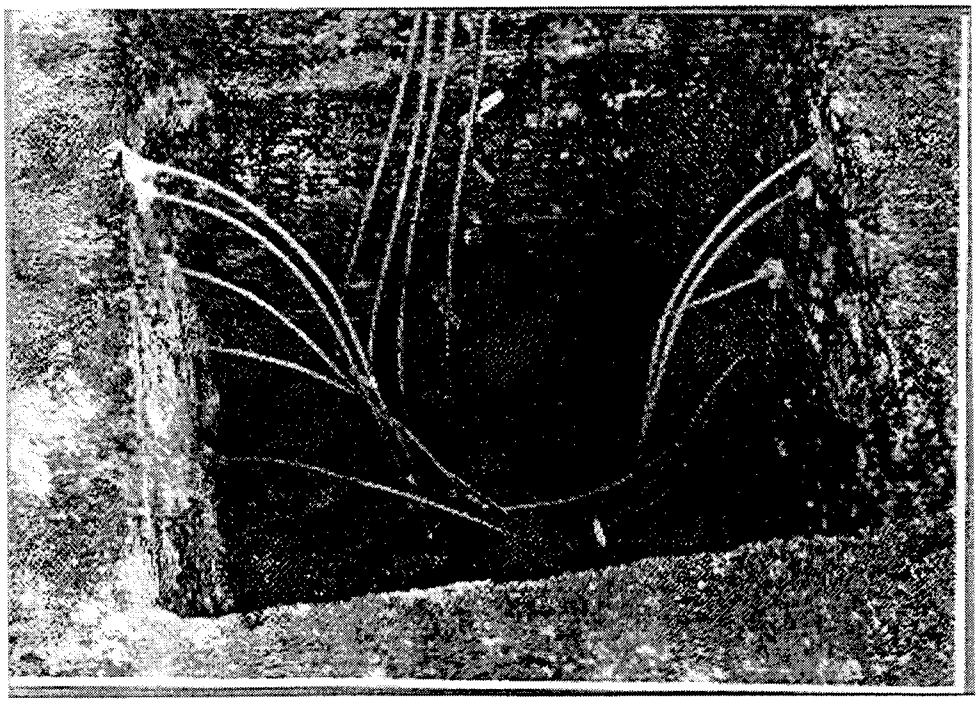

Figure 7.2.1.4 Installed Sets of Probes

Plastic (PVC) pipes were cut in half and used to hold and protect sensor cables in the hole, as shown in Figure 7.2.1.5. The sensors to be located at 20 mm and 0 mm depths were temporarily placed in a steel box to be buried in the concrete, as shown in Figure 7.2.1.6. After this, a concrete truck was called to the site and the hole was filled up with Portland cement concrete up to the surface of the intermediate asphalt layer. The steel box was laid flush with the surface, as shown in Figure 7.2.1.7.

7.2.2 Installation of Surface and 20 mm Pavement Temperature Sensors

The steel box location was referenced by two points in the road ditch using a measuring tape. The surface and 20 mm sensors installation was scheduled after the surface layer was paved over the hole, and for a day where the surface layer paving was taking place so that after installation, the hot asphalt and compactors would be available on the site.

In preparation for installation of the surface and 20 mm sensor, the steel box was located first using the reference points. A gasoline concrete saw was used to cut a block of surface layer of pavement around the steel box. The box was found fairly accurately, as shown in Figure 7.2.2.1. The steel box cover was unscrewed and the sensors and cables were pulled out, as shown in Figure 7.2.2.2. For the 20 mm sensors, a measurement was taken, and a 15 cm long horizontal hole was drilled in the side wall of the opening, as shown in Figure 7.2.2.3. For the surface sensors, a sloping trench was cut with the concrete saw that would allow locating the probe's tip (sensing part) at the surface while keeping most of the probe and cables below the surface. This trench was filled with epoxy resin in such a way that only the tip of the sensor was exposed at the pavement's surface, as shown in Figure 7.2.2.4. The cables were wrapped with tape several times to protect them from the asphalt.

After completing the installation, the box lid was put back. An asphalt tack coat was sprayed on the surface of the pavement in the block. A small amount of surface mixture was heated as shown in Figure 7.2.2.5. The asphalt was spread to cover the hole

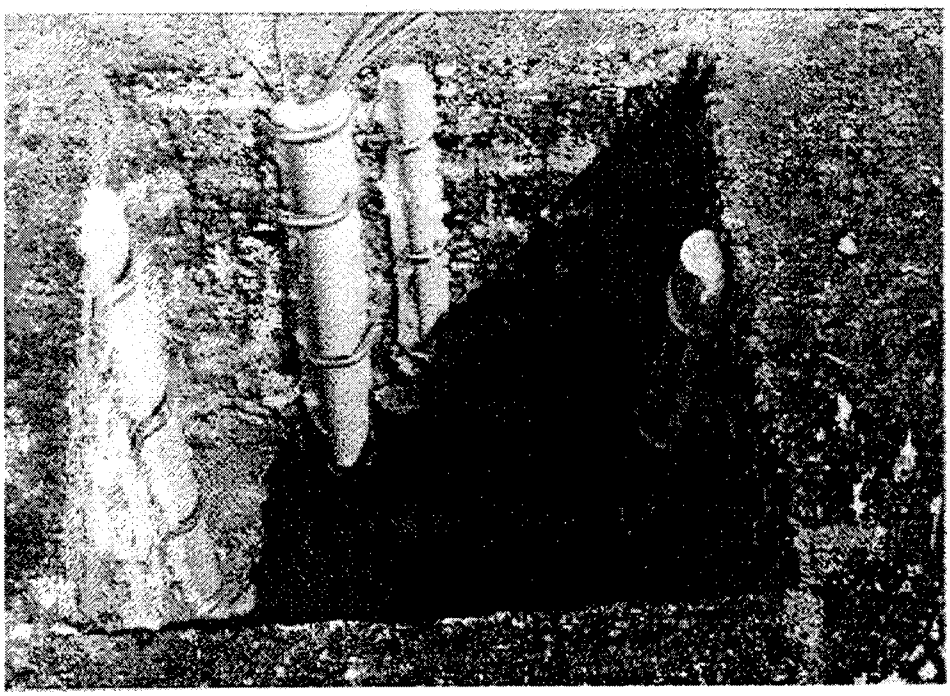

Figure 7.2.1.5 PVC Pipes Covering the Installed Probes

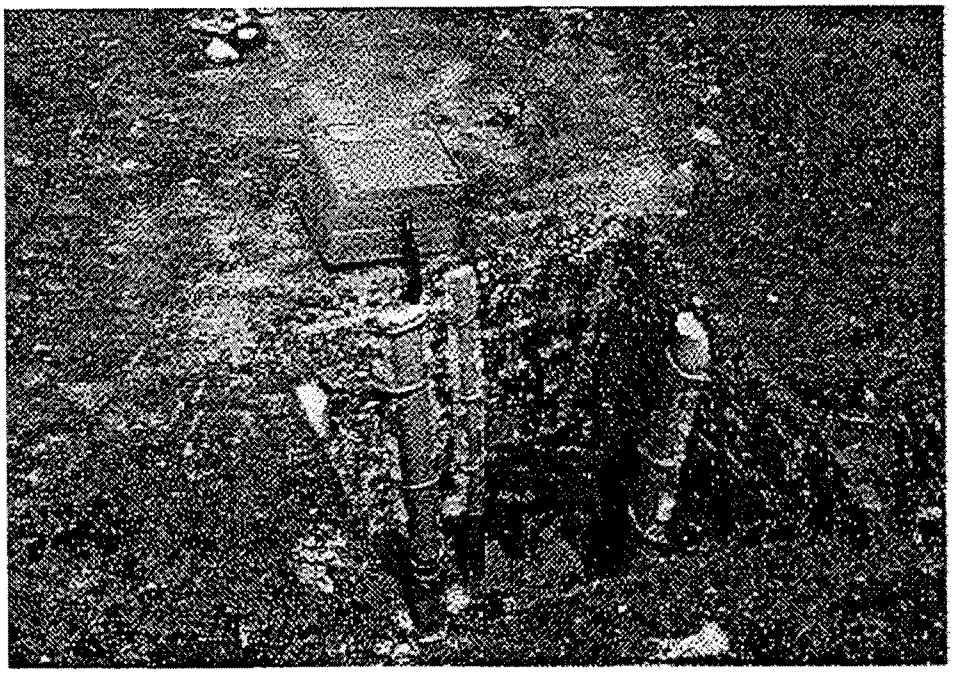

Figure 7.2.1.6 Steel Box Containing 0 and 20 mm Sensors and Cables

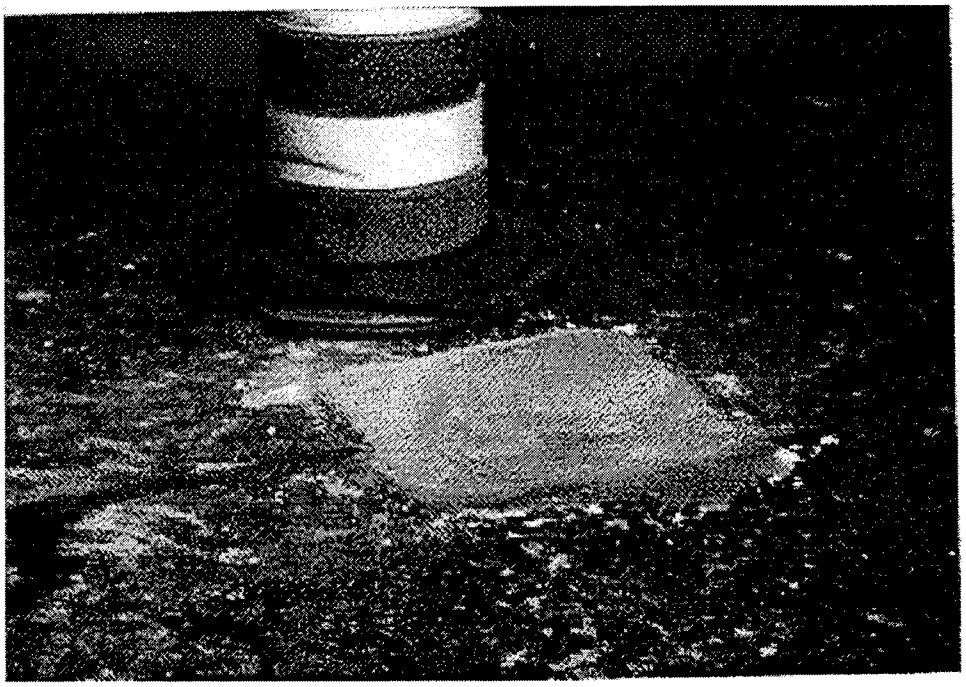

Figure 7.2.1.7 Hole Filled with Concrete with the Steel Box in Place

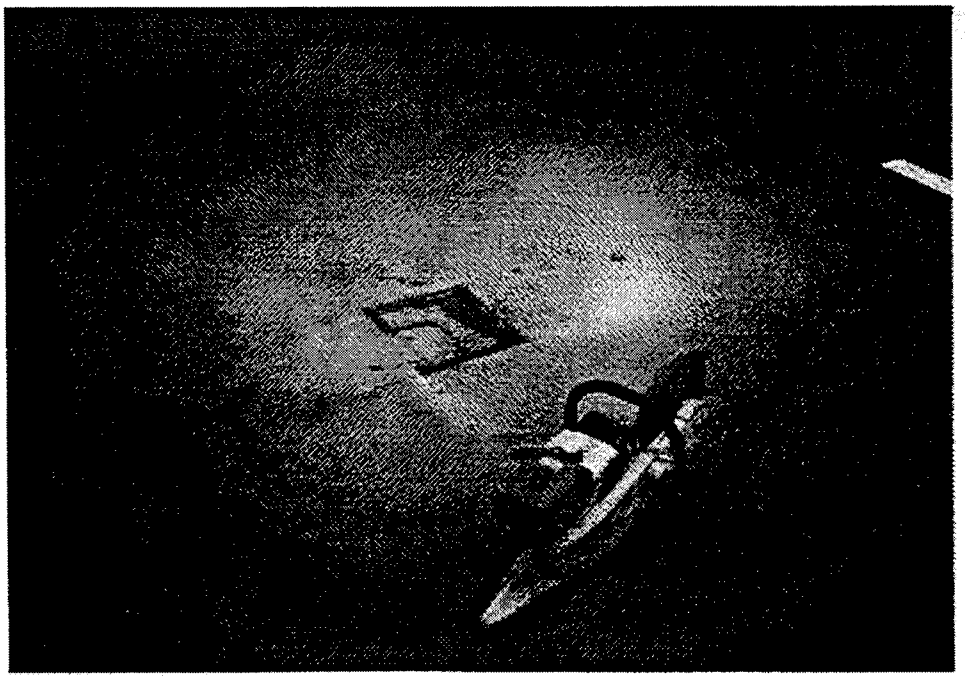

Figure 7.2.2.1 Steel Box Located and Asphalt Block Cut to Uncover the Box

Figure 7.2.2.2 Pulling the 0 and 20 mm Sensors Out of the Box

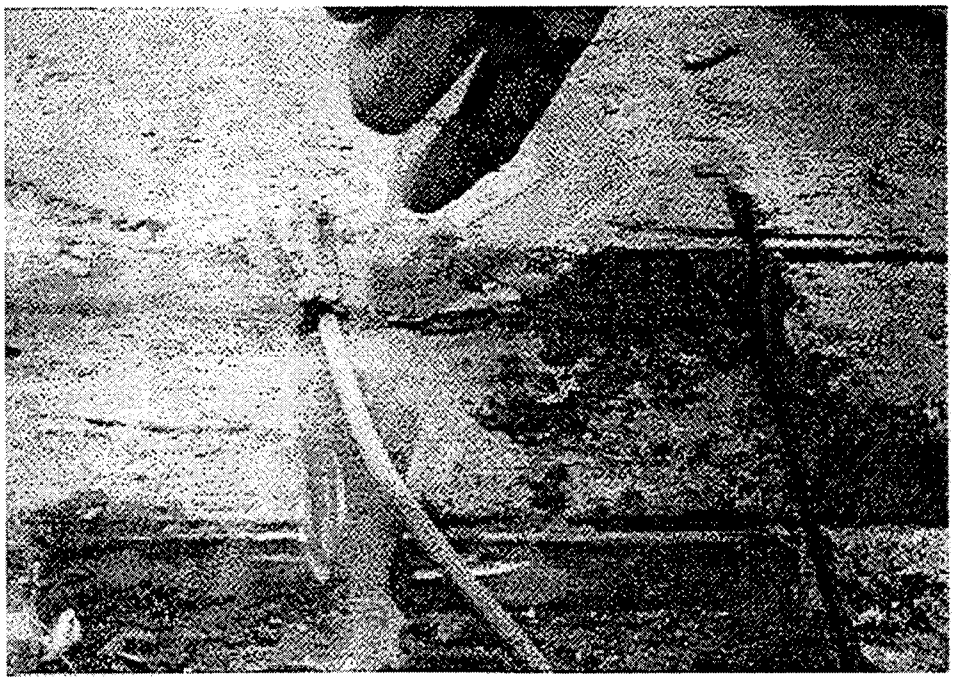

Figure 7.2.2.3 Installing a Thermocouple at 20 mm Depth

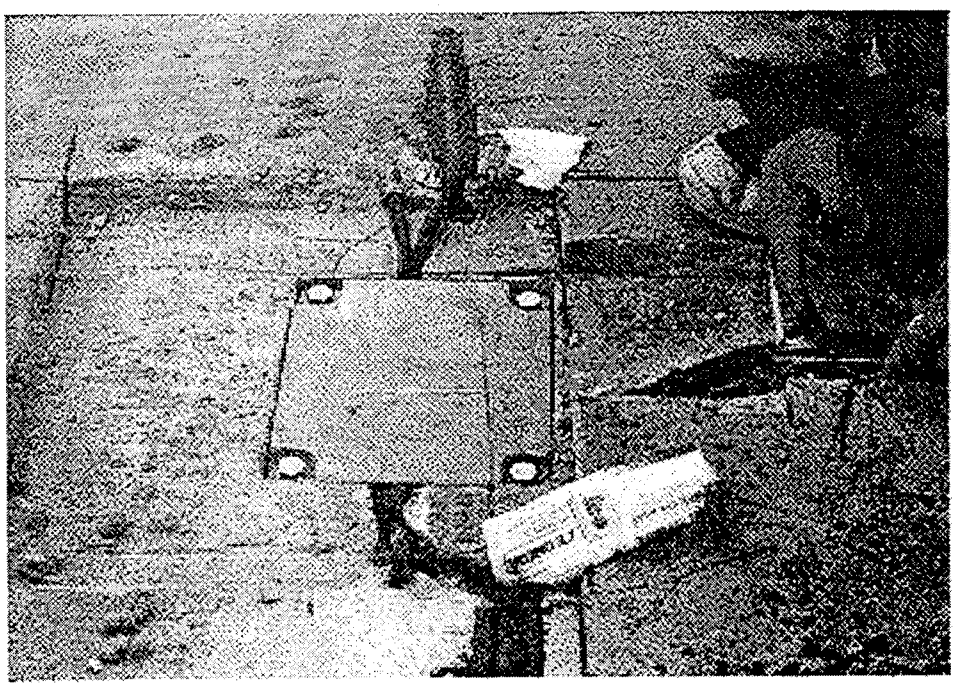

Figure 7.2.2.4 Installing the 0 mm (Surface) Sensor

Figure 7.2.2.5 Heating Up the Asphalt Mixture

Figure 7.2.2.6 Spreading Out the Heated Asphalt Mixture

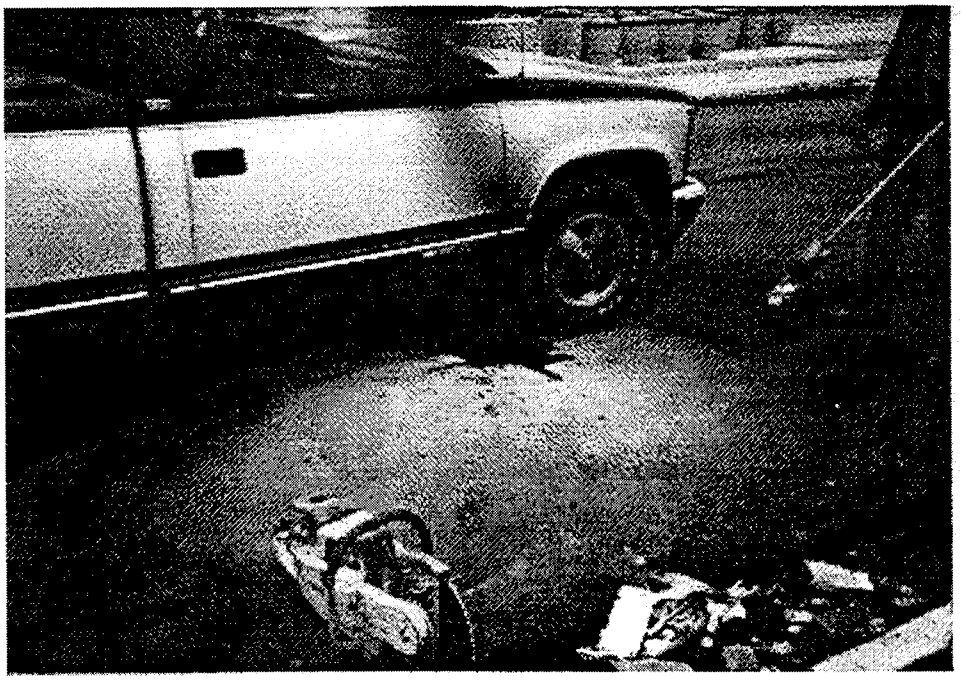

Figure 7.2.2.7 (a) Compacting the Backfilled Asphalt

Figure 7.2.2.7 (b) Compacting the Backfilled Asphalt

as shown in Figure 7.2.2.6. A truck tire and a roller were used to compact the mix in the hole, as shown in Figure 7.2.2.7.

7.3 Sensors Actual Location

The actual location of the pavement sensors varied slightly from the targeted location. All actual locations were measured and recorded. Table 7.3.1 shows the targeted and actual locations for all three sets of sensors.

Table 7.3.1 Location of Thermistor Probes and Thermocouples

Sensor Number	East Thermocouple	Thermistor	West Thermocouple
1	0.0 cm	0.0 cm	0.0 cm
2	2.5 cm	2.5 cm	2.5 cm
3	6.25 cm	6.25 cm	5.63 cm
4	12.5 cm	26.9 cm	11.25 cm
5	26.25 cm	26.88 cm	26.25 cm
6	42.25 cm	41.25 cm	41.25 cm
7	56.75 cm	56.25 cm	56.25 cm

7.4 Tower and Data acquisition system installation

A concrete foundation of about 1 m in diameter and about 50 cm deep was poured on the side of the road. The tower base was attached to the foundation with anchor bolts buried in the concrete. Figure 7.4.1 shows the leveling of the tower base. At a subsequent visit to the site, the tower was erected on the base. The solar radiation sensor was placed at the top of the tower and leveled in place. The air temperature sensor radiation shield was placed on one of the posts of the tower. The cellular phone antenna was placed at the top of the tower, and oriented towards the closest cellular tower which was about 16 km from the site. The solar panel was mounted on the south side of the tower and oriented to obtain maximum exposure to the sunlight (about 48°C from the horizontal plane). The data acquisition box was mounted at a reachable height on the tower. The sensor cables were routed from the end of the steel conduit via PVC pipes and elbows to the data acquisition box. The completed tower with the equipment on it is shown in Figure 7.4.2.

The data acquisition box contains CR10X data logger, AM416 multiplexer, DC112 modem and a Motorola transceiver. Sensors and operating devices were connected, as shown, in Figure 7.4.3. The sensors' multiplexer was surrounded by

insulation foam to maintain a constant temperature at the end of the thermocouples connected to it. A thermistor attached to the multiplexer is used as source of reference temperature for the thermocouples. Extra cables were wrapped around the box, as shown in Figure 7.4.4. A battery was connected to the datalogger and placed at the bottom of the tower. Figure 7.4.5 shows the complete tower with all the components installed.

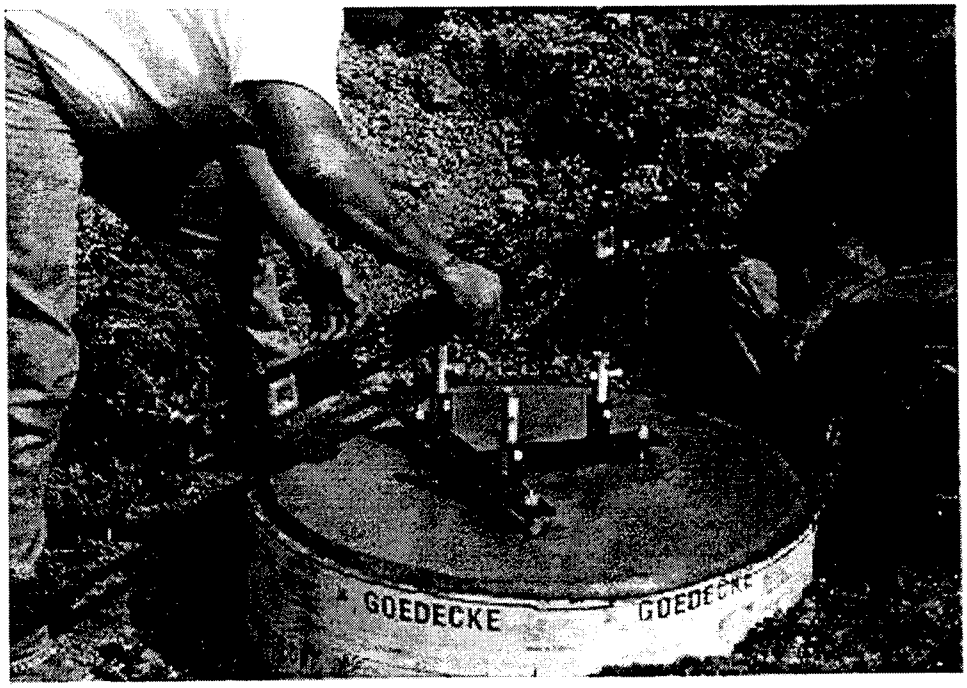

Figure 7.4.1 Levelling the Tower Base in the Concrete

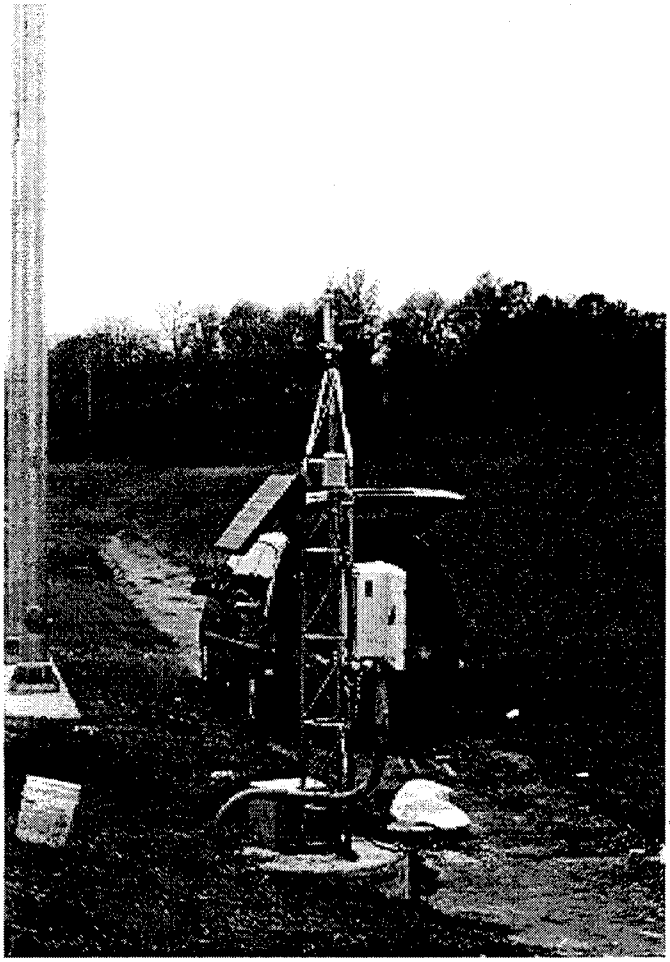

Figure 7.4.2 Mounted Tower and Instruments

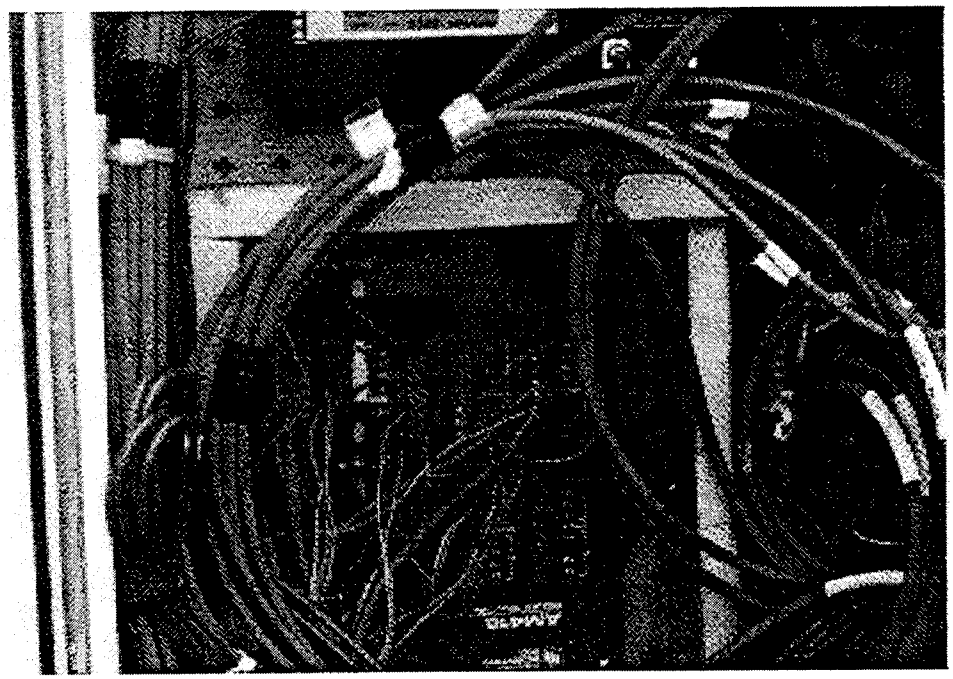

Figure 7.4.3 Wiring Connections of Sensors to the Multiplexer

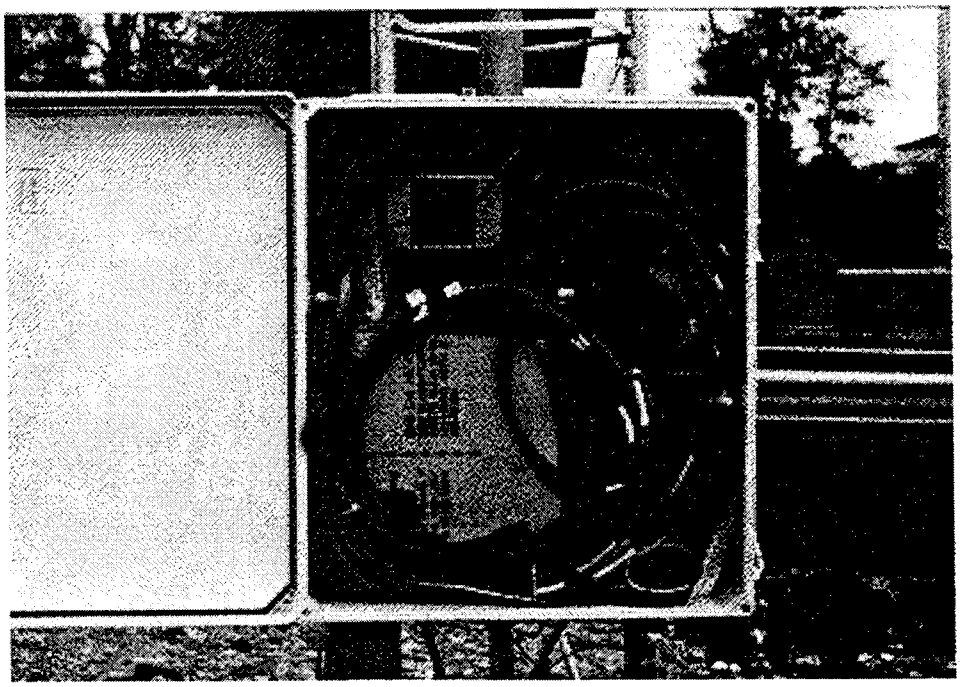

Figure 7.4.4 Instruments Box After Completing Connections

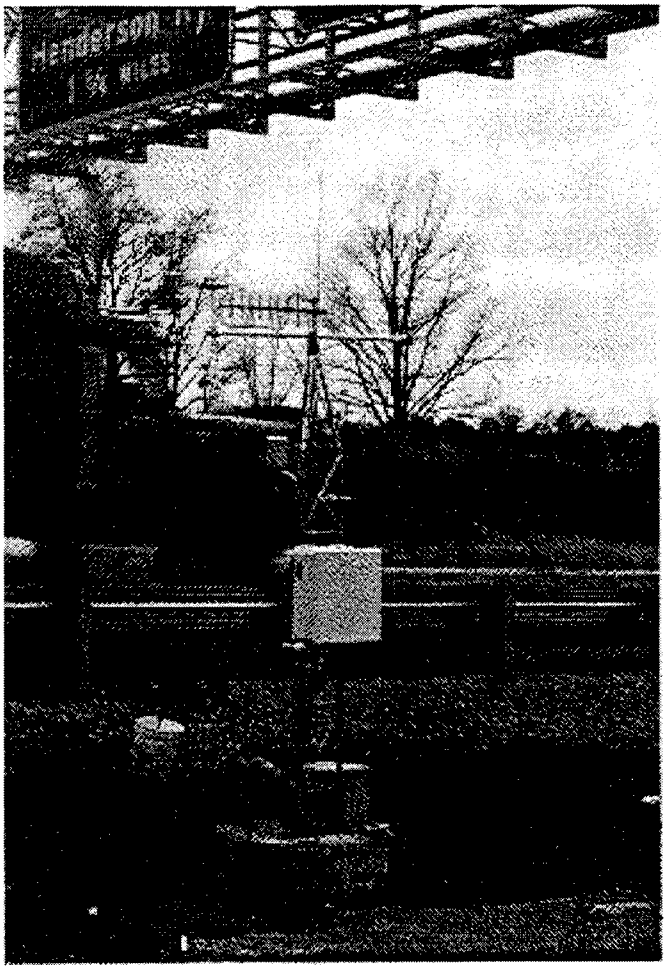

Figure 7.4.5 Tower and Equipment Ready for Operation

7.5 Site Operation

The software supplied with the data logger was used to write the data acquisition program. The readings from the solar radiation sensor are taken every minute, and the average value is stored for 15 minutes of reading. All other sensors are read every 15 minutes. All data are stored on site for a period of about two weeks. The data is then downloaded to a computer with a modem at Purdue via cellular phone. The operation of the data logger can also be controlled from Purdue, if needed.

7.6 Early Site Data and Analysis

Data acquired to date indicate that all sensors are operational. The readings from thermocouples at the opposing sides of the instrumentation hole are showing good agreement. However, data collected from thermistors do not agree with these collected from thermocouples. It appears that although thermistors are providing data, at this point this data is not reliable. The reason for that was not, as yet, identified.

To compare temperatures recorded by thermocouples in the East and West locations, sensors 1E, 1W, 2E, 2W, and 5E and 5W were selected as they were located exactly at the same depths in both sets. Figure 7.6.1 shows the temperature measurements for November 21 to 23, 1996 for those sensors, as well as the air temperature. The Figure shows the close agreement of the results. The maximum difference in temperature reading during this period was 0.23, 0.15 and 0.06°C for sensors 1, 2 and 5, respectively.

Figure 7.6.2 shows temperature data for the East set of thermocouples and the solar radiation in Watt per square meter (W/m^2) for two consecutive days. The Figure shows that sensors located deeper than 25 cm (TCE5, TCE6 and TCE7 which were located in the old pavement and subgrade) are less sensitive to the changes in the air temperature than the sensors located up to about 12 cm from the surface (sensors TCE1, TCE2, TCE3, and TCE4). The data also show that approximately around mid-day each day more solar energy was reaching the pavement surface than during any other times of the day. The effect of solar radiation on the air temperature as well as on the pavement temperature is clearly shown. For example, on the second day, at approximately noon, the pavement surface became warmer than the layers below due to sun energy absorption.

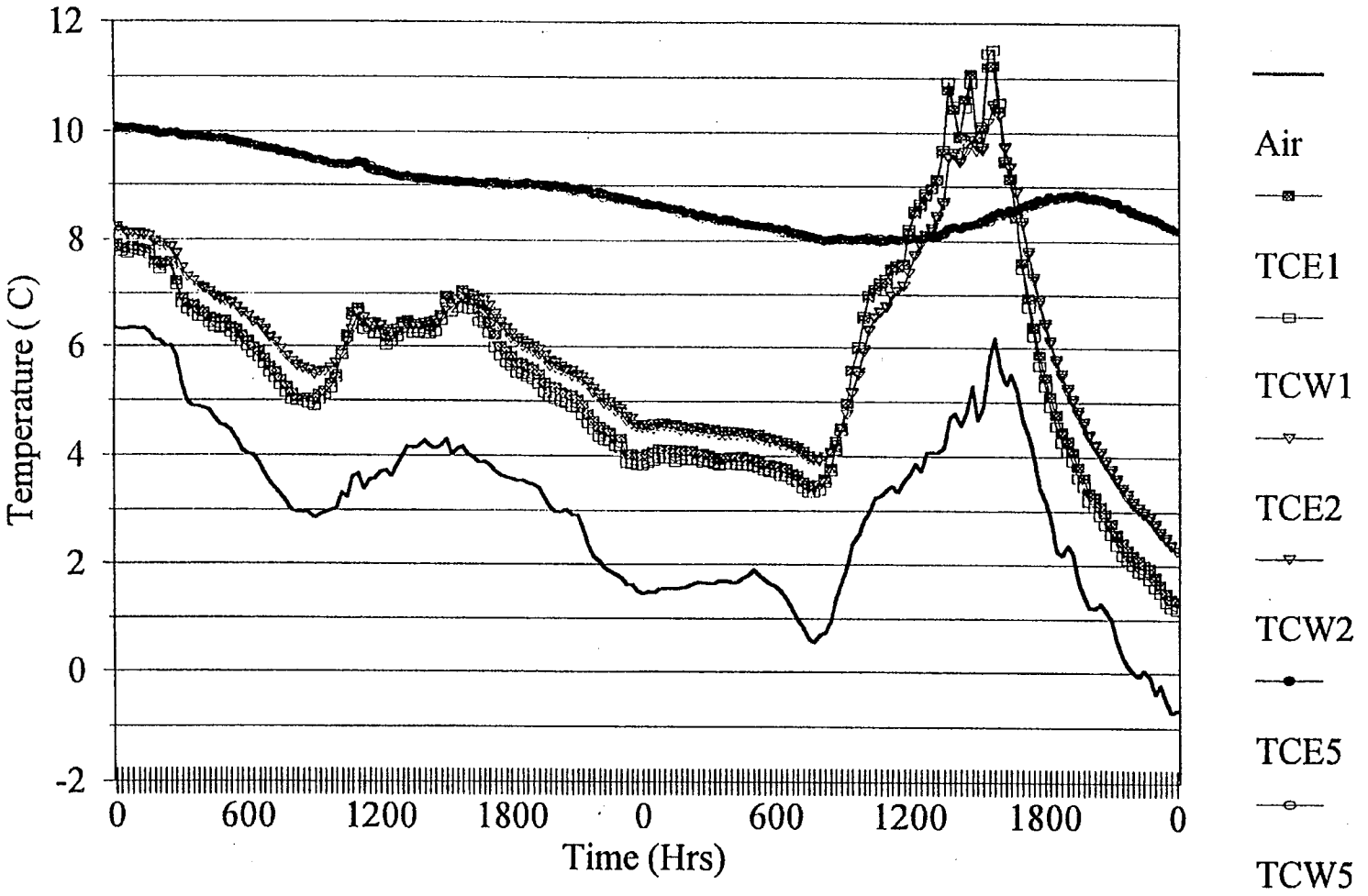

Figure 7.6.1 Temperature Measurement for November 22-23, 1996

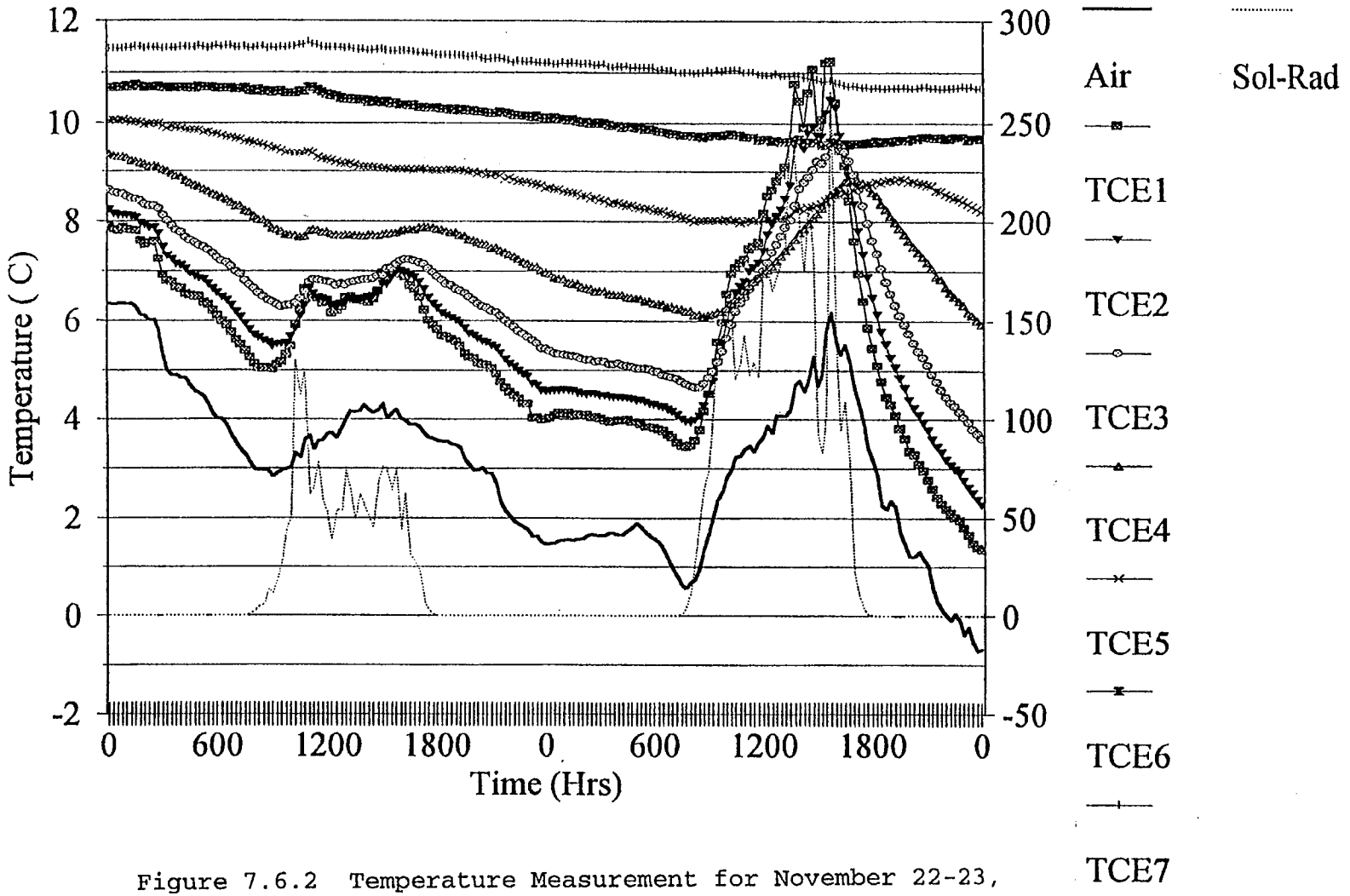

Figure 7.6.2 Temperature Measurement for November 22-23, 1996

8 SUMMARY AND CONCLUSION

Low temperature cracking resistance plays a major role in the performance of a pavement. The purpose of this research was to determine low temperature related performance parameters of asphalt used in the construction of old pavement and to verify the low temperature grading of asphalt removed from the newly constructed highway pavement on Interstate 64 in southern Indiana. For a region where low temperature cracking is of great concern, it is particularly important that care is taken in the selection of an asphalt binder to ensure adequate performance of the pavement over an extended period of time.

8.1 Adequacy of Binder Selection

The Superpave software utilizes the weather data provided by weather stations that are located closest to the site of construction, and selects the grade of asphalt binder to be used in the construction.

In the case of the construction of Interstate 64, the closest available weather station was in Evansville, Indiana. According to the weather data provided and used in the binder selection process as seen in Table 8.1.1, an asphalt binder of grade PG 64-34 would provide for a reliability of 98% on both the maximum and minimum pavement temperatures.

Table 8.1.1 Weather data from SHRP binder selection software

State: IN
County: VANDERBURGH
Weather Station:EVANSVILLE WSO AP

Longitude	87.53
Latitude	38.05
Elevation	116
Years of Climatic Data	42
Low Air Temperatures	
Lowest Low Temp., Degree C	-31
Median of annual Low Temps	-19
Mean of annual Low Temps	-20
Low Temp. Standard Deviation	5
High Air Temperatures	
Highest Mean 7-day recorded	37
Median of Mean 7-day Temps	34
Mean of Mean 7-day Temps	34
High Temp. Standard Deviation	1.7
N-Design Temperature	34
50% Reliability	
50% Reliability High Pvt Temp.	54.7
50% Reliability Low Pvt Temp.	-20
Performance Grade,>50% Reliab.	58-22
PG Actual Reliab. (High, Low)	(97,65)
98% Reliability	
98% Reliability High Pvt Temp.	58
98% Reliability Low Pvt Temp.	-30.3
Performance Grade,>98% Reliab.	64-34
PG Actual Reliab. (High, Low)	(98,98)
PG Versus Reliability	
PG (High,Low Reliability)	58-22 (97,65)
PG (High,Low Reliability)	58-28 (97,94)
PG (High,Low Reliability)	58-34 (97,98)
PG (High,Low Reliability)	64-34 (98,98)

Based on the results (presented in Chapter 6) obtained for both tank asphalt and asphalt extracted from the new pavement mix, it was verified that the asphalt binder used in the construction of the new pavement is indeed PG 64-34 grade. The asphalt material used in the base and binder layers of the existing left-in-place pavement would have been classified as a PG 64-22 if the results of the tests conducted on the binder obtained during the first series of extraction and recovery experiments performed on the cores were not altered by the solvent left behind during these operations. This is because the presence of residual solvent made the binder softer. If the solvent had been completely removed, the binder would be stiffer, and thus would classify as a higher low-temperature grade. The fact that the asphalt binder from the old pavement could at best be classified as a PG 64-22 grade indicates that it was not an adequate material to be used in the environment surrounding the highway where the pavement has been constructed. However, the material from the surface layer, which was an asphalt emulsion, could not be classified, using Superpave methods and specifications as it is still unknown if asphalt emulsions can be tested and classified in the same way as regular neat asphalt.

8.2 Effects of Extraction and Recovery Procedures on Binder Properties

A practical lesson learned from this research is that procedures as well as the solvents used in the process of extracting and recovering asphalt from existing pavement could change the properties of the material and affect the results produced. Although results of some previous research indicate that a SHRP developed procedure or a modified ASTM D2172 Method A procedure (9,11), when performed with caution at controlled temperatures, reduces the risk of aging to the material, when initially used in this research it did not produce satisfactory results. Specifically, Superpave tests performed on the extracted samples resulted in inaccurate and inconsistent data. Subsequently the procedure had to be adjusted and so tests needed to be repeated.

8.3 Monitoring of Field Performance

The site of study for this research is by no means the first pavement in the state that is using Superpave graded and selected material for construction. However, it is the first to be monitored specifically for low temperature cracking resistance. Although lab tests on the tank asphalt have indicated that the material used in the construction is the desired one, and it should withstand the effects of low temperatures, the real verification will only come from field observation of pavement performance after several years of service. At that time, it will become clearer whether the Superpave technology uses proper algorithms for asphalt binder selection to assure performance in the intended environment.

A field monitoring station has been set up at the site of the newly constructed pavement on highway I-64 in southern Indiana. This station will monitor the pavement temperatures at various depths, the air temperature and humidity, solar radiation, and the wind speed and direction. Data collected from this station will be used in the future for evaluating the algorithm currently used by the Superpave software in binder grade selection.

8.4 Conclusion

The following are the conclusions deduced from this research. These conclusions are restricted to the scope of this research.

1. The material used in the current pavement was verified as being of a PG 64-34 grading. This was confirmed by tests on both the binder from the manufacturer's tank as well as binder extracted from mixes that were placed during construction.
2. Great care needs to be taken in performing the extraction and recovery procedures to obtain binder from cores and mixes. The duration and temperature of the procedure needs to be especially closely monitored to ensure that all solvent is removed from the binder without exposing the asphalt to heat for longer than it is necessary.

3. The parity in the results for tank asphalt obtained by the research team and INDOT lab technicians show that comparable results can be obtained for Superpave binder tests performed by different operators.
4. The results obtained from the testing of binder from the intermediate and base layers of the old pavement cores may not be correct because the presence of residual solvent had made the binder softer. Therefore the binders could not be correctly classified using Superpave specification. However, it can be concluded that the binder from the base and intermediate layers would not meet the required specifications at the low temperature end even if solvent had been completely removed because it would have been classified as a PG 64-22 or less while the requirement for the pavement was a PG 64-34.
5. Asphalt emulsions have different properties than regular asphalt, and there is a need to evaluate whether asphalt emulsions can be classified as a performance graded binder using the Superpave specifications.
6. Results from the tests performed on the additionally aged old pavement binder indicate that a stiffness limit had not been reached for this material despite it having 15 years of field exposure.
7. The comparison of stiffness values obtained on material from the old pavement before and after additional aging showed a significant increase in stiffness resulting from additional aging. This suggests that the PAV aging procedure may not adequately simulate the in service aging of binder.
8. The instrumentation scenario used in this study resulted in a successful sensors installation. All the probes are operational.
9. The preliminary temperature measurements are shown to be reliable.
10. The measurements will continue, and will be used to verify and possibly refine the Superpave temperature algorithms. Local equations for Indiana could also be obtained for pavement temperature estimation.
11. The pavement will be monitored in the future to determine the validity of PG-grading in binder selection.

8.5 Recommendations

1. The problem encountered with the thermistors will be checked until the reason for the shift in results can be identified, and addressed.

2. From the instrument station, pavement temperatures should be monitored. The data should be used to evaluate the Superpave temperature algorithms. A refined Superpave model can be obtained for southern Indiana. This model would better account for the role of environmental conditions in the selection of PG graded asphalts.

3. It is recommended to use installation procedure developed during this project in future pavment instrumenation projects.

LIST OF REFERENCES

[1] U.S. Department of Transportation and Federal Highway Administration, *Background of Superpave Asphalt Mixture Design and Analysis*, February 1995.

[2] Robertson, R. E., et al., *"Chemical Properties of Asphalts and their Relationships to Pavement Performance"*, Association of Asphalt Paving Technologists, Vol. 60, 1991, pp. 413-436.

[3] U.S. Department of Transportation and Federal Highway Administration, *Background of Superpave Asphalt Binder Test Methods*, July 1994.

[4] Anderson, D. A., Christensen, D. W., and Bahia, H. *"Physical Properties of Asphalt Cement and the Development of Performance Related Specifications"*, Association of Asphalt Paving Technologists, Vol. 60, 1991, pp. 437-532.

[5] Fromm, H. J. and Phang, W. A., *"Study of Transverse Cracking of Bituminous Pavements"*, Association of Asphalt Paving Technologists, Vol. 41, pp. 383-423.

[6] Gaw, W.J., *"Measurement and Prediction of Asphalt Stiffnesses and their Uses in Developing Specifications to Control Low-Temperature Pavement Transverse Cracking"*, Low Temperature Properties of Bituminous Materials and Compacted Bituminous Paving Mixtures, ASTM Special Technical Paper 628, 1977.

[7] Moulthrop, J. S., Cominsky, R. J., Kennedy, T. W., and Harrigan, E. T., *"Strategic Highway Research Program Asphalt Research - An Overview"*, Association of Asphalt Paving Technologists, Vol. 60, pp. 403-412.

[8] Asphalt Institute and Federal Highway Administration, *"Superpave Asphalt Mixture Analysis"*, January 1996.

[9] Burr, B. L., Glover, C. J., Davison, R. R., and Billin, J. A., *"New Apparatus and Procedure for the Extraction and Recovery of Asphalt Binder from Pavement Mixtures"*, Transportation Research Record 1491, TRB, National Research Council, Washington, D.C., 1993, pp. 20-29.

[10] Burr, B. L., Davison, R. R., Glover, C. J., and Bullin, J. A., *"Solvent Removal from Asphalt"*, Transportation Research Record 1269, TRB, National Research Council, Washington, D.C., 1990, pp. 1-8.

[11] Burr, B. L., Davison, R. R., Jemison, H. B., Glover, C. J., and Bullin, J. A., *"Asphalt Hardening in Extraction Solvents"*, Transportation Research Record 1323, TRB, National Research Council, Washington, D.C., 1991, pp. 70-76.

[12] Burr, B. L., Davison, R. R., Cipione, C. A., Glover, C. J., and Bullin, J. A., *"Evaluation of Solvents for the Extraction of Residual Asphalt from Aggregates"*, Transportation Research Record 1323, TRB, National Research Council, Washington, D.C., 1991, pp. 47-52.

[13] Jung, D., Vinson, T. S., *"Low Temperature Cracking Resistance of Asphalt Concrete Mixtures"*, Association of Asphalt Paving Technologists, Vol. 62, pp. 54-92.

[14] Strategic Highway Research Program, *"Development and Validation of Prediction Models and Specifications for Asphalt Binders and Paving Mixes"*, SHRP-A-357, 1993.

[15] ASTM D-2172, *"Standard Test Methods for Quantitative Extraction of Bituminous Paving Mixtures"*, Annual Book of ASTM Standards, 1996, pp. 208-219.

[16] ASTM D-5340, *"Standard Test Method for Airport Pavement Condition Index Surveys"*, Annual Book of ASTM Standards, 1996, pp. 552-599.

[17] Busby, E. O. And Rader, L. F., *"Flexural Stiffness Properties of Asphalt Concrete at Low Temperatures"*, Association of Asphalt Paving Technologists, Vol. 41, pp. 163-187.

[18] ASTM D1856, *"Standard Test Method for Recovery of Asphalt from Solution by Abson Method"*, Annual Book of ASTM Standards, 1996, pp. 169-172.

APPENDICES

APPENDIX A – RAW TEST DATA

Table A1 DSR Results for Binder Extracted from New Pavement Mix (RTFO), First Run

DSR at 52°C

Sample	G* (kPa)	Delta (δ,°)	G*/sinδ (kPa)	Temp.(°C)
MIXA	1.353	73.20	1.413	52.0
MIXB	2.962*	67.10*	3.216*	52.0
MIXC	0.882	73.60	0.920	52.1
MIXD	2.186*	70.60*	2.317*	52.0
MIXE	0.727*	73.70*	0.757*	52.0
MIXF	1.034	62.60	1.164	52.0
Average	1.090	69.80	1.166	52.0

DSR at 58°C

Sample	G* (kPa)	Delta (δ,°)	G*/sinδ (kPa)	Temp.(°C)
MIXA	0.781	74.20	0.812	58.0
MIXB	1.684*	70.40*	1.788*	58.0
MIXC	0.540	77.00	0.554	58.0
MIXD	1.039*	73.20*	1.085*	58.0
MIXE	0.393*	78.90*	0.400*	57.9
MIXF	0.887	73.00	0.928	58.0
Average	0.736	74.73	0.765	58.0

* Data points not used in calculations

Table A1 DSR Results for Binder Extracted from New Pavement Mix (RTFO), First Run, Cont'd

DSR at 64°C

Sample	G* (kPa)	Delta (δ,°)	G*/sinδ (kPa)	Temp.(°C)
MIXA	0.461	77.80	0.472	63.9
MIXB	0.726*	79.80*	0.737*	64.0
MIXC	0.307	79.80	0.323	64.0
MIXD	0.592*	76.30*	0.609*	64.0
MIXE	0.483*	78.20*	0.493*	64.0
MIXF	0.599	80.20	0.608	64.0
Average	0.456	79.27	0.468	64.0

Table A2 DSR Results for Binder Extracted from New Pavement Mix (RTFO), Second Run

DSR at 58°C

Sample	G* (kPa)	Delta (δ,°)	G*/sinδ (kPa)	Temp.(°C)
MIXA	4.1233	65.10	4.5341	58.0
MIXB	4.2331	65.00	4.6722	58.0
MIXC	3.5985	65.00	3.9704	58.0
MIXD	4.3523	66.20	4.7568	58.0
Average	3.9850	65.03	4.3922	58.0

DSR at 64°C

Sample	G* (kPa)	Delta (δ,°)	G*/sinδ (kPa)	Temp.(°C)
MIXA	2.0612	66.80	2.2423	64.0
MIXB	2.1538	66.90	2.3417	64.0
MIXC	2.0963	67.10	2.2763	63.9
MIXD	2.2599	67.90	2.4392	64.0
Average	2.1038	66.93	2.2868	64.0

DSR at 70°C

Sample	G* (MPa)	Delta (δ,°)	G*/sinδ (kPa)	Temp.(°C)
MIXA	1.2702	69.30	1.3574	70.0
MIXB	1.2949	69.50	1.3824	70.0
MIXC	1.1421	69.60	1.2188	70.0
MIXD	1.2535	70.60	1.3294	70.0
Average	1.2357	69.47	1.3195	70.0

Table A3 DSR Results for Binder Extracted from New Pavement Mix (After PAV), First Run

DSR at 19°C

Sample	G* (kPa)	Delta (δ,°)	G*sinδ (kPa)	Temp. (°C)
MIXPA	1,293.5	30.20	650.7	19.0
MIXPB	935.3	41.60	621.0	18.9
MIXPC	982.6	38.70	614.4	19.0
MIXPD	1,117.4	33.80	614.4	19.0
Average	1,082.2	36.08	625.1	19.0

Table A4 DSR Results for Binder Extracted from New Pavement Mix (After PAV), Second Run

DSR at 19°C

Sample	G* (kPa)	Delta (δ,°)	G*sinδ (kPa)	Temp. (°C)
MIXPA	3,240.7	47.90	2,403.8	19.0
MIXPB	3,459.9	46.90	2,528.3	18.9
MIXPC	3,652.3	45.70	2,615.8	19.1
MIXPD	3,641.4	45.70	2,607.0	19.0
MIXPE	3,643.0	47.50	2,685.4	19.0
MIXPF	3623.4	46.0	2607.60	18.9
Average	3,498.6	46.55	2,538.7	19.0

Table A5 BBR Results for Binder Extracted from New Pavement Mix (After PAV), First Run

BBR at -24°C

Sample	m-value	Stiffness (MPa)
A	0.306	280.2
B	0.338	165.4
Average	0.322	222.8

Table A6 BBR Results for Binder Extracted from New Pavement Mix (After PAV), Second Run

BBR at -24°C

Sample	m-value	Stiffness (MPa)
A	0.314	264.6
B	0.322	249.0
Average	0.318	256.8

Table A7 DSR Results of Tank Asphalt Binder

Tested by INDOT (Original)

DSR At 64°C

Sample	G* (kPa)	Delta (δ,°)	G*/sinδ (kPa)	Temp.(°C)
ORIG1	1.173	71.58	1.236	64.0
ORIG2	1.061	73.19	1.109	64.0
ORIG3	1.199	70.92	1.269	64.0
ORIG4	1.042	72.17	1.095	64.0
ORIG5	1.083	69.41	1.157	64.0
Average	1.112	71.45	1.173	64.0

Table A8 DSR Results of Tank Asphalt Binder

Tested by INDOT (After RTFO)

DSR At 64°C

Sample	G* (kPa)	Delta (δ,°)	G*/sinδ (kPa)	Temp.(°C)
RTFO1	2.383	65.57	2.619	64.0
RTFO2	2.410	67.36	2.611	64.0
RTFO3	2.079	67.27	2.255	64.0
RTFO4	2.467	66.30	2.693	64.0
RTFO5	2.326	66.06	2.545	64.0
Average	2.333	66.51	2.545	64.0

Table A9 DSR Results of Tank Asphalt Binder

Tested by INDOT (After PAV)

DSR At 19°C

Sample	G* (kPa)	Delta (δ,°)	G*sinδ (kPa)	Temp. (°C)
PAV1	3,386	46.87	2,472	19.0
PAV2	3,118	47.81	2,310	19.0
PAV3	2,759	48.83	2,077	19.0
PAV4	3,344	47.61	2,464	19.0
PAV5	2,440	49.39	1,852	19.0
Average	3,009	48.10	2,235	19.0

Table A10 BBR Results for Tank Asphalt Binder

Tested by INDOT (After PAV)

BBR at -24°C

Sample	m-value	Stiffness (MPa)
PAV1	0.277	263.0
PAV2	0.309	281.0
PAV3	0.302	229.0
PAV4	0.309	247.0
PAV5	0.312	216.0
Average	0.302	247.2

Table A11 DSR Results for Tank Asphalt Binder

Tested by Research Team (Original)

DSR At 64°C

Sample	G* (kPa)	Delta (δ,°)	G*/sinδ (kPa)	Temp.(°C)
ORIGA	0.994	72.40	1.043	64.0
ORIGB	1.179	64.10	1.311	64.0
ORIGC	1.155	71.80	1.216	64.0
ORIGD	1.224	71.00	1.294	64.0
ORIGE	1.047	72.10	1.100	64.0
ORIGF	1.011	72.10	1.062	64.0
ORIGG	0.931	72.80	0.975	64.0
ORIGH	0.930	73.00	0.973	64.0
Average	1.059	71.16	1.122	64.0

Table A12 DSR Results for Tank Asphalt Binder

Tested by Research Team (After RTFO)

DSR at 64°C

Sample	G* (kPa)	Delta (δ,°)	G*/sinδ (kPa)	Temp.(°C)
RTFOA	1.972	67.90	2.129	64.0
RTFOB	2.045	67.50	2.231	64.0
RTFOC	2.153	66.00	2.357	64.0
RTFOD	2.118	66.50	2.310	64.0
RTFOE	2.063	66.80	2.444	64.0
RTFOF	2.040	66.70	2.220	64.0
RTFOG	2.044	66.90	2.222	64.0
RTFOH	2.060	66.60	2.245	64.0
Average	2.062	66.86	2.270	64.0

Table A13 DSR Results for Tank Asphalt Binder

Tested by Research Team (After PAV)

DSR at 19°C

Sample	G* (kPa)	Delta (δ,°)	G*sinδ (kPa)	Temp. (°C)
PAVA	2,462	48.80	1,902	19.0
PAVB	2,562	48.60	1,922	19.0
PAVC	3,127	48.10	2,364	19.0
PAVD	2,946	48.10	2,194	19.0
PAVE	2,983	48.50	2,234	19.0
PAVF	3,128	48.90	2,357	19.0
PAVG	2,384	48.50	1,786	19.0
PAVH	3,090	48.20	2,305	19.0
Average	2,835	48.46	2,133	19.0

Table A14 BBR Results for Tank Asphalt Binder

Tested by Research Team (After PAV)

BBR at -24°C

Sample	m-value	Stiffness (MPa)
A	0.306	311
B	0.301	313.2
C	0.307	289.4
D	0.333*	173.3*
Average	0.305	305

Table A15 DSR Results for Surface Binder
Extracted from old pavement (PAV)

DSR at 7°C

Sample	G* (kPa)	Delta (δ,°)	G*sinδ (kPa)	Temp. (°C)
SFCA01	3,468	36.10	2,044	7.1
SFCB01	319*	72.80*	305*	6.9
SFCC01	7,829	30.60	3,989	7
SFCD01	30,104*	22.80*	11,656*	6.9
SFCE01	34,948*	21.70*	12,994*	6.9
SFCF01	6,110	31.90	3,228	7.1
SFCG01	12,594	26.90	5,693	7.1
SFCH01	10,818	29.90	5,398	7.0
SFCJ01	18,081	25.10	7,659	7.0
SFCK01	4,978	34.50	2,819	7.0
SFCL01	1,528*	38.50*	952*	7.0
SFCM01	15,203	27.60	7,038	7.0
SFCN01	20,382	25.30	8,714	7.0
SFCP01	17,653	23.30	6,939	6.9
Average	11,712	29.12	5,352	7.0

DSR at 10°C

Sample	G* (kPa)	Delta (δ,°)	G*sinδ (kPa)	Temp. (°C)
SFCA02	2,904	36.90	1,742	10.0
SFCB02	90*	49.81*	69*	10.0
SFCC02	6,493	31.90	3,435	10.1
SFCD02	25,266*	24.20*	10,347*	9.9
SFCE02	31,091*	21.50*	11,409*	9.9
SFCF02	4,371	34.70	2,487	9.9
SFCG02	10,585	28.80	5,093	10.0
SFCH02	8,854	29.50	4,367	10.0
SFCJ02	14,898	27.80	6,955	10.0
SFCL02	1,626*	38.40*	1,011*	10.0
SFCM02	12,747	27.70	5,930	10.0
SFCN02	17,578	26.40	7,187	9.9
SFCP02	14,773	26.10	6,492	9.9
Average	10,356	29.98	4,854	10.0

Table A15 DSR Results for Surface Binder
Extracted from old pavement (PAV), Continued

DSR at 13°C

Sample	G* (kPa)	Delta (δ,°)	G*sinδ (kPa)	Temp. (°C)
SFCA03	2,214	38.50	1,378	13.0
SFCB03	554*	37.90*	341*	13.0
SFCC03	4,973	33.90	2,772	13.0
SFCD03	20,023*	25.80*	8,799*	13.0
SFCE03	24,497*	25.60*	10,597*	12.9
SFCF03	3,157	37.50	1,921	12.9
SFCG03	8,282	30.50	4,204	13.0
SFCH03	6,803	31.30	3,535	12.9
SFCJ03	11,878	29.10	5,779	13.0
SFCL03	1,451*	40.50*	942*	13.0
SFCM03	10,111	29.30	4,955	13.0
SFCN03	13,951	28.00	6,557	12.9
SFCP03	11,786	28.40	5,598	12.9
Average	8,128	31.83	4,078	13.0

Table A16 BBR Results for Asphalt Extracted
from Surface Layer of Old Pavement (PAV)

BBR at -6°C

Sample	m-value	Stiffness (MPa)
A	0.273	69.09
B	0.271	69.93
Average	0.272	69.51

Table A17 DSR Results for Asphalt Extracted from Binder Layer of Old Pavement (PAV)

DSR at 7°C

Sample	G* (kPa)	Delta (δ,°)	G*sinδ (kPa)	Temp. (°C)
BINA01	6,219	34.50	3,522	7.0
BINB01	9,380	34.10	5,263	6.9
BINC01	59,185	19.00	19,231	6.9
BIND01	13,226	31.40	6,896	6.9
BINE01	32,898	22.20	12,409	7.0
BINF01	76,949	17.10	22,515	7.0
BING01	14,667	30.20	7,377	7.1
BINH01	16,908	29.20	8,250	7.1
BINJ01	22,221	27.40	10,211	6.9
BINK01	43,343	21.50	15,899	6.9
BINL01	34,464	25.40	14,783	7.0
BINM01	51,214	22.10	19,268	7.0
BINN01	67,216	17.60	20,324	7.0
Average	34,453	25.52	12,765	7.0

DSR at 10°C

Sample	G* (kPa)	Delta (δ,°)	G*sinδ (kPa)	Temp. (°C)
BINA02	7,368	34.80	4,201	10.0
BINB02	8,121	34.20	4,569	10.0
BINC02	52,343	19.50	17,457	9.9
BIND02	11,136	31.40	5,805	10.0
BINE02	27,999	25.20	11,931	10.0
BINF02	66,594	17.20	19,648	10.0
BING02	11,098	32.30	5,993	10.0
BINH02	13,830	30.30	6,984	10.0
BINJ02	19,329	28.50	9,219	10.0
BINK02	37,055	23.30	14,658	9.9
BINL02	28,164	27.70	13,092	10.0
BINM02	43,469	23.90	17,611	10.0
BINN02	60,599	18.90	19,629	10.0
Average	29,777	26.71	11,600	10.0

Table A17 DSR Results for Asphalt Extracted from Binder Layer of Old Pavement (PAV), Cont'd

DSR at 13°C

Sample	G* (kPa)	Delta (δ,°)	G*sinδ (kPa)	Temp. (°C)
BINA03	5,991	36.30	3,548	13.1
BINB03	6,170	36.50	3,673	12.9
BINC03	45,124	21.80	16,727	12.9
BIND03	8,434	33.20	4,612	13.1
BINE03	22,062	26.80	9,954	13.0
BINF03	59,048	18.30	18,548	13.0
BING03	8,200	33.90	4,574	13.0
BINH03	10,753	32.10	5,516	13.0
BINJ03	14,602	30.40	7,387	13.0
BINK03	30,766	23.20	12,136	12.9
BINL03	23,841	28.90	11,522	13.0
BINM03	41,146	24.30	16,932	13.1
BINN03	49,186	20.40	17,145	13.0
Average	25,025	28.16	10,175	13.0

DSR at 16°C

Sample	G* (kPa)	Delta (δ,°)	G*sinδ (kPa)	Temp. (°C)
BINA04	4,365	38.00	2,851	16.0
BINB04	4,499	38.50	2,798	16.0
BINC04	36,193	25.60	15,644	15.9
BIND04	6,478	35.10	3,723	15.9
BINE04	17,279	27.80	8,052	16.1
BINF04	49,114	21.30	17,866	16.0
BING04	5,946	36.00	3,497	15.9
BINH04	7,967	34.50	4,507	16.0
BINJ04	11,070	32.70	5,986	16.0
BINK04	24,198	26.90	10,963	15.9
BINL04	19,593	30.70	10,003	16.0
BINM04	33,962	25.70	14,728	16.0
BINN04	38,604	21.90	14,399	16.0
Average	19,944	30.36	8,848	16.0

Table A17 DSR Results for Asphalt Extracted from Binder Layer of Old Pavement (PAV), Continued

DSR at 19°C

Sample	G* (kPa)	Delta (δ,°)	G*sinδ (kPa)	Temp. (°C)
BINA05	3,434	40.20	2,218	19.1
BINB05	3,218	40.80	2,102	19.0
BINC05	29,306	25.20	12,488	19.0
BIND05	4,770	37.30	2,894	18.9
BINE05	13,225	30.60	6,741	19.0
BINF05	38,700	24.60	16,116	18.9
BING05	4,146	38.60	2,585	19.0
BINH05	5,793	37.00	3,486	19.0
BINJ05	8,059	35.80	4,719	19.0
BINK05	18,991	27.90	8,879	19.0
BINL05	17,776	31.50	9,288	18.9
BINM05	30,567	26.40	13,591	19.0
BINN05	29,414	22.70	11,351	19.0
Average	15,954	32.20	7,420	19.0

DSR at 22°C

Sample	G* (kPa)	Delta (δ,°)	G*sinδ (kPa)	Temp. (°C)
BINA06	2,458	42.70	1,668	22.10
BINB06	2,273	43.30	1,559	21.90
BINC06	22,970	26.60	10,284	22.00
BIND06	3,706	39.20	2,342	22.00
BINE06	9,605	33.70	5,329	22.00
BINF06	30,016	26.30	13,277	22.00
BING06	3,688	41.80	2,458	22.00
BINH06	4,059	39.80	2,599	22.00
BINJ06	5,764	37.90	3,543	22.00
BINK06	14,004	31.00	7,207	22.00
BINL06	14,118	33.60	7,813	22.00
BINM06	22,005	27.70	10,229	22.00
BINN06	22,747	24.20	9,325	22.00
Average	12,109	34.45	5,972	22.00

Table A17 DSR Results for Asphalt Extracted from Binder Layer of Old Pavement (PAV), Cont'd

DSR at 25°C

Sample	G* (kPa)	Delta (δ,°)	G*sinδ (kPa)	Temp. (°C)
BINA07	1,746	45.30	1,241	25.0
BINB07	1,576	45.90	1,131	25.0
BINC07	17,599	30.10	8,819	25.0
BIND07	2,110	42.70	1,431	25.0
BINE07	7,012	35.70	4,092	25.0
BINF07	22,859	26.90	10,351	25.0
BING07	2,796	45.30	1,987	25.0
BINH07	3,517	48.90	2,650	25.0
BINJ07	4,087	40.80	2,672	25.0
BINK07	10,507	32.50	5,647	25.0
BINL07	10,489	37.40	6,370	25.0
BINM07	18,729	29.50	9,232	25.0
BINN07	17,525	25.10	7,434	25.0
Average	9,273	37.39	4,851	25.0

Table A18 BBR Results for Asphalt Binder Extracted from Binder Layer of Old Pavement (PAV)

BBR at -12°C

Sample	m-value	Stiffness (MPa)
A	0.268	123.7
B	0.264	145.9
C	0.424	19.28
D	0.628*	5.713*
Average	0.319	96

Table A19 BBR Results of Asphalt Extracted from Binder Layer of Old Pavement (After Additional PAV)

BBR(with PAV) at -6°C

Sample	m-value	Stiffness (MPa)
A	0.244	117.8
B	0.241	134
Average	0.243	125.9

BBR(with PAV) at -12°C

Sample	m-value	Stiffness (MPa)
A	0.210	236
B	0.200	234.2
Average	0.205	235.1

Table A20 DSR Results for Asphalt Binder Extracted from Base Layer of Old Pavement (PAV)

DSR at 7°C

Sample	G* (kPa)	Delta (δ,°)	G*sinδ (kPa)	Temp. (°C)
BASA01	6,558*	33.70*	3,642*	6.9
BASB01	16,940	28.80	8,171	6.9
BASC01	27,046	27.50	12,482	6.9
BASD01	24,998	31.40	13,022	6.9
BASE01	50,280	24.20	20,600	6.9
BASF01	36,883	27.30	16,805	6.9
BASG01	36,750	25.20	15,639	6.9
BASH01	72,388*	20.00*	24,797*	6.9
Average	32,150	27.40	14,453	6.9

DSR at 10°C

Sample	G* (kPa)	Delta (δ,°)	G*sinδ (kPa)	Temp. (°C)
BASA02	2,028*	35.00*	2,884*	10.0
BASB02	17,952	28.90	8,675	10.0
BASC02	22,190	30.10	11,121	9.9
BASD02	22,190	30.00	11,106	9.9
BASE02	42,586	22.90	16,599	10.1
BASF02	28,645	27.80	13,343	10.1
BASG02	32,102	27.80	14,951	9.9
BASH02	65,502*	24.80*	27,496*	9.9
Average	27,611	27.92	12,633	10.0

Table A20 DSR Results for Asphalt Binder Extracted from Base Layer of Old Pavement (PAV), Continued

DSR at 13°C

Sample	G* (kPa)	Delta (δ,°)	G*sinδ (kPa)	Temp. (°C)
BASA03	4,193*	37.10*	2,527*	13.0
BASB03	14,736	34.30	8,309	13.0
BASC03	17,054	31.40	8,879	12.9
BASD03	17,628	32.90	9,570	12.9
BASE03	33,376	25.30	14,288	12.9
BASF03	22,608	31.00	11,644	13.1
BASG03	25,159	29.30	12,298	12.9
BASH03	49,681*	20.40*	17,336*	12.9
Average	21,760	30.70	10,831	13.0

DSR at 16°C

Sample	G* (kPa)	Delta (δ,°)	G*sinδ (kPa)	Temp. (°C)
BASA04	4,199*	37.40*	2,551*	16.0
BASB04	10,879	35.30	6,280	16.0
BASC04	12,916	34.70	7,353	15.9
BASD04	13,545	33.40	7,450	15.9
BASE04	25,908	26.90	11,727	15.9
BASF04	17,115	34.00	9,579	15.9
BASG04	18,935	30.50	9,604	15.9
BASH04	41,769*	24.20*	17,103*	15.9
Average	16,550	32.47	8,665	15.9

Table A20 DSR Results for Asphalt Binder Extracted from Base Layer of Old Pavement (PAV), Cont'd

DSR at 19°C

Sample	G* (kPa)	Delta (δ,°)	G*sinδ (kPa)	Temp. (°C)
BASA05	3,106*	40.00*	1,997*	18.9
BASB05	7,820	37.80	4,789	19.0
BASC05	9,669	35.10	5,558	19.0
BASD05	10,074	35.90	5,908	19.0
BASE05	19,373	31.10	9,998	19.0
BASF05	12,325	35.80	7,213	19.0
BASG05	14,171	34.10	7,948	19.0
BASH05	32,892*	26.30*	14,568*	18.9
Average	12,239	34.97	6,902	19.0

DSR at 22°C

Sample	G* (kPa)	Delta (δ,°)	G*sinδ (kPa)	Temp. (°C)
BASA06	2,254*	42.40*	1,520*	22.0
BASB06	5,602	40.10	3,609	22.1
BASC06	6,919	38.40	4,294	21.9
BASD06	7,071	38.50	4,403	22.0
BASE06	14,441	34.20	8,118	22.0
BASF06	8,760	38.70	5,474	22.0
BASG06	10,010	37.20	6,052	22.0
BASH06	25,958*	30.30*	13,086*	22.0
Average	8,800	37.85	5,325	22.0

Table A20 DSR Results for Asphalt Binder Extracted from Base Layer of Old Pavement (PAV), Cont'd

DSR at 25°C

Sample	G* (kPa)	Delta (δ,°)	G*sinδ (kPa)	Temp. (°C)
BASA07	1,602*	45.20*	1,137*	25.0
BASB07	3,886,900	43.10	2,657	25.0
BASC07	4,827	40.80	3,157	25.0
BASD07	4,994	41.60	3,312	25.0
BASE07	10,402	36.00	6,120	24.9
BASF07	6,452	41.40	4,266	25.0
BASG07	7,038	40.00	4,519	25.0
BASH07	18,118*	31.80*	9,560*	25.0
Average	653,436	40.48	4,005	25.0

Table A21 BBR Results for Asphalt Extracted from Base Layer of Old Pavement (PAV)

BBR at -12°C

Sample	m-value	Stiffness (MPa)
A	0.398	37.34
B	0.293	118.1
C	0.569*	8.471*
D	0.425	22.43
Average	0.372	59.29

Table A22 BBR Results for Asphalt Extracted from Base Layer of Old Pavement (After Additional PAV)

BBR (with PAV) at -6°C

Sample	m-value	Stiffness (MPa)
A	0.255	149.8
B	0.255	163.9
Average	0.255	156.85

BBR (with PAV) at -12°C

Sample	m-value	Stiffness (MPa)
A	0.206	261.2
B	0.214	263.2
Average	0.210	262.2

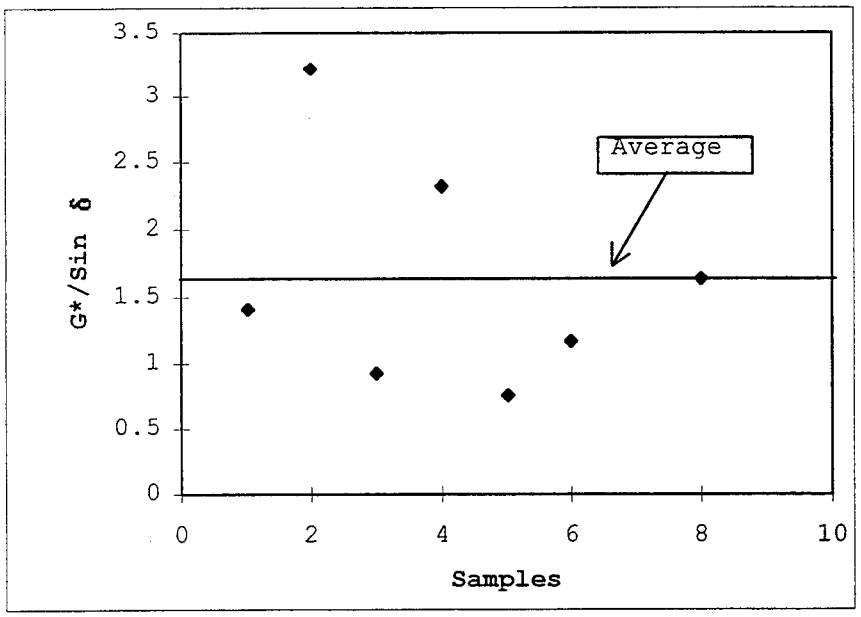

Figure A1.1 Data Distribution of DSR Test on Mix Binder, First Run, at 52°C

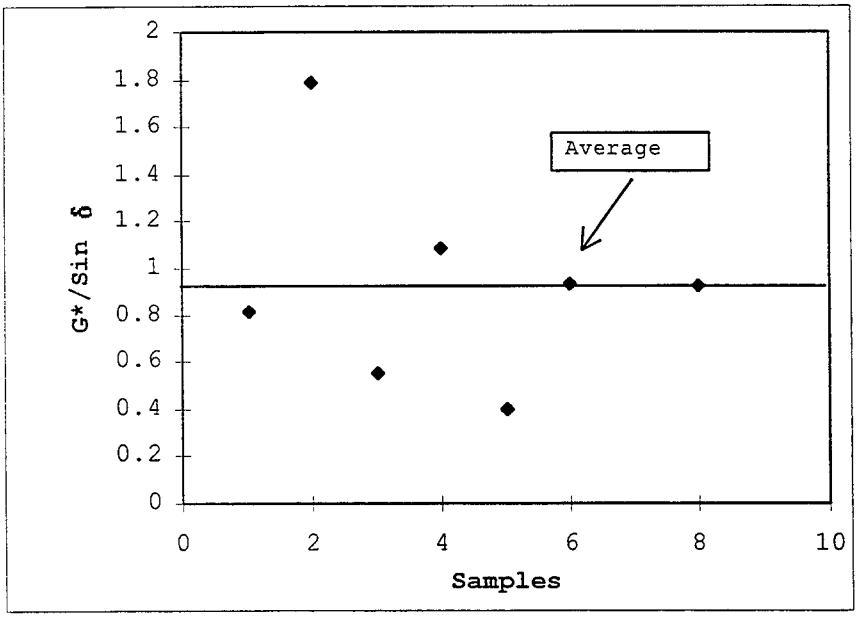

Figure A1.2 Data Distribution of DSR Test on Mix Binder, First Run, at 58°C

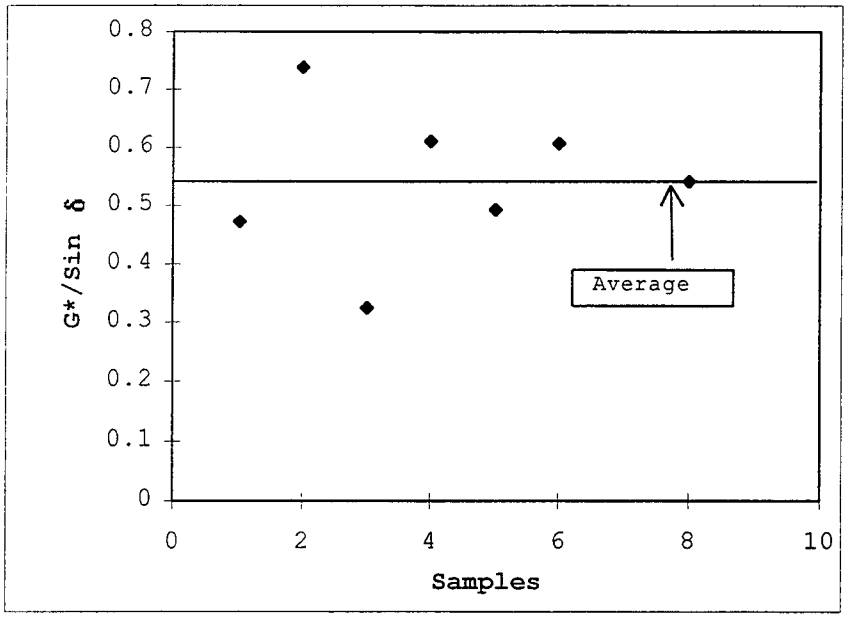

Figure A1.3 Data Distribution of DSR Test on Mix Binder, First Run, at 64°C

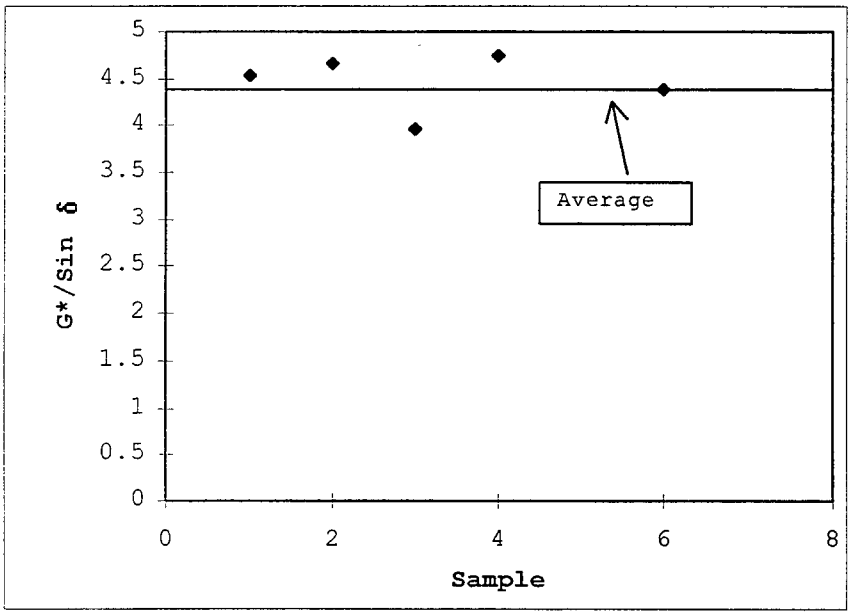

Figure A2.1 Data Distribution of DSR Test on Mix Binder, Second Run, at 58°C

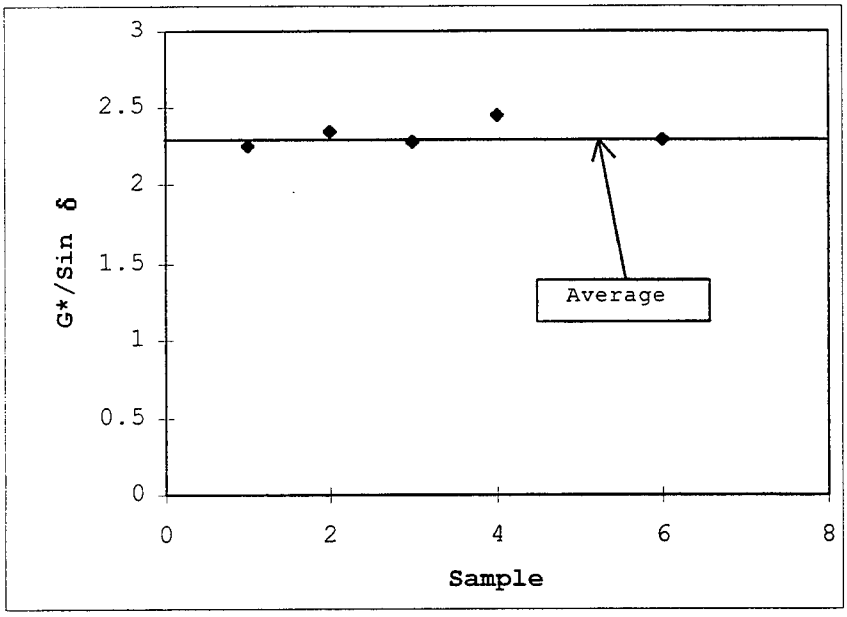

Figure A2.2 Data Distribution of DSR Test on Mix Binder, Second Run, at 64°C

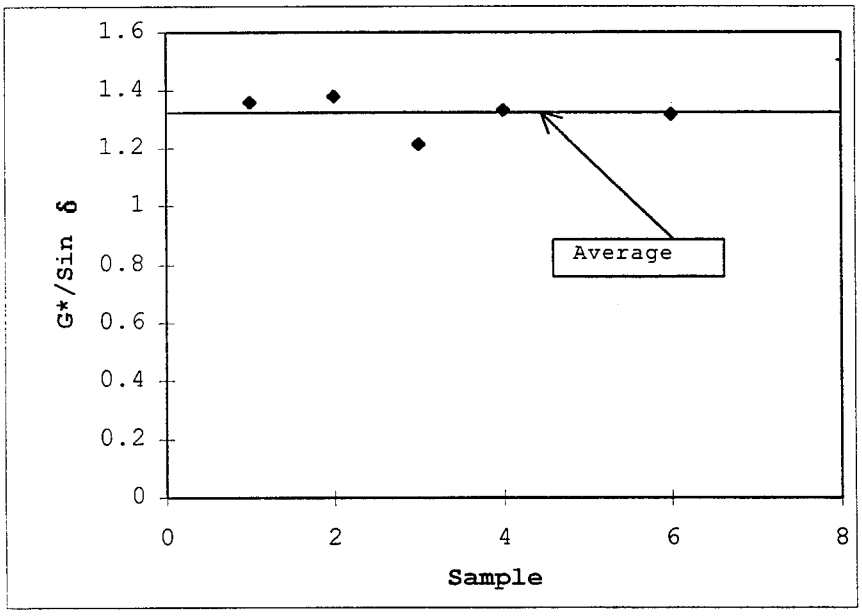

Figure A2.3 Data Distribution of DSR Test on Mix Binder, Second Run, at 70°C

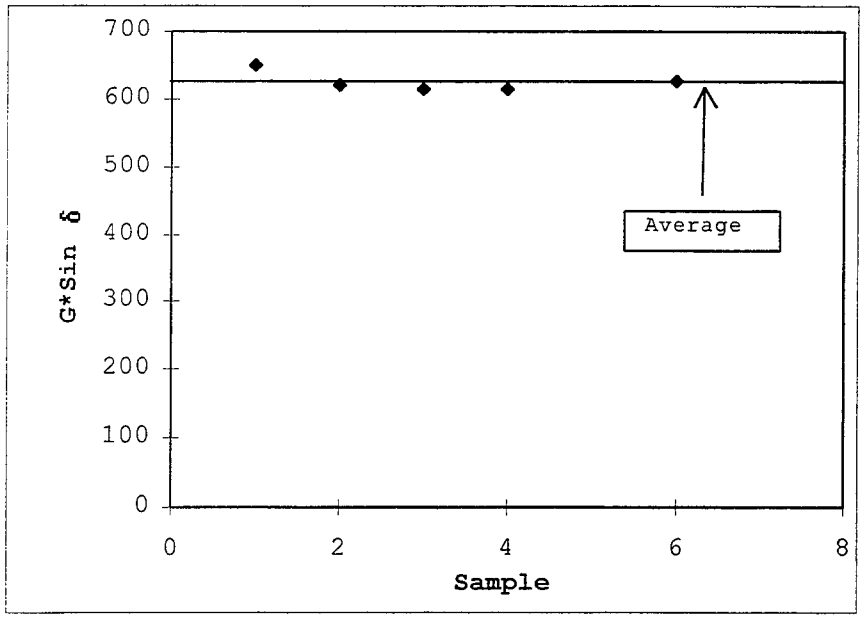

Figure A3.1 Data Distribution of DSR Test on PAV-Aged Mix Binder, First Run, at 19°C

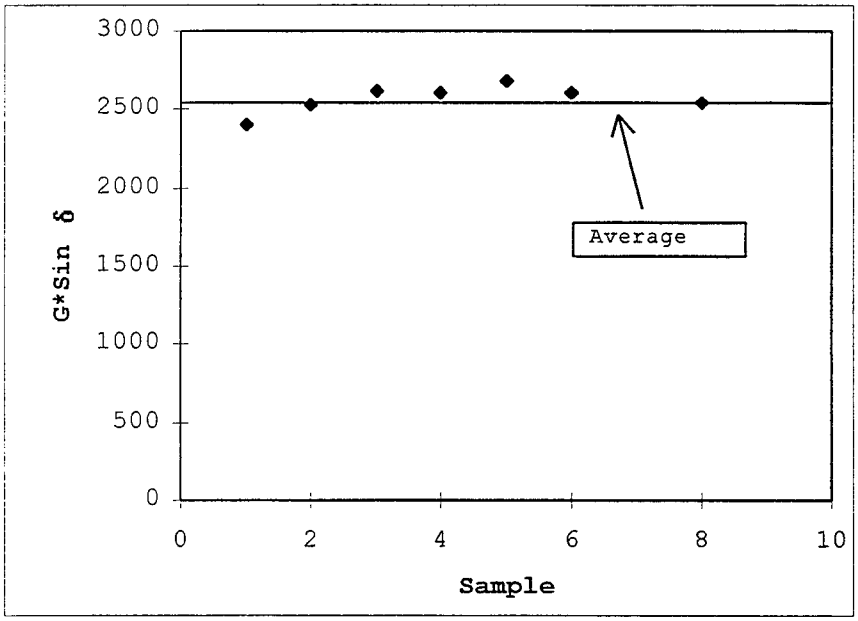

Figure A4.1 Data Distribution of DSR Test on PAV-Aged Mix Binder, Second Run, at 19°C

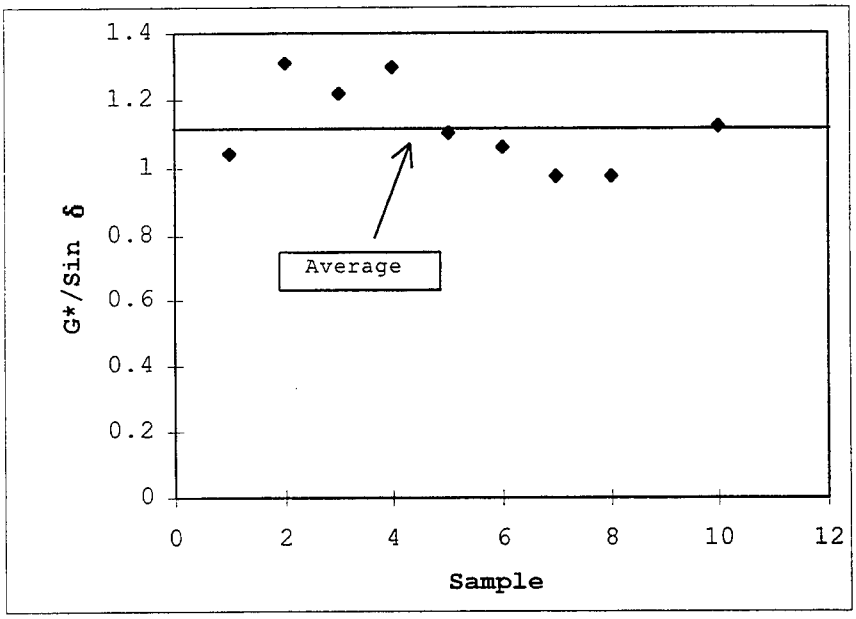

Figure A11.1 Data Distribution of DSR Test on Original Tank Asphalt, 64°C

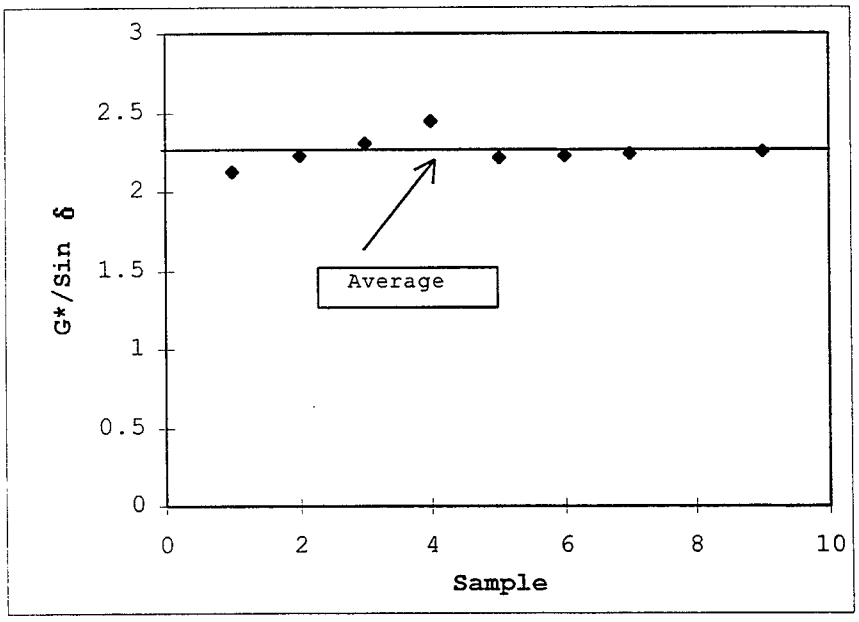

Figure A12.1 Data Distribution of DSR Test on Original Tank Asphalt (RTFO), at 64°C

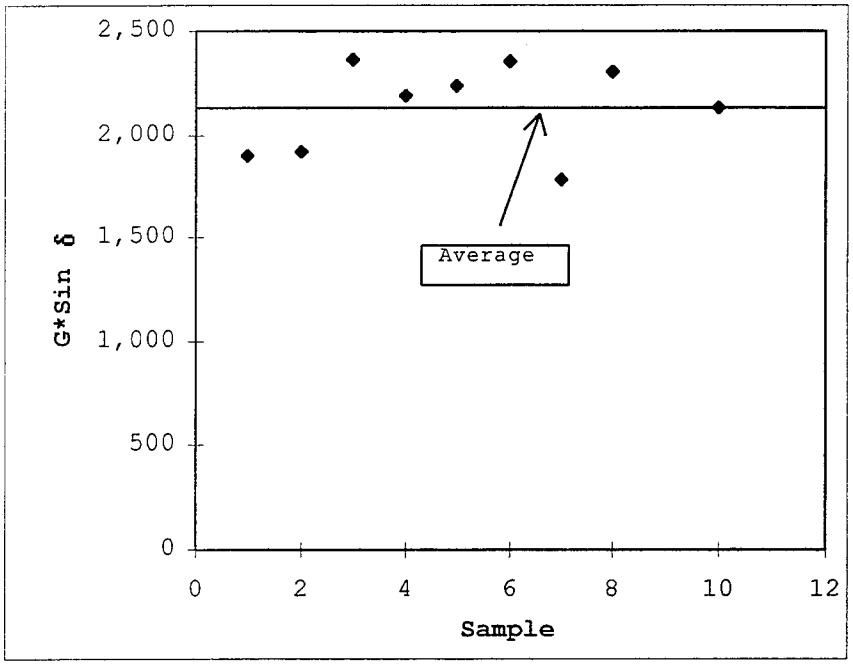

Figure A13.2 Data Distribution of DSR Test on Original Tank Asphalt (PAV), at 19°C

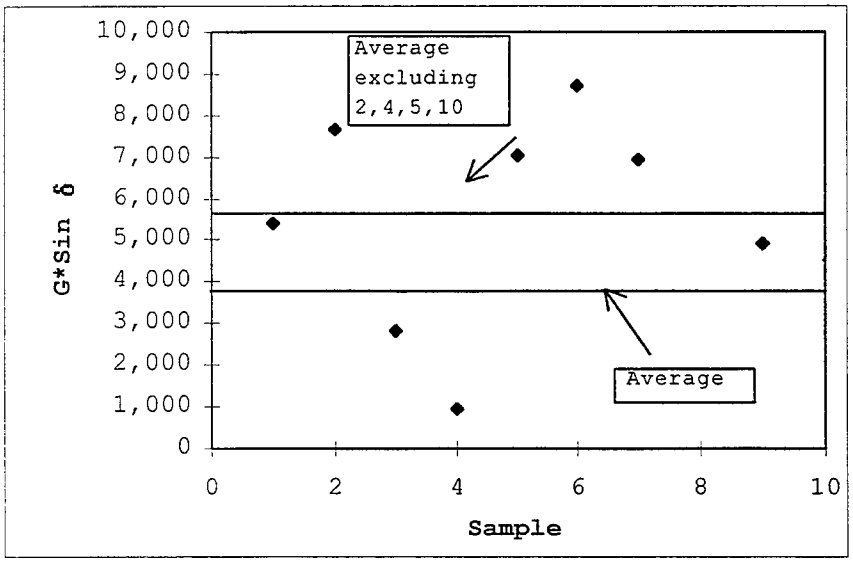

Figure A15.1 Data Distribution of DSR Test on Old Pavement Surface Binder, at 7°C

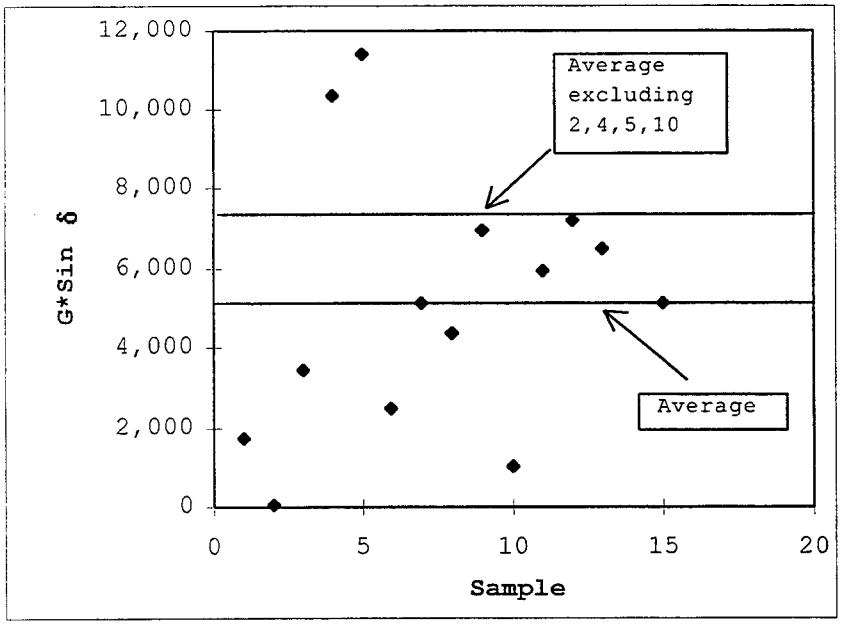

Figure A15.2 Data Distribution of DSR Test on Old Pavement Surface Binder, at 10°C

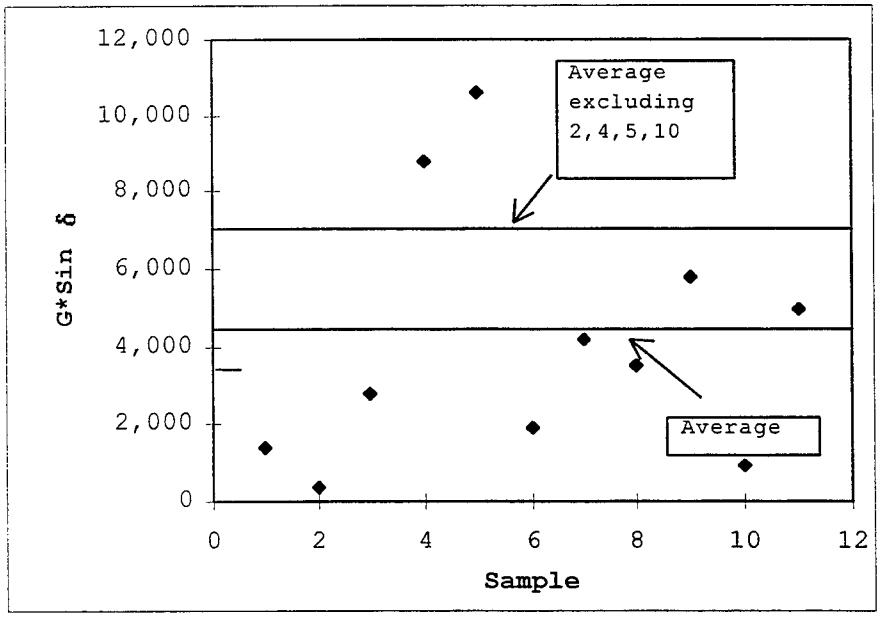

Figure A15.3 Data Distribution of DSR Test on Old Pavement Surface Binder, at 13°C

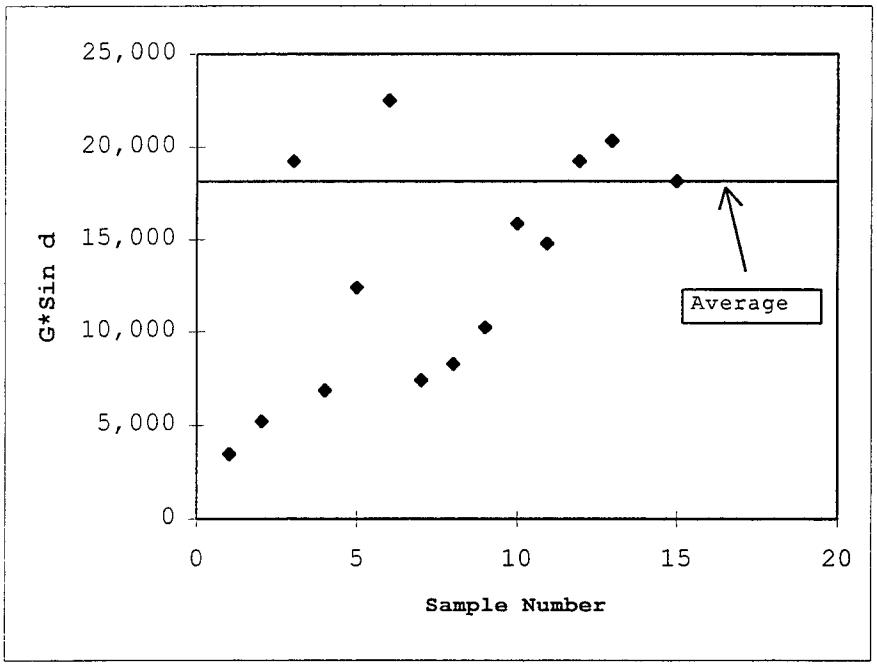

Figure A17.1 Data Distribution of DSR Test on
Old Pavement Intermediate Binder, at 7°C

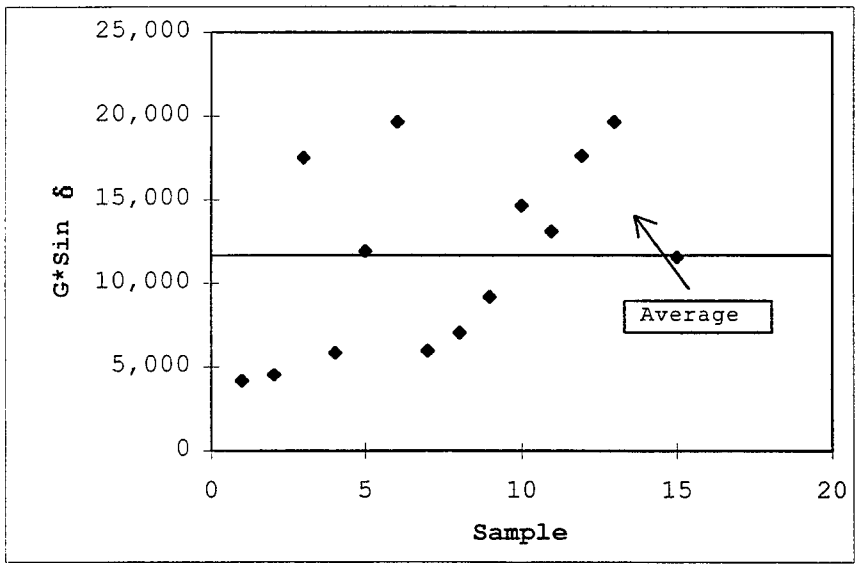

Figure A17.2 Data Distribution of DSR Test on
Old Pavement Intermediate Binder, at 10°C

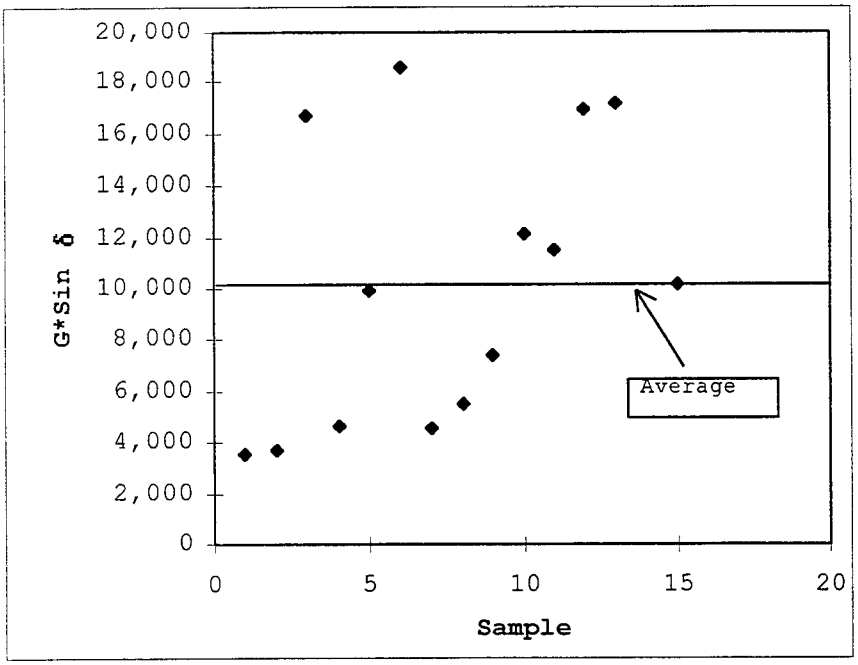

Figure A17.3 Data Distribution of DSR Test on
Old Pavement Intermediate Binder, at 13°C

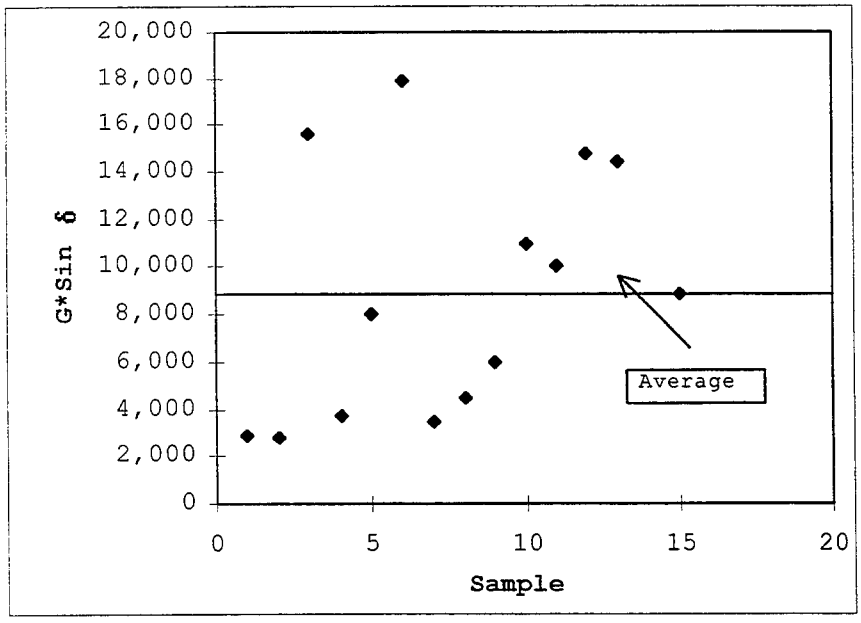

Figure A17.4 Data Distribution of DSR Test on
Old Pavement Intermediate Binder, at 16°C

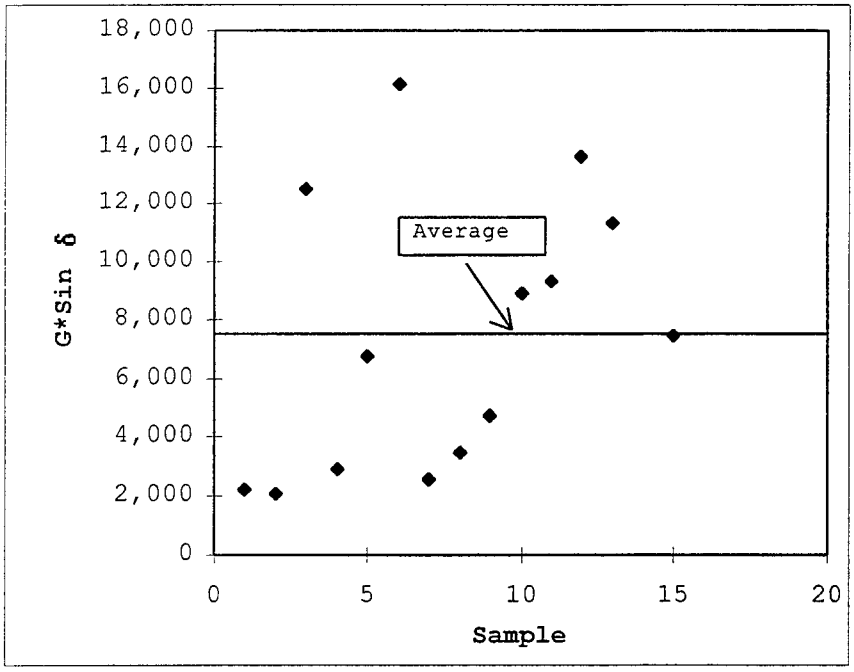

Figure A17.5 Data Distribution of DSR Test on Old Pavement Intermediate Binder, at 19°C

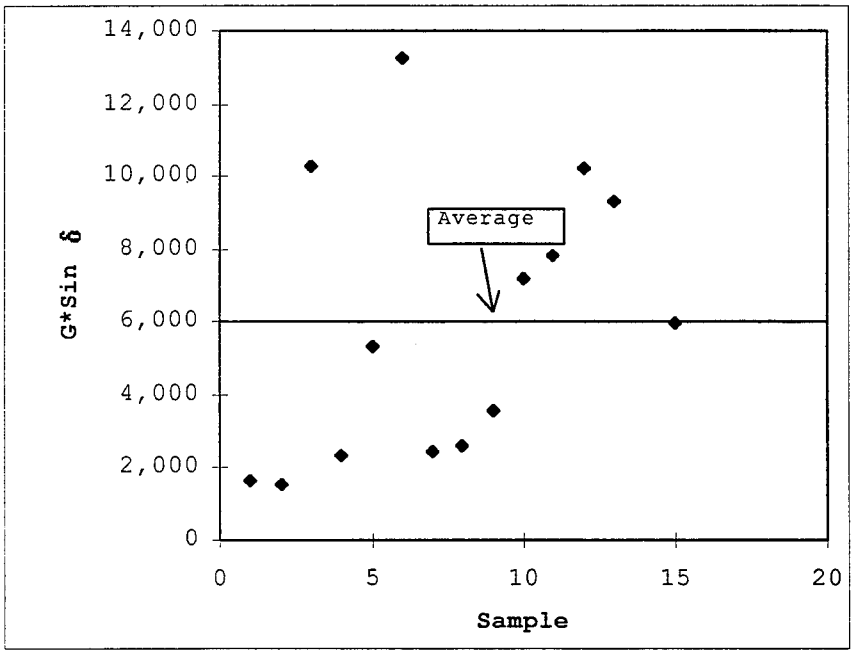

Figure A17.6 Data Distribution of DSR Test on Old Pavement Intermediate Binder, at 22°C

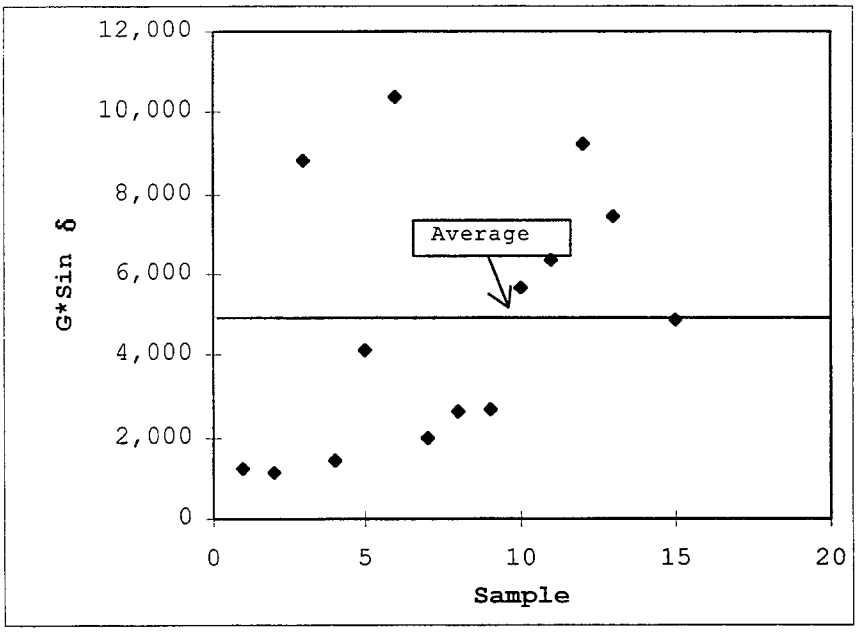

Figure A17.7 Data Distribution of DSR Test on
Old Pavement Intermediate Binder, at 25°C

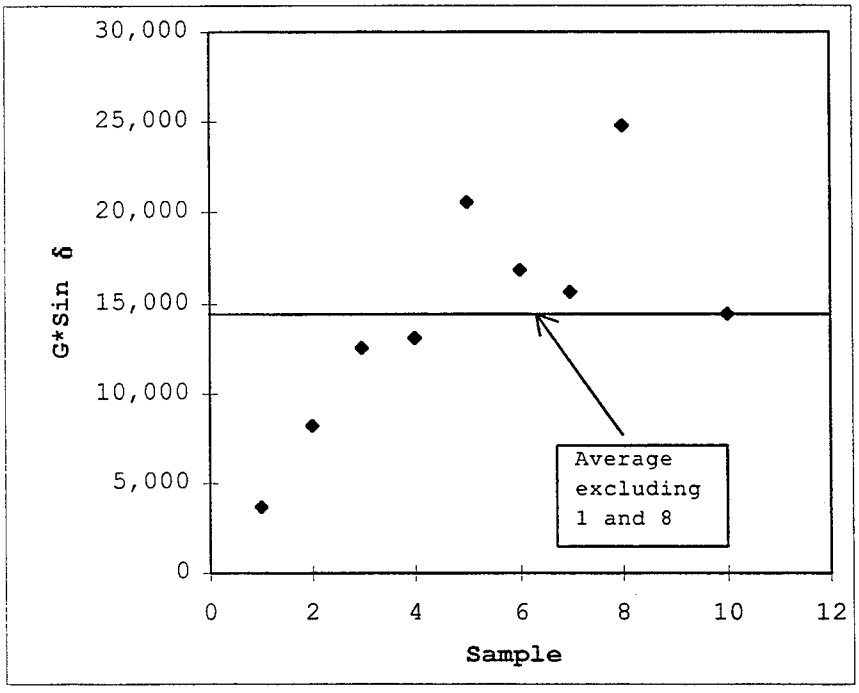

Figure A19.1 Data Distribution of DSR Test on
Old Pavement Base Binder, at 7°C

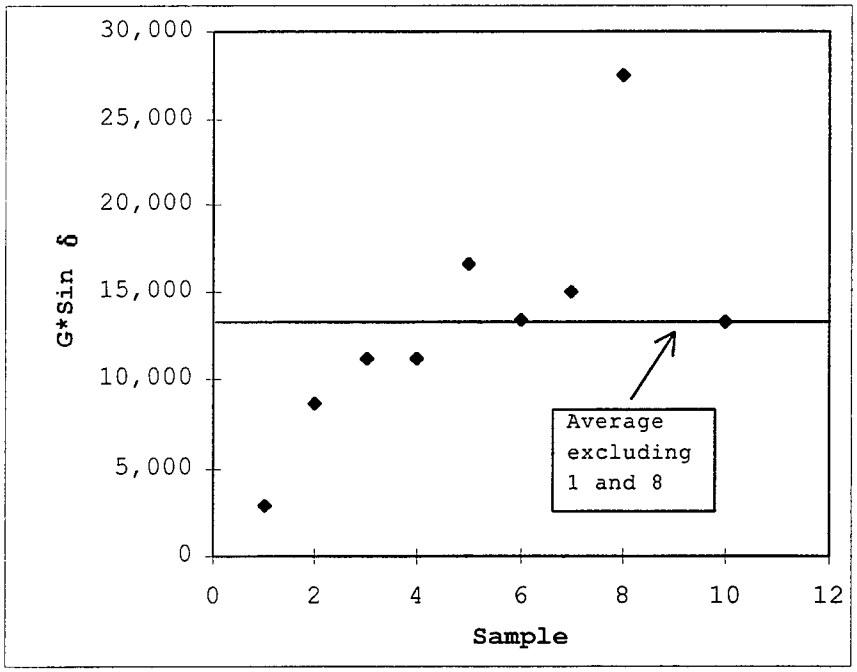

Figure A19.2 Data Distribution of DSR Test on
Old Pavement Base Binder, at 10°C

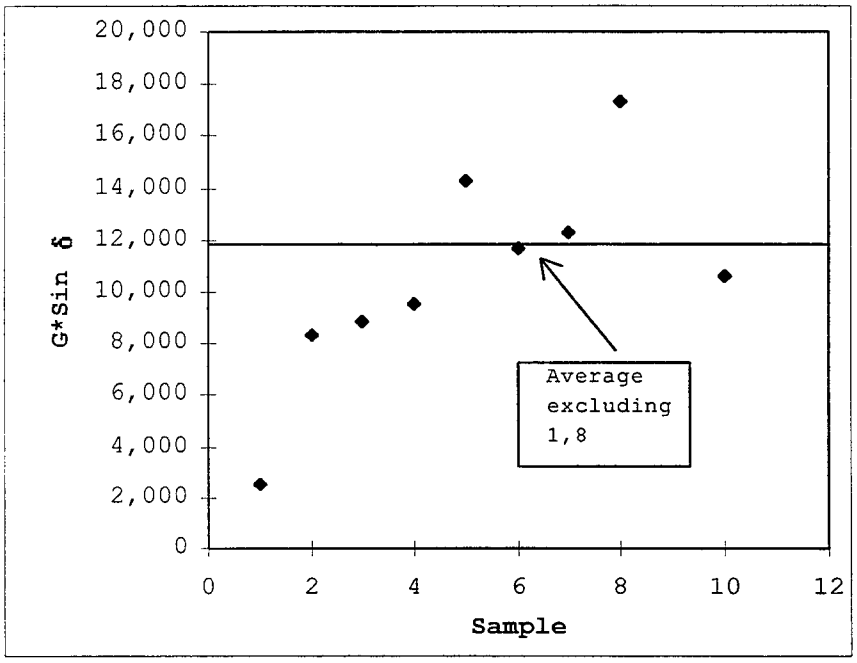

Figure A19.3 Data Distribution of DSR Test on
Old Pavement Base Binder, at 13°C

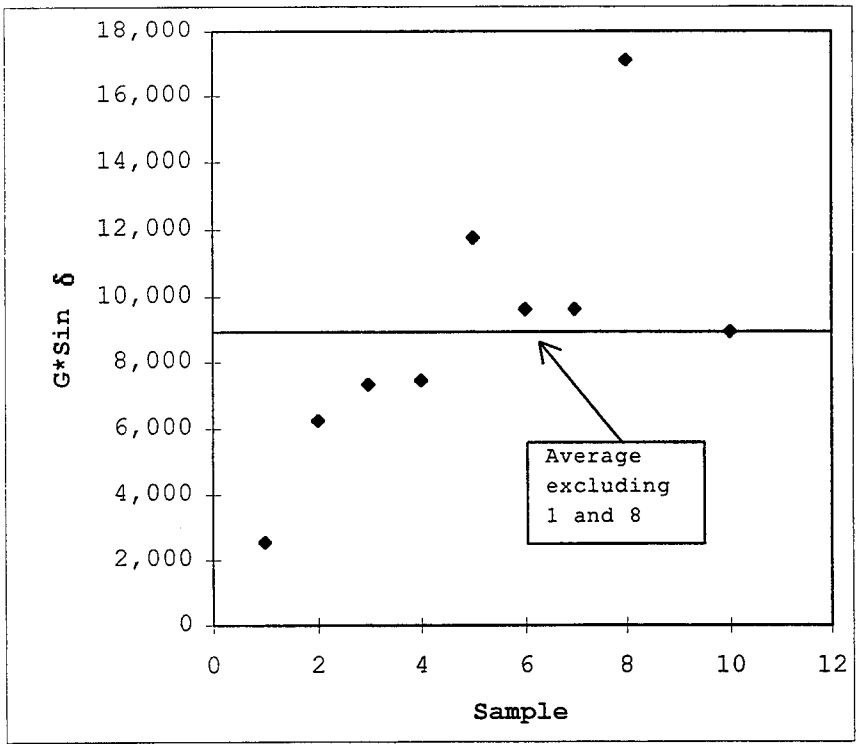

Figure A19.4 Data Distribution of DSR Test on
Old Pavement Base Binder, at 16°C

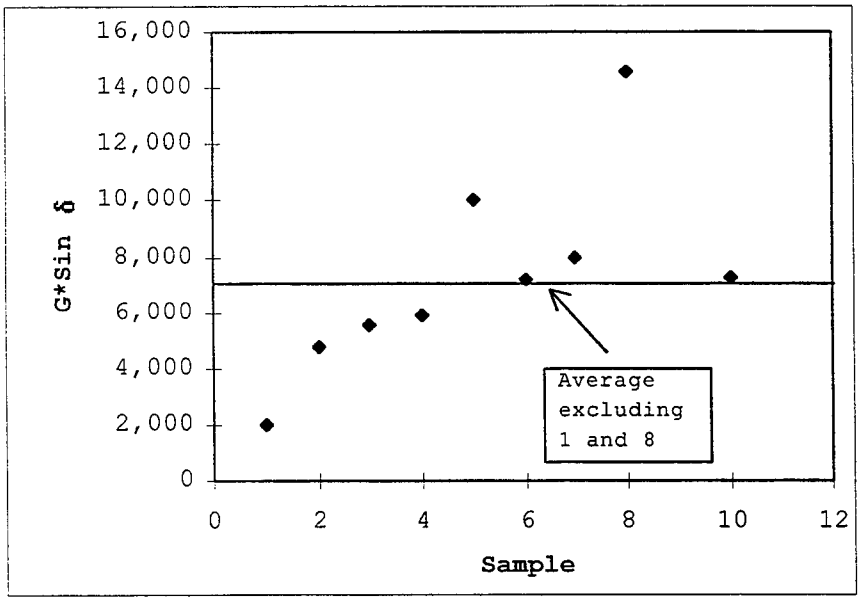

Figure A19.5 Data Distribution of DSR Test on
Old Pavement Base Binder, at 19°C

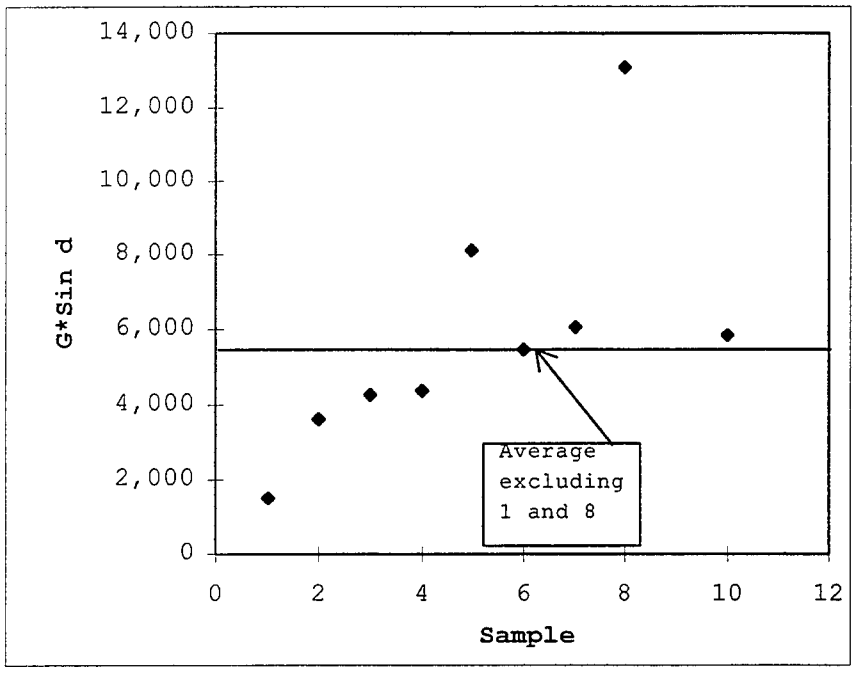

Figure A19.6 Data Distribution of DSR Test on
Old Pavement Base Binder, at 22°C

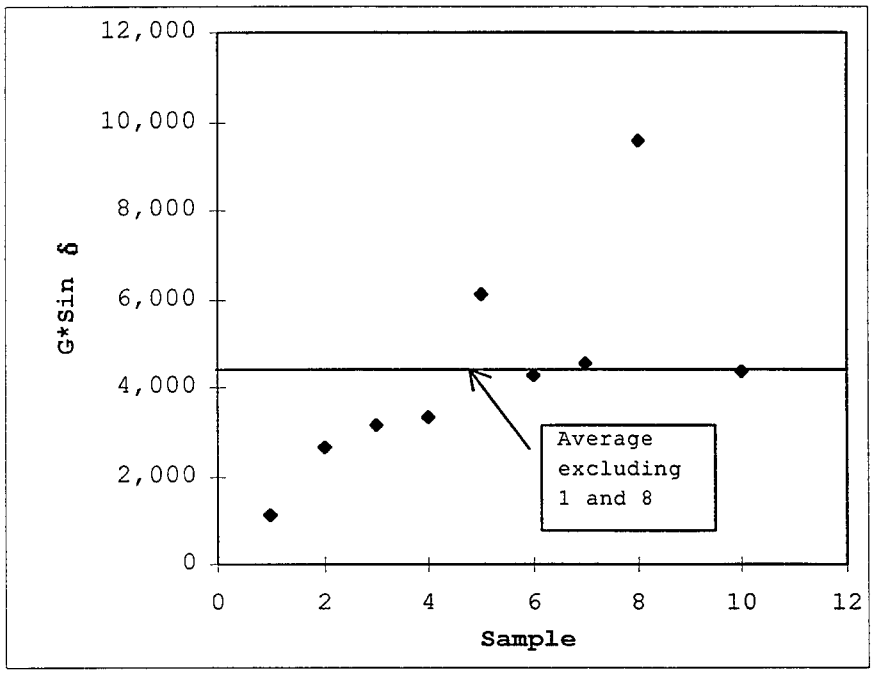

Figure A19.7 Data Distribution of DSR Test on
Old Pavement Base Binder, at 25°C

APPENDIX B – TECHNICAL NOTES ON INSTRUMENTATION

APPENDIX B - TECHNICAL NOTES ON INSTRUMENTATION

B.1 Datalogger Operating System

The operating software was downloaded to the CR10X unit before installing the datalogger at the site. The datalogger uses a special code that can be typed directly via CR10KD (CR10 Key Board) or can be created on separate computer using PC208 software provided by Campbell Scientific and then downloaded. The datalogger in general performs a set of sensor readings and stores the data into input locations. Processing instructions are applied to the values at the input locations. The processed values are then stored until downloaded. The operating program consists of a set of instructions to perform the readings and direct the acquired values into the final storage. The program consists of two main instruction Tables (Table 1 and 2) and a third instruction Table for subroutines (Table 3). Following is a listing of the program used on the I-64 site with the previously mentioned set of sensors. Note that if different type or number of sensors were used, this program would have to be modified.

Table B.1.1 CR10 Operating Program for I-64 Site

```
;{CR10}
*Table 1 Program
 01: 60.0     Execution Interval (seconds)

1: Volt (Diff) (P2)
 1: 1        Reps
 2: 22       ± 7.5 mV 60 Hz Rejection Range
 3: 4        DIFF Channel
 4: 4        Loc [ Sol_Rad   ]
 5: 200      Mult
 6: 0        Offset

2: If time is (P92)
 1: 0        Minutes (Seconds --) into a
 2: 15       Interval (same units as above)
 3: 1        Call Subroutine 1

3: If time is (P92)
 1: 600      Minutes (Seconds --) into a
 2: 1440     Interval (same units as above)
 3: 43       Set Port 3 High

4: If time is (P92)
 1: 660      Minutes (Seconds --) into a
 2: 1440     Interval (same units as above)
 3: 53       Set Port 3 Low

*Table 2 Program
 02: 0.0     Execution Interval (seconds)

*Table 3 Subroutines

1: Beginning of Subroutine (P85)
 1: 1        Subroutine 1

2: Temp (107) (P11)
 1: 2        Reps
 2: 4        SE Channel
 3: 1        Excite all reps w/Exchan 1
 4: 1        Loc [ Ref_Temp  ]
 5: 1        Mult
 6: 0        Offset
3: Do (P86)
```

1: 44 Set Port 4 High

4: Excitation with Delay (P22)
1: 1 Ex Channel
2: 0 Delay W/Ex (units = 0.01 sec)
3: 15 Delay After Ex (units = 0.01 sec)
4: 0 mV Excitation

5: Volts (SE) (P1)
1: 1 Reps
2: 5 ± 2500 mV Slow Range
3: 6 SE Channel
4: 3 Loc [RH]
5: 0.1 Mult
6: 0 Offset

6: Do (P86)
1: 54 Set Port 4 Low

7: Do (P86)
1: 41 Set Port 1 High

8: Beginning of Loop (P87)
1: 0 Delay
2: 14 Loop Count

9: Do (P86)
1: 72 Pulse Port 2

10: Excitation with Delay (P22)
1: 1 Ex Channel
2: 2 Delay W/Ex (units = 0.01 sec)
3: 0 Delay After Ex (units = 0.01 sec)
4: 0 mV Excitation

11: Thermocouple Temp (DIFF) (P14)
1: 1 Reps
2: 2 ± 7.5 mV Slow Range
3: 1 DIFF Channel
4: 1 Type T (Copper-Constantan)
5: 1 Ref Temp Loc [Ref_Temp]
6: 5 -- Loc [TCE1]
7: 1.0 Mult
8: 0 Offset

12: Excite-Delay (SE) (P4)
1: 1 Reps
2: 5 ± 2500 mV Slow Range
3: 3 SE Channel
4: 2 Excite all reps w/Exchan 2
5: 0 Delay (units 0.01 sec)
6: 2500 mV Excitation
7: 19 -- Loc [TS1]
8: 1 Mult
9: 0 Offset

13: End (P95)

14: Do (P86)
1: 51 Set Port 1 Low

15: Batt Voltage (P10)
1: 26 Loc [Bat_Vol]

16: Do (P86)
1: 10 Set Output Flag High

17: Real Time (P77)
1: 110 Day,Hour/Minute

18: Sample (P70)
1: 3 Reps
2: 1 Loc [Ref_Temp]

19: Average (P71)
1: 1 Reps
2: 4 Loc [Sol_Rad]

20: Sample (P70)
1: 21 Reps
2: 5 Loc [TCE1]

21: Sample (P70)
1: 1 Reps
2: 26 Loc [Bat_Vol]
22: End (P95)
End Program

-Input Locations-
1 Ref_Temp 5 2 1
2 RH_Temp 17 1 1
3 RH 1 1 1
4 Sol_Rad 1 1 1
5 TCE1 5 1 1
6 TCW1 1 1 0
7 TCE2 1 1 0
8 TCW2 1 1 0
9 TCE3 1 1 0
10 TCW3 1 1 0
11 TCE4 1 1 0
12 TCW4 1 1 0
13 TCE5 1 1 0
14 TCW5 1 1 0
15 TCE6 1 1 0
16 TCW6 1 1 0
17 TCE7 1 1 0
18 TCW7 1 1 0
19 TS1 1 1 1
20 TS2 1 1 0
21 TS3 1 1 0
22 TS4 1 1 0
23 TS5 1 1 0
24 TS6 1 1 0
25 TS7 1 1 0
26 Bat_VoL 1 1 1
27 _____ 0 0 0
28 _____ 0 0 0
-Program Security-
0000
0000
0000
-Mode 4-
-Final Storage Area 2-
0

B.2. Telecommunication with the Site

The site is located on I-64 and equipped with a CR10X datalogger, a DC112 modem and a cellular phone with an established phone number through a cellular provider. On the other end, at Purdue University, a PC computer is set up with a modem connected to a regular phone line, with PC208 software. The software contains several modules. Either of GT (Graphic Terminal Ver 3.0) program or Telcom (Telecommunication Ver 7.2) program could be used to connect to the site.

The modem uses an initialization file "modem.ini" with the following lines:

AT&F
AT&K0&C1&D0&V0

The set of commands for communication with the site is stored in the file "I64.stn", so called station file, shown in Table B.2.1. The CR10X datalogger provides storage area that can be partitioned into two final storage areas named final storage area 1 and 2. In our case, all final storage space was allocated to final storage area 1. The commands in the I64.stn file specify downloading data from final storage area 1 in ASCII comma delineated format. Dialing from Purdue requires dialing "9" for external signal, therefore the site telephone number was included in the I64 station file as "9,xxx-xxxx" where the "," represents 2 seconds modem hold.

Table B.2.1 I-64 Station File "I64.stn"

Required Parameters	Station Parameter
Telecommunication Parameters for station	I64
Datalogger Type	CR10
Use Asynchronous Communication Adapter	COM3
Communications Baud Rate	1200
Data File Format	Comma Delineated ASCII
Final Storage Area	Area 1
Interface Device	Hayes Modem
Number	9,xxx-xxxx

In the CR10 operating program shown above, the phone was setup to be turned on by a relay for one hour (from 10 am to 11 am) daily. However, if no communication is established with the phone, the phone would only drain 0.38 amps (standby mode). In case the communication is established, the phone would drain 2.1 amps (on-line mode). Therefore, it is recommended that the on-line time should be kept to a minimum as the battery used provides only about 80 amp.hour of reserve capacity. The datalogger system will shut down if the voltage drops below 9.6 volts. The use of a solar panel on this site provides more security and constantly recharges the battery to around 14.0 volts in peak recharge time.

B.3 Data Downloading and Formatting

The data is stored in an ASCII format. It is downloaded in the same format. It is then inserted into a spreadsheet which parses the data into separate columns. The order of data in the final storage is the same as in the input location storage as described below.

B.4 Sensor Information

The following table (Table B.4.1) shows the models and brief description for each type of sensor used in this study. The input locations are also indicated. All equipment was purchased from Campbell Scientific, Inc., except the pavement thermistors, which were purchased from Omega Engineering, Inc.

All the probes were supplied with the wiring and operating manuals. Since the thermistors were purchased from Omega and had to be adapted to the Campbell datalogger, additional resistors had to be added. The thermistors operation is described in the following section.

B.5 Thermistor Operation

Since the datalogger was supplied by a different company, it could not take the thermistors input without adding additional resistors to the circuit.

The thermistor probes supplied by Omega are actually composed of two thermistor-composites ($R_{c1}$and R_{c2}), as shown in Figure B.5.1. The probe also contains

two resistors R_1 and R_2. The circuit shown in Figure B.5.1 would linearize the response of the thermistor probe in a given range depending on the combination of resistors used as shown in Table B.5.1 below.

Table B.5.1 Resistor Combination for Linearizing Temperature Response

Resistor Kit (Omega Reference number)	Fixed Resistors	Temperature Linear Range
44201	R_1 = 3200 Ω R_2 = 6250 Ω	0 to 100°C
44203	R_1 = 18,700 Ω R_2 = 35,250 Ω	-30 to 50°C

Although the circuit in Figure B.5.1 could linearize the thermistor's response over relatively wide range of temperatures, the standard circuit solution equation provided by Omega (Equation B.5.1) is applicable only in the temperature range shown in Table B.5.1.

Since these ranges did not cover the expected range of temperature for the pavement, a custom equation was developed utilizing the 44203 resistor kit. The original Equation provided by Omega for this kit was in the form:

$$E_{out}\text{-}ve = -0.0067966\, E_{in}\, T + 0.65107\, E_{in} \qquad \text{(B.5.1)}$$

In order to develop a new set of correlation coefficients for the custom equation, the following equation needed to be evaluated:

$$T = a + b_1 E + b_2 E^2 + b_3 E^4 + b_4 E^6 + b_2 5E^8 + b_6 E^{10} + b_7 E^{12} + b_8 E^{14}$$

(B.5.2)

Where,

T = temperature (°C)

E = $E_{out\text{-}ve}$ divided by E_{in}.

This equation represents a 14th order polynomial in which parameter, E, is a function of resistance of thermistor composite resistors R_{c1} and R_{c2}. The solution process required the use of previously established relationship between resistance and temperature for R_{c1} and R_{c2} components. The relationship was supplied by Omega (22), and was utilized in circuit equation shown below (Equation B.5.3). This equation provides the value of E_{out}-ve for every temperature point analyzed.

$$E_{out}\text{-}ve = Ein \frac{(R_2 + R_{c1})}{R_{c1} + R_{c1} + R_2} \frac{1}{R_T} \quad \text{(B.5.3)}$$

Where,

$$R_T = \frac{R_1 R_{c1} + R_1 R_{c2} + R_1 R_2 + R_2 R_{c2} + R_{c1} R_{c2}}{R_{c1} + R_{c2} + R_2} \quad \text{(B.5.4)}$$

Where,

E_{in} = excitation voltage (taken 2500 mV),

$E_{out\text{-}ve}$ = voltage across part of the circuit (see Figure B.5.1),

R_1, R_2 = fixed resistors,

R_{c1}, R_{c2} = thermistor composite resistors,

R_T = total resistance of the circuit.

A total of 130 temperature-resistance (-30°C to 100°C) points were used in establishing the correlation coefficient for the custom Equation B.5.2. The resulting R^2-value was 0.999997, indicating a high degree of correlation between parameter E and temperature. The coefficients established for the custom equation are given in Table B.5.2

Table B.5.2 Correlation Coefficients for the Custom Equation

Coefficient	Value
a	148.7
b_1	-660.5
b_2	1579.4
b_3	-7454.9
b_4	35993.6
b_5	-120899
b_6	259813.9
b_7	-338166
b_8	242021.6
b_9	-72985.9

Figure B.5.2 shows the plots of both the custom equation (Equation B.5.2) and Omega linear equation (Equation B.5.1) for the 44203 resistor kit for the temperatures varying from -30°C to 100°C. Both curves are essentially identical for the range of temperatures from -30°C to 50°C. The temperature error for the linear Omega equation is 0.15°C while the temperature error for the custom equation ranges from 0.08°C to -0.12°C. However, the custom curve deviates significantly from the Omega curve for the temperature range from 50°C to 100° C. As shown in Figures B.5.3 and B.5.4, the error associated with the use of Omega equation in that range is much larger than this associated with the use of the custom equation due to non linear response of thermistors in that range.

Since the custom equation was more accurate, it was used in connection with the thermistor data.

B.5.1 Thermistor Wiring Circuits

Figure B.5.1.1 shows a schematic of the thermistor wiring. One R_1 resistance was used between the AM416 and the CR10. However seven R_2 were used, each connected to one thermistor.

B.5.1 Thermistor Wiring Circuits

Figure B.5.1.1 shows a schematic of the thermistor wiring. One R_1 resistance was used between the AM416 and the CR10. However seven R_2 were used, each connected to one thermistor.

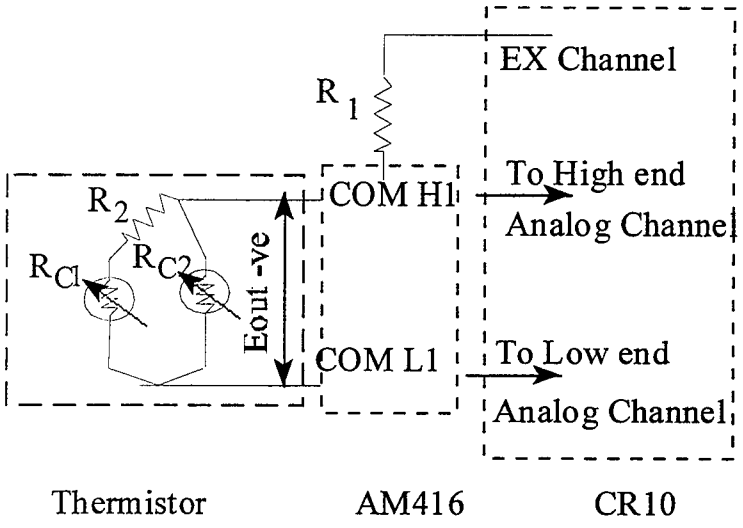

Figure B.5.1.1 Thermistor Connections

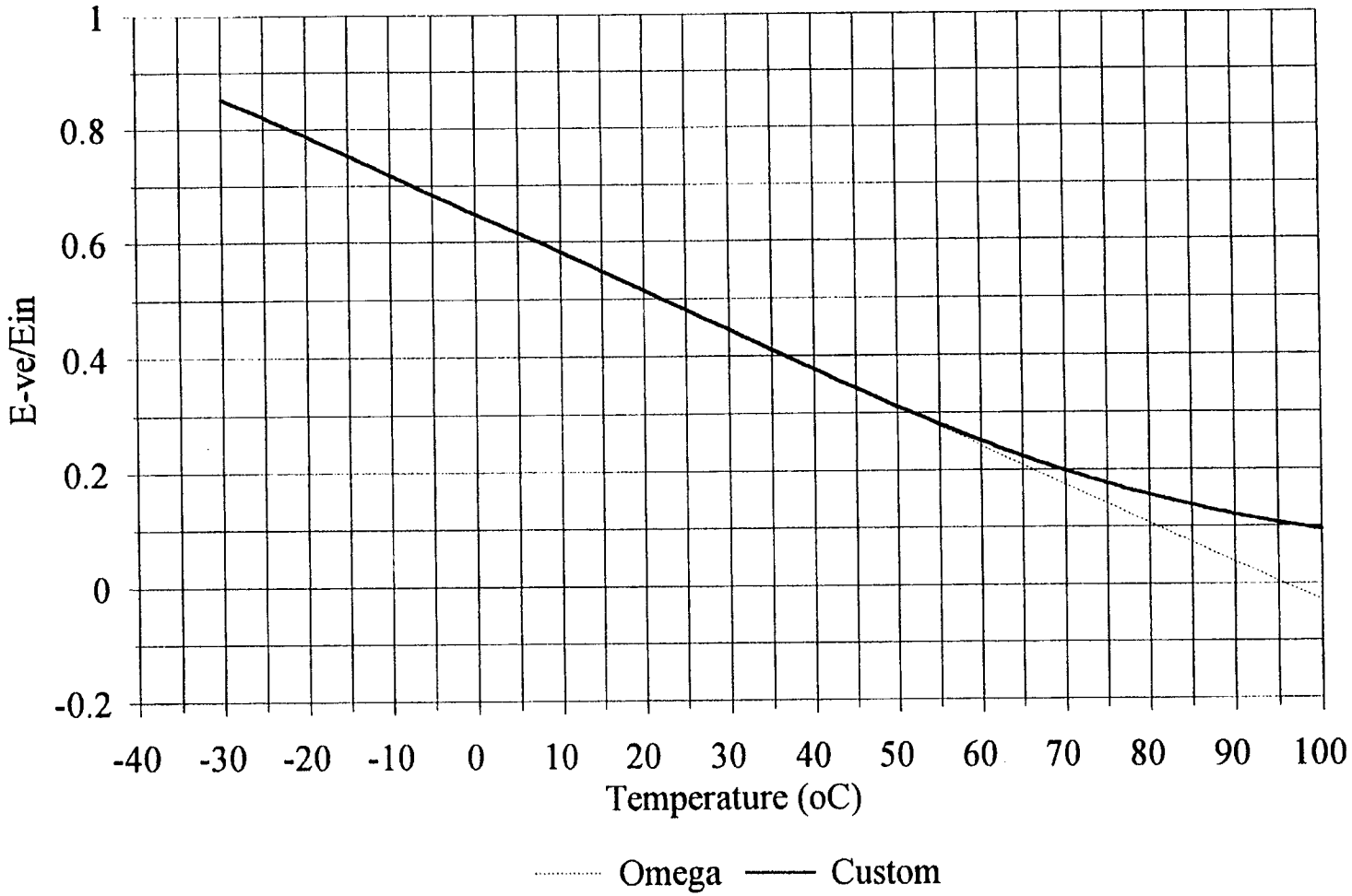

Figure B.5.2 Comparison of Omega and Custom Regression Equation

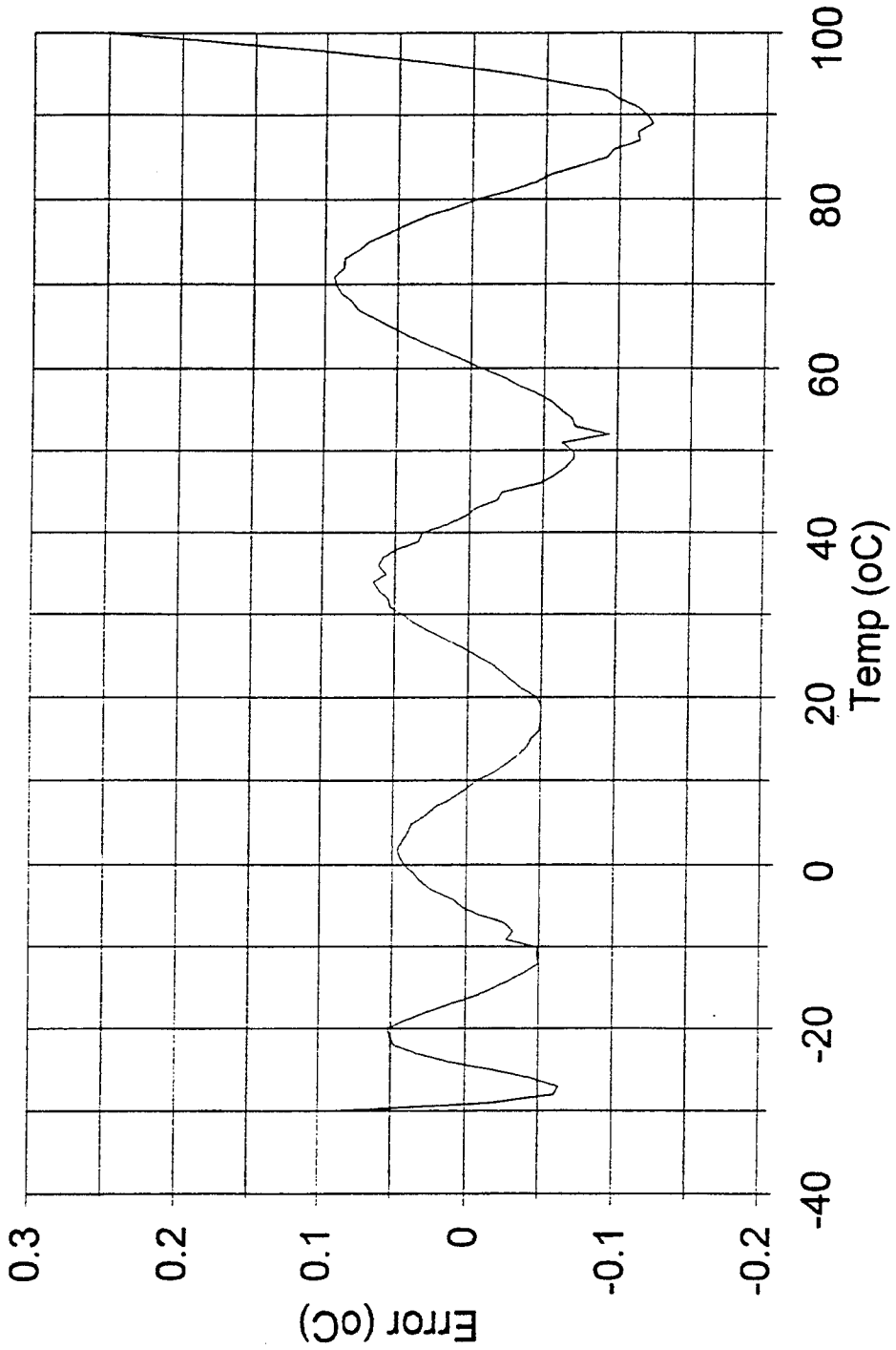

Figure B.5.3 Error in Estimated Temperature from Custom Regression Model

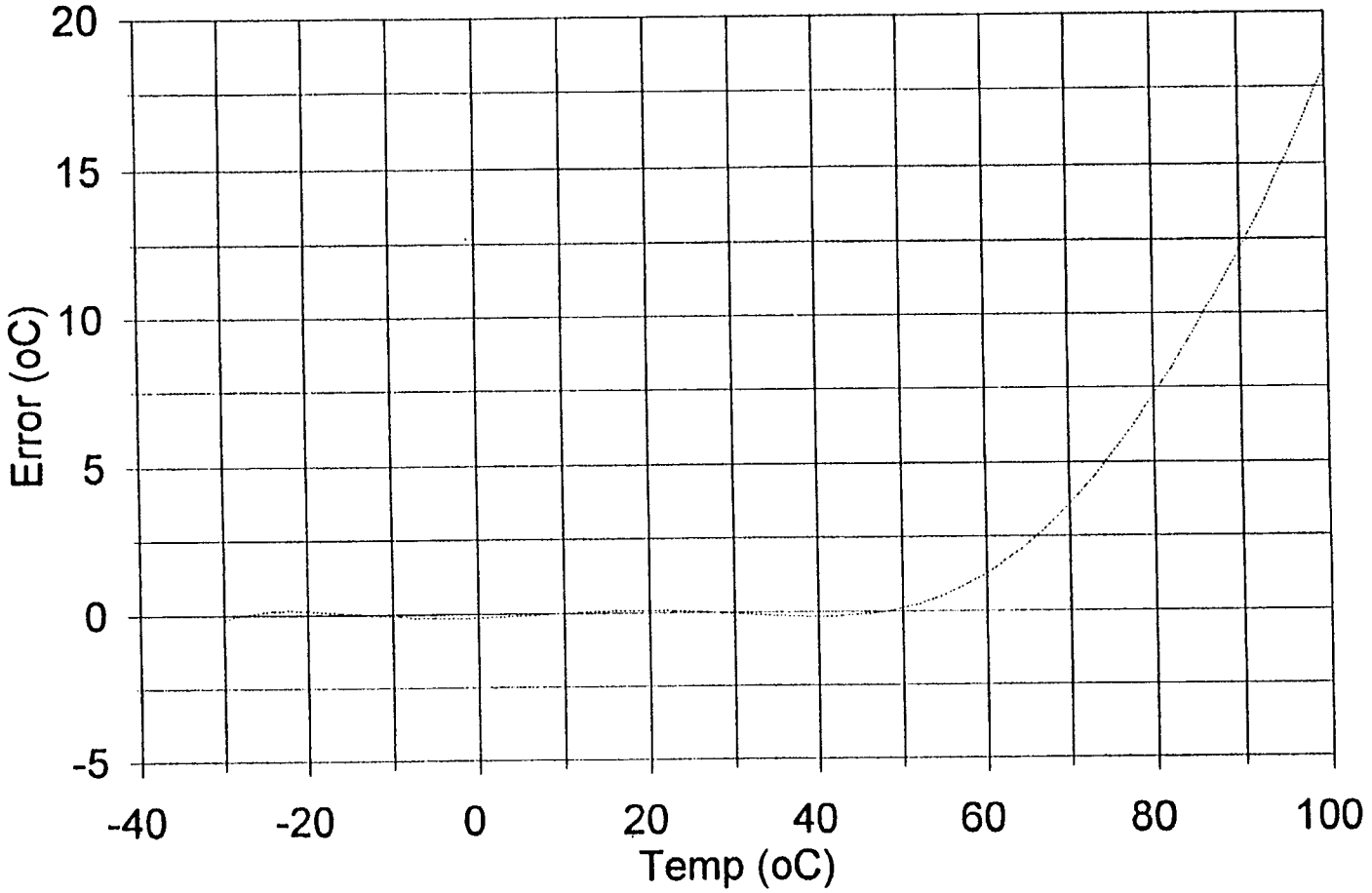

Figure B.5.4 Error in Estimated Temperature from Omega Linear Model

APPENDIX C – EVALUATION OF LOW-TEMPERATURE CRACKING POTENTIAL

APPENDIX C - EVALUATION OF LOW TEMPERATURE CRACKING POTENTIAL

The project discussed in this report is a 21-km stretch of highway I-64 in southwestern Indiana, which showed considerable pavement distress due to thermal cracking. As a part of the rehabilitation scheme for this stretch of the highway, the cracked, upper 50-mm thick layer was removed and overlaid with Superpave mix with PG 64-34 binder. This was the binder specified for the project location utilizing the Superpave binder selection program. Installation of temperature probes in the pavement and weather station allowed the air and pavement temperatures to be continuously monitored.

In the Superpave methodology, binder selection is driven by low and high pavement temperature prediction algorithms developed during SHRP research. The current Superpave procedure assumes that the design minimum pavement temperature is the same as the minimum air temperature. Comparisons between minimum air and observed pavement temperatures at test sites from all over United States and Canada have shown this to be a very conservative estimate. It has been observed that minimum pavement temperatures are considerably warmer (about 10°C) than minimum air temperatures. Some performance graded binders are capable of withstanding very low temperatures. Such binders tend to be modified, which will often double their prices. Improper and extremely conservative estimates of pavement temperatures could lead to unnecessary project expense.

C.1. Evaluation of Pavement Temperature Algorithms

In this section, the existing pavement temperature algorithms are evaluated using data collected from the existing weather station. The station has been in service since its installation in 1996 and records air temperature, humidity and solar radiation at every 15-

minute intervals. Pavement temperatures detected by the temperature sensors installed at various depths in the pavement are also recorded. Though both thermistors and thermocouples were installed, only the data collected from thermocouples were used for validation, since not all the thermistors were functional. Figure C.1 shows the location of these thermocouples in the pavement.

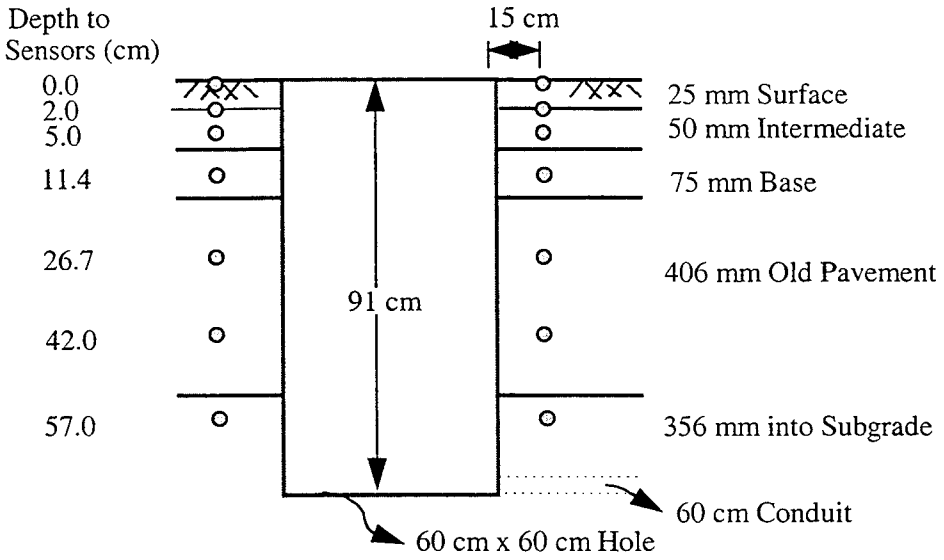

Figure C.1. Location of thermocouples in the pavement

The existing low pavement temperature prediction models evaluated in this report are a) SHRP Model and C-SHRP Model b) LTPP (SMP) Model c) Han Model and d) University of WI Model. Only low temperature models will be discussed in this report.

C.1.a. SHRP and C-SHRP Models

The SHRP model was based on theoretical heat transfer modelling and regression analysis. The factors considered in developing this model were air temperature, latitude, solar absorption and wind speed. The model assumes solar radiation of 0.9 W/m^2 and wind speed of 4.5 m/s. SHRP model uses the mean lowest air temperature as the design low

pavement temperature at the surface, for any given site. This overestimates the pavement temperature and is thus a very conservative. The Canadian SHRP or C-SHRP model developed by W. Robertson (1) is preferred, which is as follows:

$$T_{min} = 0.859\ T_{air} + 1.7$$

where T_{min} = Low AC pavement temperature at the surface, °C,

T_{air} = Mean low air temperature, °C.

C.1.b. LTPP (SMP) Model

The Seasonal Monitoring Program (SMP) of LTPP was commenced in 1991 and included 30 test sites in its initial phase. Its objective was to validate of models relating environmental conditions and field properties of pavement materials by providing data gathered at various sites located all over North America. This model is an empirical model developed by A. Mohseni and M. Symons (2, 3) and accounts for different environmental factors, similar to the SHRP model. However, in contrast to SHRP model, solar absorption and wind speed were not assumed.

Using the LTPP model, the low pavement temperature at any depth is estimated by:

$$T_{min} = -1.56 + 0.72\ T_{air} - 0.004\ lat^2 + 6.26\ \log(H+25) + z\ (4.4 + 0.52\sigma^2_{air})^{0.5}$$

where T_{min} = Low AC pavement temperature at any depth H, °C

T_{air} = Mean low air temperature, °C

Lat = Latitude of the test section, degrees

H = Depth to surface, mm

σ_{air} = Standard deviation of the mean low air temperature, °C

z = Standard normal distribution value, z = 2.055 for 98% reliability

Range of surface temperatures considered during the development of the model varied from –65° to 10°C and the maximum difference between air and pavement surface temperatures was limited to 35°C. This model ensures that pavement temperatures increase with depth.

Data from other SMP sites were used to validate this model. The temperature estimates given by LTPP model were compared to the estimates obtained from SHRP and C-SHRP models. SHRP estimates were about 12°C higher (more negative) than SMP model,

while C-SHRP model estimates were about 8°C higher (at high latitudes). At higher latitudes, differences between C-SHRP and LTPP model were more significant. It was also observed that, for depths greater than 200 mm the pavement temperatures predicted by SHRP model were disproportionately high.

C.1.c. Han Model

This model was developed by E. Lukanen and C. Han of the Braun Intertec Corporation and E. Skok, Jr. of the Minnesota Asphalt Pavement Association (4). They used the same database as the LTPP model, but included 15 additional sites for validation purposes. They chose a single minimum and maximum temperature point from each season whereas Mohseni and Symons chose several points in developing their model. Therefore, the results provided by Han model are similar to those of LTPP model, though the final form of the equation is slightly different. The equation for predicting minimum pavement temperatures at any depth are:

$$T_{d(min)} = -0.15 - 1.9\,\phi + 0.06\,\phi^2 - 0.0007\,\phi^3 + 0.59\,T_{a(min)} + 5.2\,\ln(d + 25)$$

where $T_{d(min)}$ = Minimum pavement temperature at any depth, °C,

$T_{a(min)}$ = Low air temperature, °C.

ϕ = Latitude, degrees

d = Depth from surface, mm

C.1.d. University of WI Model

This model was developed by P. Bosscher, et al. (5), of the Asphalt Pavement Research Group at the University of Wisconsin. It was based on two, instrumented test sections constructed on US-53 in Trempealeau County, WI. This model was developed from data collected for 22 months, with temperature probes inserted only up to a depth of 100 mm. The equation for low pavement temperature is

$$T_{d(min)} = T_{pav@6.4mm(min)} - [0.00123\,T_{pav@6.4mm(min)}\,(d - 6.4)] + 0.0146\,(d - 6.4)$$

where $T_{d(min)}$ = Minimum pavement temperature at any depth, °C,

$T_{pav@6.4mm(min)}$ = Minimum pavement temperature at depth of 6.4 mm, °C,

$= 0.768 + 0.687\ T_{air(min)}$

$T_{air(min)}$ = Minimum air temperature, °C

d = depth from surface, mm

This model is valid only when the air temperature is below –5°C. Predictions made by U. of WI model (UW model) at a depth of 6.4 mm were compared with estimates obtained from LTPP and SHRP models at the same depth. Comparisons were also made with observed pavement temperatures at a depth of 6.4 mm. Good correlation was found between LTPP and UW models and with observed pavement temperatures. SHRP model predicted much colder temperatures and did not show good agreement with observed pavement temperatures.

C.2. Evaluation of Temperature Models using Test Site Data

For the purpose of analysis, the air temperature values recorded at a nearby Evansville weather station were used. Data at this station have been recorded for over 42 years. The mean of the lowest annual temperatures during this period was -20°C with a standard deviation of 5°.

Figure C.2 shows the variations in monthly high and low air and pavement temperatures observed at the test site on I-64. Data collected from the December '96 through November '98 were used in analysis. Also, shown in the graph are pavement temperatures at 25 mm below the surface. Although the high temperature binder grade selection using the Superpave software requires that the design high temperature at 20 mm be known, the sensor at this test site was located at 25 mm and hence these values are shown. It can be seen from the graph that the minimum pavement temperature never falls below that of the minimum air temperature. The highest pavement temperature was about 20° higher that the air temperature. The difference between air and pavement temperatures drops as the air temperature drops. The pavement temperature at 25 mm is slightly lower than that at the surface and stays parallel to it for most part.

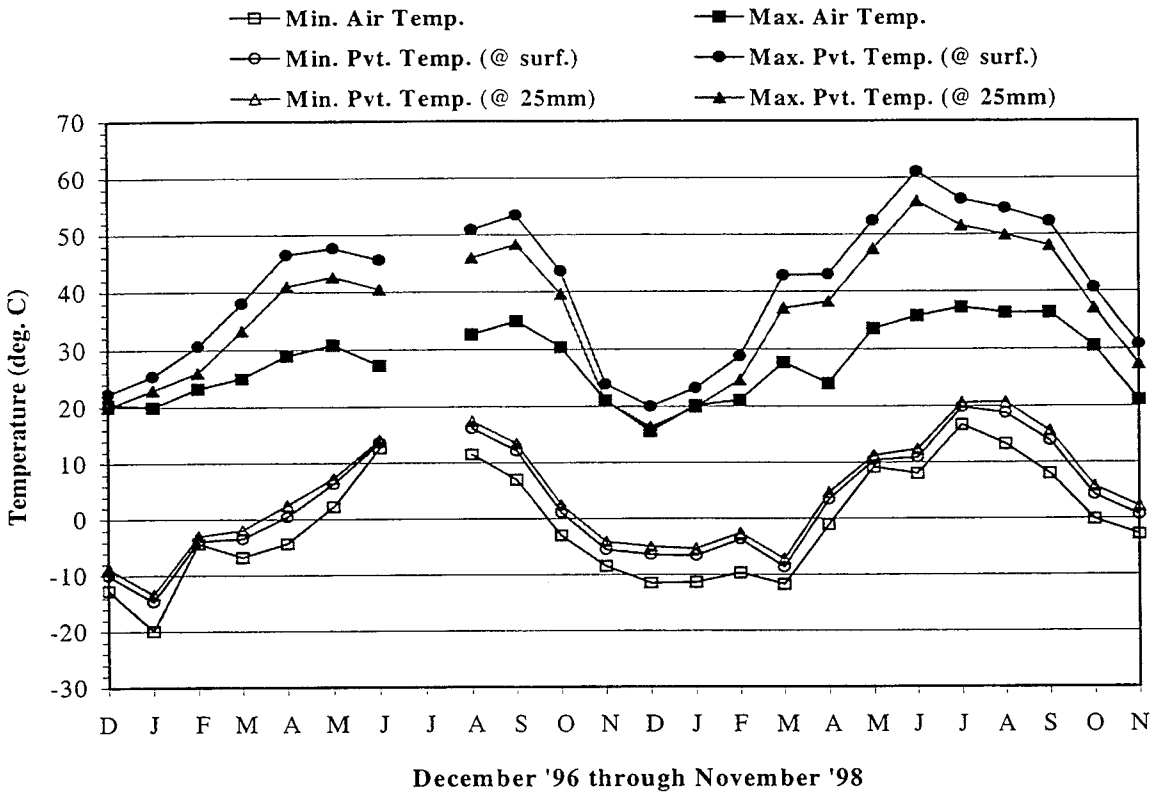

Figure C.2. Observed monthly variations in air and pavement temperatures at test site

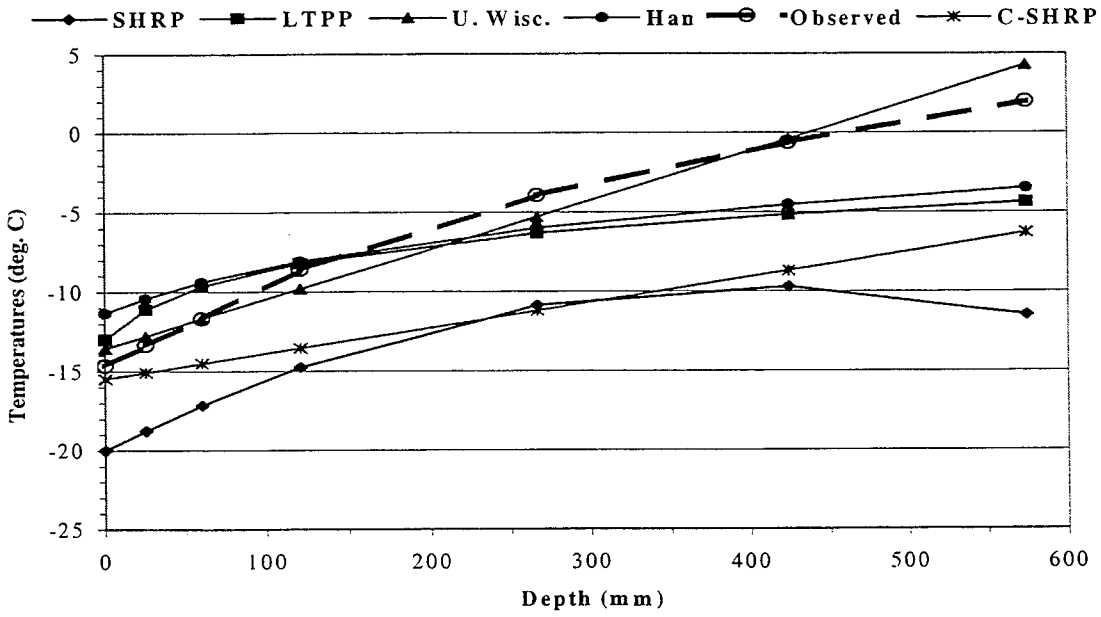

Figure C.3. Predicted and observed minimum pavement temperatures

Figure C.3 shows the variations in minimum temperature with depth. The temperature estimates shown in this figure are for 50% reliability. As can be seen, Han and LTPP models give very similar prediction and overestimate the observed pavement temperature by about 2 - 4 degrees at the surface. Beyond a depth of 250 mm, Han and LTPP model predictions are much lower than those observed. SHRP gives very conservative values at all depths. C-SHRP values are very close to observed values near the pavement surface. However, C-SHRP values are much lower than those observed at greater depths. The University of Wisconsin model predicts values that are close to the observed values at all depths, despite the fact that data were available only up to a depth of 100 mm.

C.3. Binder Selection Based on Model Predictions

The binder grade chosen for the site was PG 64-34 based on data from Evansville station and SHRP model. This grade gives a reliability of 99.7 % for the low temperature. The estimated pavement temperature at this reliability using the various models was calculated and summarized in Table C.1.

Table C.1. Estimated minimum pavement temperature at 99.7% reliability

Model	Estimated T_{min} (°C)
SHRP	-34.0
LTPP	-26.8
Univ. of WI	-27.6
Han	-25.3
C-SHRP	-29.5
Observed*	-28.7

Corresponding to the predicted temperatures, binder grades were selected for at least the same reliability. This is tabulated in Table C.2. But this reliability is very high and quite unnecessary. Usually, a reliability of 98 % is considered satisfactory. Table C.3 shows the

binder grades based on 98% reliability. Review of the data in Table C.3 indicates that Han, LTPP, and C-SHRP models all predicted the same binder grade. The choice of binder grade predicted by University of Wisconsin model conforms with observed temperature range at the site. In spite of the fact that this model was based on data collected up to a depth of 100 mm, the model seems to be giving the best estimates of the expected field conditions. All the binder grades selected based on temperatures predicted by the models as well as that based on actual recorded temperatures were higher (less negative) than the binder grade selected based on the current Superpave model. However, the reader should keep in mind that the observations were based on only 2 years of data and may need to be modified as more data becomes available.

Table C.2. Estimated low temperature binder grade at 99.7% (at least) reliability

Model	Grade
SHRP	-34
LTPP	-28
Univ. of WI	-28
Han	-28
C-SHRP	-34
Observed	-34

Table C.3. Estimated low temperature binder grade at 98% (at least) reliability

Model	Asphalt Grades
SHRP	-34
LTPP	-22
Univ. of WI	-28
Han	-22
C-SHRP	-28
Observed	-28

C.4. Indirect Tensile Testing

The low temperature behavior of HMA mixes can be evaluated using the Superpave Indirect Tension Tester (IDT). This device is used to perform creep compliance and tensile strength tests at low temperatures, as per Superpave protocols (AASHTO TP-9). Test results, such as slope of the creep compliance curve (m), Poisson ratio (ν), and tensile strength, obtained from these tests are used in the Superpave thermal-crack prediction models, to assess the potential of a given pavement to develop cracking at low temperatures.

As a part of this study, SGC samples were prepared using the same Superpave mix design as that used in intermediate course of the new overlay. The binder used in this test section was PG 64-34. The IDT test protocol (TP-9) requires that the samples be compacted to 7% air voids and that three replicates be tested at each temperature. This study deviated from the test protocol in that the compaction of samples was terminated at different values of N (compactive effort) rather than upon reaching 7% air voids. This was done to study the change in air voids with compactive effort. Additionally, only one sample was prepared at each level of compactive effort. For each value of N, the percentage of air voids was determined from the bulk specific gravity of each specimen and reported in Tables C.6 – C.8. The N values used in this study were 80, 109, 125 and 150 gyrations. The required sample size for IDT testing is 150 mm diameter and 51 mm thickness. These samples were obtained from the SGC compacted samples by sawing to the required thickness.

It was also a part of the research objective to study the influence of gyratory machine and operator on the compactive effort. To this end, samples were compacted to the aforementioned N values, using Pine and Troxler machines. One set of Troxler samples was prepared by the researcher while two sets of Pine samples were compacted by two different operators. One set of the Pine samples was prepared by the researcher and the other by a technician from INDOT's Materials and Testing Laboratory, in Indianapolis, IN

As per test protocols (TP-9), low temperature creep tests were performed at -20°, -10° and 0°C. The samples were diametrically loaded at a constant, ram-displacement rate of 12.5 mm/minute. The applied load was held for 100s and the corresponding horizontal and vertical displacements were noted. Tensile strength tests were performed at –10°C, with a

constant, ram-displacement rate of 50 mm/minute. The increase in load with time was recorded until failure of specimen occurred. The tensile strength of the material was calculated using procedure discussed elsewhere (11). The strength values for the different specimens compacted to different N values are shown in Tables C.6 – C.8.

Table C.6. Percent air voids and tensile strength of Pine IDT specimens (DOT)

No. of Gyrations, N	% Air Voids	Strength, MPa (psi)
80	5.8	1.9 (279)
109	4.2	N/A
125	4.0	2.3 (337)
150	2.4	2.2 (319)

Table C.7. Percent air voids and tensile strength of Pine IDT specimens (researcher)

No. of Gyrations, N	% Air Voids	Strength, MPa (psi)
80	2.8	3.0 (436)
109	2.8	3.2 (470)
125	2.2	3.4 (496)
150	1.5	2.8 (414)

Table C.8. Percent air voids and tensile strength of Troxler IDT specimens (researcher)

No. of Gyrations, N	% Air Voids	Strength, MPa (psi)
80	4.5	3.2 (459)
109	4.6	2.9 (403)
125	3.5	0.2 (36)*
150	2.7	2.1 (303)

*Outlier

In cold weather, asphalt pavement will crack when the pavement temperature falls below the so-called "critical temperature". Below the critical temperature, the thermal stresses generated in the pavement will exceed the tensile strength of the pavement material. The thermal cracking potential of HMA can be assessed by studying its creep behavior and

tensile strength at low temperatures. Models have been developed by Roque and others (6, 7, 9, 10) to predict thermal cracking as a function of time. Since HMA is a linear, viscoelastic material, its mechanical properties are time and temperature dependent. It is therefore essential to understand its properties over a range of temperatures and loading times, in order to reasonably predict its long-term performance. Stiffness of a material can be characterized by its compliance. Raw test data from creep compliance tests performed at the three temperatures are used in developing the master creep curve of the material. The resulting master creep curve shows the change in compliance with loading time. The master creep curve is used to generate the relaxation modulus function, which in turn, is used to estimate the thermal (tensile) stresses developed in the pavement, as a function of temperature.

In this study, raw test data from the IDT creep tests were directly input into the "Ltstress" program (subsequently referred to as IDT model) developed by Don Christensen (12) to obtain the master creep compliance curve and ultimately the plot of thermal stress as a function of temperature. In developing this plot, following default values were used:

Coefficient of thermal expansion of the mixture ..... 1.5×10^{-5} in/in/°F

Starting pavement temperature..... 40°F

Pavement cooling rate ..... 10°F/hr

The thermal stress versus temperature plot (Figure C.4) can be used to determine the critical pavement temperature. The critical pavement temperature can be estimated by drawing a horizontal line from the known value of stress (tensile strength from IDT test), to where it intercepts the curve and reading the corresponding temperature on the abscissa. The values of T_c determined for each of the samples are listed in Table C.9. These values can be compared with the minimum pavement temperature predicted by various low-temperature models (Table C.10) in order to assess the ability of the given mix to resist thermal cracking. For a well-chosen binder, the critical temperature of the binder will be lower (more negative) than the critical or fracture temperature of pavement, as predicted by IDT testing of the mix.

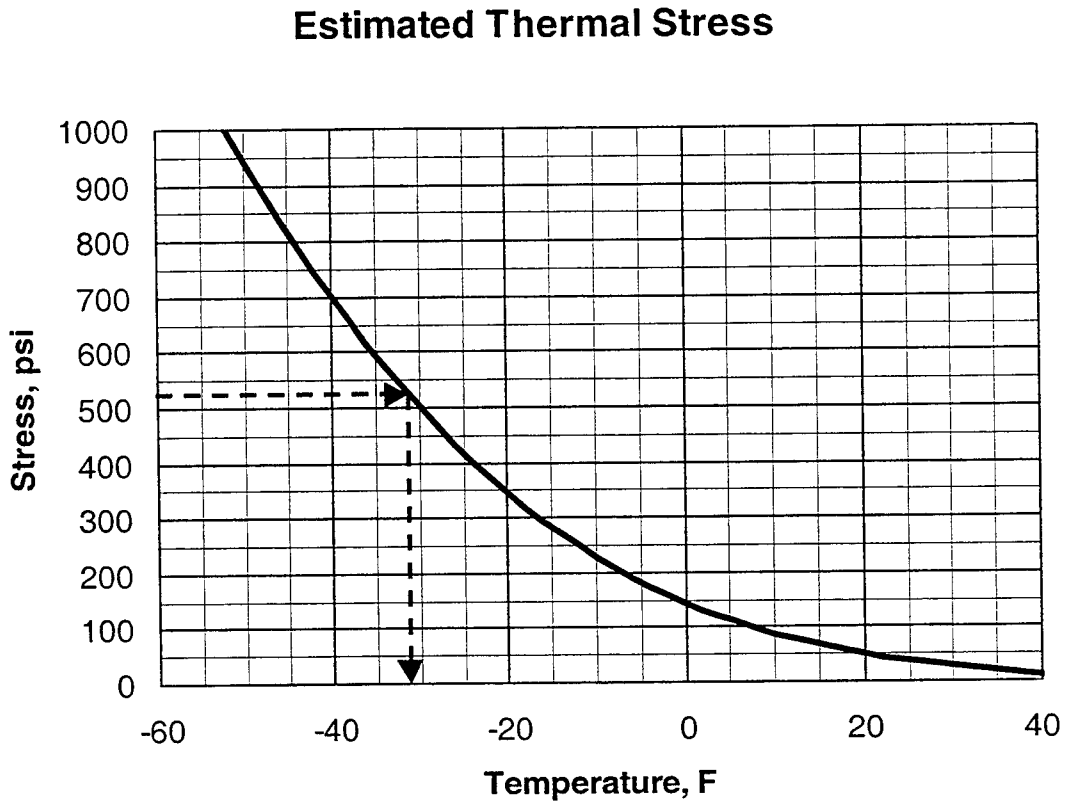

Figure C.4. Examples of thermal stress versus temperature plot

Table C.9. Critical pavement binder temperatures

Gyrations, N	T_c, °C
80	-22.5
109	N/A
125	-27.0
150	-25.0

Table C.10. Predicted minimum pavement temperatures (98% reliability)

Model	$T_{min(pav)}$, °C
SHRP	-30.3
C-SHRP	-25.8
LTPP	-23.3
Han	-21.8
Univ. of WI	-23.9
Observed*	-28.7

*Direct observation

The IDT model was developed based on samples compacted to 7% air voids. The sample compacted to 80 gyrations had air voids closest (6%) to this value. Comparison of the critical temperature for this sample (-22.5°C) with the minimum pavement temperature predicted by models discussed in this study indicate that all models yielded values close to the T_c obtained from IDT testing. SHRP model gave the conservative estimate. LTPP, Han and University of Wisconsin model estimates were quite similar to the value predicted by IDT model. However, temperature observed in the pavement was lower (more negative) than that predicted by models and by IDT testing, except for SHRP model. In spite of that, no thermal cracking was observed in the pavement during the period of data collection. It should be noted that due to the limited number of samples tested, the estimates of T_c using IDT data are not very reliable. In addition, the IDT model does not account for effect of aging hardening that occurs in the pavement over time.

In summary, the low temperatures predicted by various models, as well as the actual low temperature recorded in the pavement at the test site were higher than the lowest temperature that the binder can withstand without cracking (-34°C). This implies that the chosen binder should perform adequately at this particular location.

REFERENCES

1. W. D. Robertson, "Using the SHRP Specifications to Select Asphalt Binders for Low Temperature Service", presented at SUPERPAVE Conference, Reno, NV, 1993.
2. A. Mohseni and M. Symons, "Effect of Improved LTPP AC Pavement Temperature Models on SUPERPAVE Performance Grades", *Transportation Research Board*, No. 1609, pp. , 1998.
3. A. Mohseni and M. Symons, "Improved AC Pavement Temperature Models from LTPP Seasonal Data", *Transportation Research Board*, No. 1609, pp. ,1998.
4. E. O. Lukanen, C. Han and E. L. Skok, Jr., "Probabilistic Method of Asphalt Binder Selection Based on Pavement Temperature", *Transportation Research Record*, No. 1609, pp. 12 – 20, 1998.
5. P. J. Bosscher, H. U. Bahia, S. Thomas and J. S. Russell, "Relationship Between Pavement Temperature and Weather Data—Wisconsin Field Study to Verify Superpave Algorithm", *Transportation Research Record*, No.1609, pp. 1 – 11, 1998.
6. W. G.Buttlar and R. Roque, "Development and Evaluation of Strategic Highway Research Program Measurement and Analysis System for Indirect Tensile Testing at Low Temperatures", *Transportation Research Record*, No. 1454, pp. 162 – 171, 1994.
7. D.R. Hiltunen and R. Roque, "A Mechanics-Based Prediction Model for Thermal Cracking of Asphaltic Concrete Pavements", Journal of *Association of Asphalt Paving Technologists*, Vol. 63, pp. 81 – 117, 1994.
8. W.G.Buttlar and R. Roque, "Evaluation of Empirical and Theoretical Models to Determine Asphalt Mixture Stiffnesses at Low Temperatures", Journal of *Association of Asphalt Paving Technologists*, Vol. , pp. 99 – 141, 199?.
9. R. Roque, D. R. Hiltunen and W.G. Buttlar, "Thermal Cracking Performance and Design of Mixtures Using Superpave", Journal of *Association of Asphalt Paving Technologists*, Vol. 64, pp. 718 – 735, 1996.
10. D. R. Hiltunen and R. Roque, "The Use of Time-Temperature Superposition to Fundamentally Characterize Asphaltic Concrete Mixtures at Low Temperatures",

Engineering Properties of Asphalt Mixtures and Relationship to their Performance, ASTM STP 1265, Eds., G. A. Huber and D. S. Decker, pp. 74 – 93, 1995.

11. "Superpave Asphalt Mixture Analysis—Course Text", Federal Highway Administration, Office of Technology Applications, Washington D. C., May 1996.
12. D. Christensen, "Analysis of Creep Data from Indirect Tension Test on Asphalt Concrete", Journal of *Association of Asphalt Paving Technologists*, Vol. 67, pp. 458 – 493, 1998.
13. R. M. Anderson, D. E. Walker and P. A. Turner, "Low Temperature Evaluation of Kentucky PG 70-22 Asphalt Binders", paper submitted for presentation at the 78th Annual Meeting of *Transportation Research Board*, Washington D.C., 1999.